Dissertation zur Erlangung des Doktorgrades der Fakultät für Chemie
und Pharmazie der Ludwig-Maximilians-Universität München

Post-translational modifications in Inflammasome Signalling

Fionán Ulrich Ó Dúill
aus
Neuendettelsau, Deutschland

2020

Erklärung

Diese Dissertation wurde im Sinne von § 7 der Promotionsordnung vom 28. November 2011 von Herrn Prof. Dr. Hornung betreut.

Eidesstattliche Versicherung

Diese Dissertation wurde eigenständig und ohne unerlaubte Hilfe erarbeitet.

München, 01.10.2020

_____

Fionán Ó Dúill

Dissertation eingereicht am 13.10.2020

1. Gutachter: Prof. Dr. Veit Hornung

2. Gutachter: Prof. Dr. Julian Stingele

Mündliche Prüfung am 20.11.2020

Do mo theaghlach agus mo chairde.

Table of contents

1. Introduction

1.1. The Immune System

The immune system is a multifaceted host defence mechanism, which protects organisms against pathogen invasion. In vertebrates, two major branches of the immune response exist: the innate and the adaptive immune system (Figure 1).

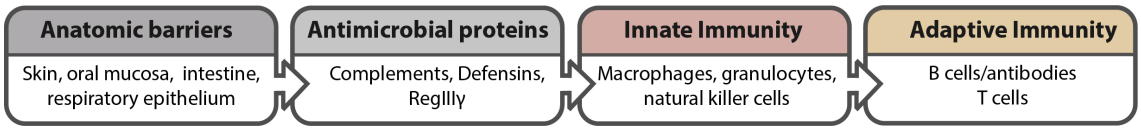

***Figure 1* Several levels of defence against pathogens.** The epithelial surface acts as a first anatomic barrier. In close proximity to this barrier, chemical and enzymatic systems act as a second, antimicrobial barrier. If these barriers are breached, the rapid innate immune cells and the slower but highly specialised adaptive immune system actively target the pathogen. (Fig. adapted from (*1*))

The innate immune system, which can be found in all multicellular organisms, rapidly acts as the first line of defence on a broad array of pathogens through recognition of distinct conserved foreign patterns, so-called pathogen-associated molecular patterns (PAMPs) (*2, 3*). This response is mediated mostly by monocytes, macrophages and dendritic cells, which directly interact with invading pathogens through germline-encoded receptors that are termed pathogen recognition receptors (PRRs). Pathogen clearance occurs either directly - through specialised engulfing cells, which break apart internalised pathogen utilising low pH and digestive enzymes - or indirectly through the release of antimicrobial peptides as well as cytokines and chemokines (*4*). Macrophages and dendritic cells also act as antigen-presenting cells (APCs) to further facilitate an adaptive immune response (*5*).

The adaptive immune response is primarily mediated by B- and T lymphocytes. Somatic recombination and clonal expansion processes lead to a great diversity of antigen receptors that can target specific epitopes present on invading microorganisms, infected cells or toxins (*6*). As no germline-encoded receptors are inherited, in contrast to the innate system, protection by the adaptive immune system takes days rather than hours. However, the adaptive immune system provides a specific and diverse long term immune-memory that is the basis of effective vaccination (*7*). B lymphocytes secrete the

antigen receptors in the form of antibodies, providing humoral protection, while T lymphocytes express antigen-receptors on their cell surface, contributing to the recognition of infected cells in a cell-based immune response. Antigen presentation through APCs and the presence of pro-inflammatory cytokines is necessary for the adaptive response, demonstrating the synergistic crosstalk between the innate and the adaptive immune system (*8, 9*).

The ability of the immune system to differentiate self from non-self and to produce adequate protection against infection requires complex regulation. Dysregulation leads to disease: in most autoinflammatory diseases the innate immune system directly causes uncontrolled inflammation, whereas in autoimmune diseases the innate immune system generally activates the adaptive immunity which, in turn, is responsible for an unbeneficial inflammatory process (*10*).

1.2. The Innate Immune System

The role of the innate immune system is to prevent infection, respond to pathogens and to prepare and activate the adaptive immune system to provide long-lasting protection.

As the first line of defence, our body utilises physical, chemical and physiological barriers that prevent the intrusion and colonisation of pathogens (Table 1) (*11*). Antimicrobial proteins present in mucosal barriers, and the pH value of the skin and the gastrointestinal tract combat microbes directly at these sites (*12*).

	Skin	Gut	Lungs	Eyes/nose/mouth
Mechanical	Epithelial cells joined by tight junctions			
	Longitudinal flow of air or fluid	Longitudinal flow of air or fluid	Movement of mucus by cilia	Tears Nasal cilia
Chemical	Fatty acids	Low pH	Pulmonary surfactant	Enzymes in tears and saliva (lysozyme)
		Enzymes (pepsin)		
	β-defensins, lamellar bodies, cathelicidin	α-defensins, RegIII (lectidins), Cathelicidin	α-defensins, cathelicidin	β-defensins Histatins
Microbiological	Normal microbiota			

***Table 1* Barriers preventing pathogens from entering.** Epithelial barriers provide mechanical, chemical and microbiological barriers against infection. Modified from (*1*).

When pathogens overcome these barriers, they come in contact with the humoral and cellular components of the innate immune system. The humoral components such as ficolins, collectins and pentraxins recognise different elements on the surface of microorganisms, opsonising them and facilitating their uptake by effector cells (*13*). Specialised engulfing cells such as macrophages and dendritic cells break apart the internalised pathogens through low pH, the presence of acid hydrolases, reactive oxygen and nitrogen intermediates and digestive enzymes (*4*).

Besides this immediate clearance of infectious agents, which is effective against bacteria, fungi, viruses and parasites; a broad mechanism of the innate immune system is the induction of cell death of infected cells, leading to the destruction of the habitat in which intracellular pathogens can proliferate. This cell-intrinsic cell death can be induced in the forms of apoptosis, pyroptosis or necroptosis, the latter two leading to the release of intracellular content and immune mediators which further activate bystander immune cells (*14*). Lytic cell death, tissue damage and infection lead to an immediate inflammatory response, termed acute phase response, driven primarily by macrophages (*15*). The subsequent secretion of a broad spectrum of cytokines and chemokines has profound effects on cellular function. These functions include the activation of granulopoiesis, which leads to the production of large numbers of granulocytes, such as neutrophils (*16*). Cytokines also lead to changes in expression patterns of immune and endothelial cells (*17*). Endothelial cells upregulate intracellular adhesion molecules (ICAMs) which interact with many leucocytes, slowing their rate of passage, thus facilitating migration in a process called leucocyte rolling (*18, 19*). Chemokines, a subclass of cytokines which attract leukocytes expressing the correspondent chemokine receptor, guide the cells to their destination.

Increased blood flow enhances the recruitment of immune cells and leads to swelling, redness and heat, which comprise the hallmarks of inflammation (*15*). The cytokine influence upon the hypothalamus causes a distinct fever response (*20, 21*).

1.3. Pathogen Recognition Receptors

The mounting of an appropriate immune response to pathogens depends on their detection (*3*). For this purpose, innate immune cells are equipped with a set of germline-encoded pattern recognition receptors (PRRs), that can detect a variety of molecules (Figure 2). They can bind to and thus be activated by pathogen-associated molecular patterns (PAMPs) which consist of conserved microbial components such as lipopolysaccharide (LPS), a major component of the outer cell membrane of Gram-negative bacteria (*22, 23*).

PRRs also have the ability to detect damage-associated molecular patterns (DAMPs), which are released during cell damage or necrotic or programmed lytic cell death. For example, the catabolite uric acid can be released by injured tissue and form crystals that in turn can activate the NLRP3 inflammasome through cell membrane perturbation (*24*). PRRs can, therefore, react to "non-self" by detecting microbial molecular structures not shared by the host as well as "self" molecules that are mislocalised in pathological or stressful conditions (Figure 2).

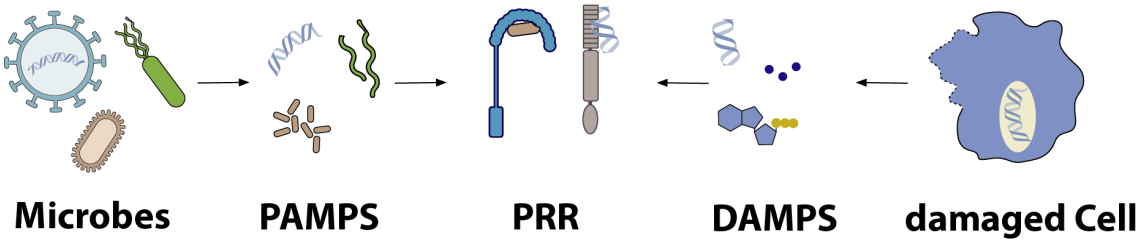

***Figure 2* Activation of the innate immune system by PAMPs and DAMPs.** Pathogens such as bacteria, fungi and viruses are recognised by detecting conserved structures called pathogen-associated molecular patterns (PAMPs). Likewise, danger stemming from the loss of cellular integrity can be sensed in the form of danger-associated molecular patterns (PAMPs). In both cases, germ-line encoded pattern recognition receptors (PRRs) recognise these ligands and induce an immune response.

PRRs can be subdivided into two main classes based on their localisation in the cell: membrane-bound TLRs (Toll-Like Receptors) and CLRs (C-Type Lectin Receptors) monitor the extracellular space and the endolysosomal system. In contrast, cytoplasmatic PRRs such as Nod-Like Receptors (NLRs), RIG-I-Like Receptors (RLRs) and AIM2-Like Receptors (ALRs) monitor the intracellular environment (*25, 26*).

1.4. Membrane-bound PRRs

The extensively studied TLRs are type I membrane proteins that detect an extensive range of extracellular pathogens. Binding and recognition of their ligands is mediated by an extracellular or luminal N-terminal leucine-rich repeat (LRR) domain.

In humans, ten functional TLRs are known (Table 2) (*22, 27*).

TLR3, TLR7/8 and TLR9 sense the presence of nucleic acid species in the endosome. TLR3 recognises double-stranded (ds)RNA species, while TLR7 and eight heterodimers detect degradation products of single-stranded RNA, and TLR9 binds unmethylated CpGs found in bacterial DNA (*28-32*).

TLR2 detects a variety of agents, ranging from acetylated lipoprotein and lipoteichoic aid to peptidoglycans and fungal cell wall components (*33-35*). It forms heterodimers with TLR6 and TLR1 for the recognition of triacylated and diacylated lipoproteins, respectively (*33, 36, 37*). The synthetic triacylated lipopeptide Pam3CSK4 is broadly used to specifically target TLR1/2 when studying the role of individual TLRs (*38*).

Early work implicated TLR2 to also play a role in LPS binding (*39*). However Poltorak *et al.* and Hoshina *et al.* were able to show in independent experiments that this was not the case: TLR4, in association with myeloid differentiation factor 2 (MD2) is responsible for LPS binding (*35, 40-44*). The soluble and circulating LPS binding protein (LBP) facilitates the trafficking of LPS to the TLR4-MD-2 complex resulting in signal transduction (*45, 46*).

The cell wall component of gram-negative bacteria LPS induces a rapid inflammatory response and is a key signal in early infection (*47, 48*). It is composed of a lipid A hydrophobic anchor, a nonrepeating oligosaccharide and a distal polysaccharide (*48*). TLR4 can directly recognise the lipid A moiety; however, some bacteria adapted to impair this binding through modifications such as acetylation and phosphorylation (*49-51*).

While TLR4 plays a key role in response to gram-negative bacteria, TLR5 recognises flagellin, which many gram-negative and positive bacteria use for mobility and adhesion (*52, 53*).

Localisation	TLR	Ligand	Activating Pathogens
Plasma membrane	TLR1/TLR2	Triacyl lipoprotein	Bacteria, mycoplasma
	TLR6/TLR2	Diacyl lipoprotein, Zymosan Lipoteichoic acid	Bacteria, mycoplasma, parasites, fungi
	TLR4	LPS	Bacteria, viruses
	TLR5	Flagellin	Bacteria
	TLR6	Diacyl lipoprotein	Bacteria, viruses
Endosome	TLR3	dsRNA	Virus
	TLR7	RNA degradation products	Virus, Bacteria
	TLR8	RNA degradation products	Virus, Bacteria
	TLR9	CpG-DNA	Virus, Bacteria, Protozoa
	TLR10	Unknown, possibly a negative regulator	

Table 2: **Localisation and role of Toll-like receptors (TLRs).** Individual TLRs with specific localisation and microbial ligand specificity. Modified from (*54*).

TLR engagement initiates a complex downstream signalling pathway through interactions of the cytoplasmic Toll/Interleukin-1 (TIR) domain with the adaptor proteins (Figure 3). TLR2, 5, 7 and 9 recruits myeloid differentiation primary response gene 88 (MyD88), while TLR3 recruits TIR-domain containing adaptor protein inducing IFNb (TRIF), both of which will be discussed in more detail below (*55*). TLR4 can bind both MyD88 and TRIF in the presence of adapter molecules.

TLR dimerisation leads to MyD88 association via TIR-TIR domain interaction (*56*). The TIR domain-containing adaptor protein (TIRAP, also known as MAL) is also associated at the TIR upon TLR4, TLR1/2 and TLR2/5 activation (*56-59*). The large helical signal complex of multiple MyD88 molecules termed the myddosome can recruit the cytosolic interleukin-1 receptor-associated kinases (IRAK1,2,4) (*60, 61*). The phosphorylation of IRAK1 through IRAK4 leads to the activation of the E3-ubiquitin ligase TNF-receptor associated factor 6 (TRAF6) which in turn auto-ubiquitinates, forming long K63-linked chains which act as protein scaffolds for downstream recruitment of signalling molecules (*62*).

Analogous to MyD88, TRIF, together with the adapter TRAM (TRIF-related adaptor molecule), binds TLR3 and TLR4 leading to the activation of TRAF3 and TRAF6 (*58, 63, 64*). TRAF3 forms K63-linked ubiquitin chains and thus recruits the kinases TBK1 (TANK-binding kinase1) and IKKε resulting in the phosphorylation of IRF3 and initiating type I interferon signalling (*65*).

Mediated by TAK1 binding proteins (TAB2 and TAB3), TGFβ-activated kinase (TAK1) binds to the ubiquitin scaffold on TRAF6 and triggers its activation (*66*). This activated kinase complex can drive both the transcription factor Nuclear Factor-κB (NF-κB) and mitogen-activated protein kinase (MAPK) signalling (*67*). For NF-κB signalling TAK1 phosphorylates the IκB kinase (IKK) complex which is composed of Ikkα, IKKβ and IKKγ (also known as NF-κB essential modifier, NEMO) (*68-70*). NEMO binds to polyubiquitin chains bringing the complex into close proximity to TAK1. TAK1 is thought to phosphorylate IKKβ, which in turn phosphorylates IκBα resulting in its ubiquitination and degradation via the proteasome. The RelA-p50 heterodimer freed thereupon can translocate to the nucleus and induce gene expression (*68*).
The MAPK pathway signals through JNK (c-Jun N-terminal kinase) and P38 resulting in the nuclear translocation of the transcription factor AP-1 (Activating protein-1), promoting pro-inflammatory and pro-survival genes (*71, 72*).

These transcription factors, with their binding specificity to distinct DNA motifs, induce the expression of various pro-inflammatory genes, including those coding for cytokines and chemokines, and also the regulation of inflammasomes. Tight regulation of their activity, as described for NF-κB in the following section, is therefore essential.

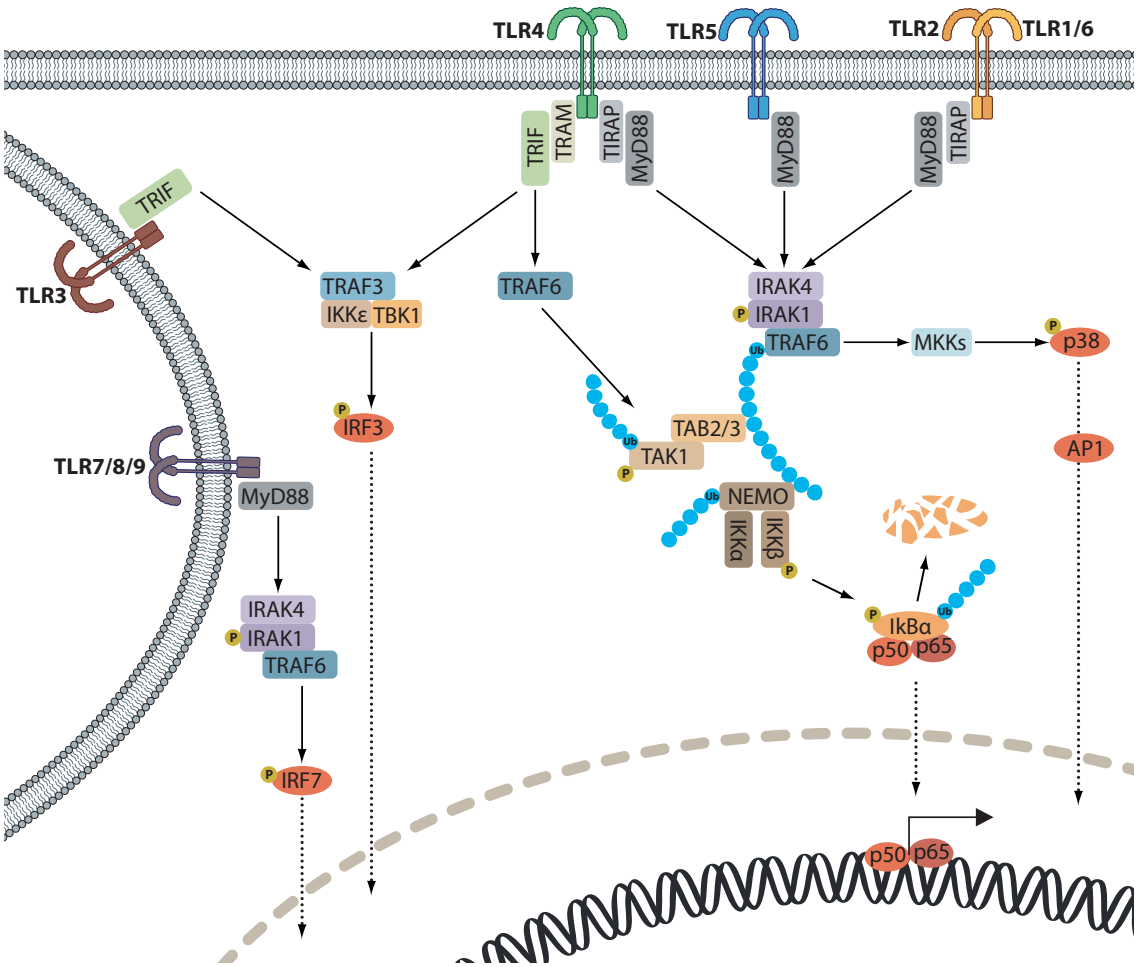

***Figure 3* TLR signalling pathways.** Upon respective ligand binding, TLRs form dimers and recruit adaptor proteins to the cytoplasmic domains of the receptor. Downstream signalling leads to the translocation of transcription factors to the nucleus. One of the main pathways, the NF-κB signalling, is highly regulated by kinases (TAK1, IKKs) and ubiquitinases, which provide the scaffolding for the signalling complexes.

1.5. NF-κB signalling and the IKK family Kinases

As observed in the previous chapter, TLR engagement often leads to downstream NF-κB activation. In vertebrates, the NF-κB transcription factor family consists of a heterogeneous group of proteins (Figure 4), including the TAD containing RELA (p65), and RELB (RelB) and REL (c-Rel) as well as ankyrin repeat containing NF-κB1 (p50/p105) and NF-κB2 (p52/p100) (*73*). In unstimulated cells, NF-κB dimers are tightly bound by inhibitory proteins (IκBs), restraining them to the cytosol and thus inhibiting DNA binding, only to be freed upon stimulation.

The strongly conserved RHD (Rel homology domain) enables the subunits to form various homo- and heterodimers and allows the binding of DNA as well as the

interaction with inhibitory proteins (*74, 75*). The IκB (Inhibitor of κB) proteins bind the RHD of the NF-κB dimers via their ankyrin repeats (ARD), masking their C-terminal NLS, thus preventing the translocation to the nucleus. Phosphorylation of the inhibitory factors following stimulation leads to rapid K48 polyubiquitination and proteasomal degradation. Once freed by this process, the transcription factors are able to translocate to the nucleus and induce gene expression. Indeed ubiquitination events on NF-κB proteins such as p65, p100 and p105 have also been reported, adding an additional layer of protection by limiting their availability and dimerization (*76, 77*) (*78, 79*).

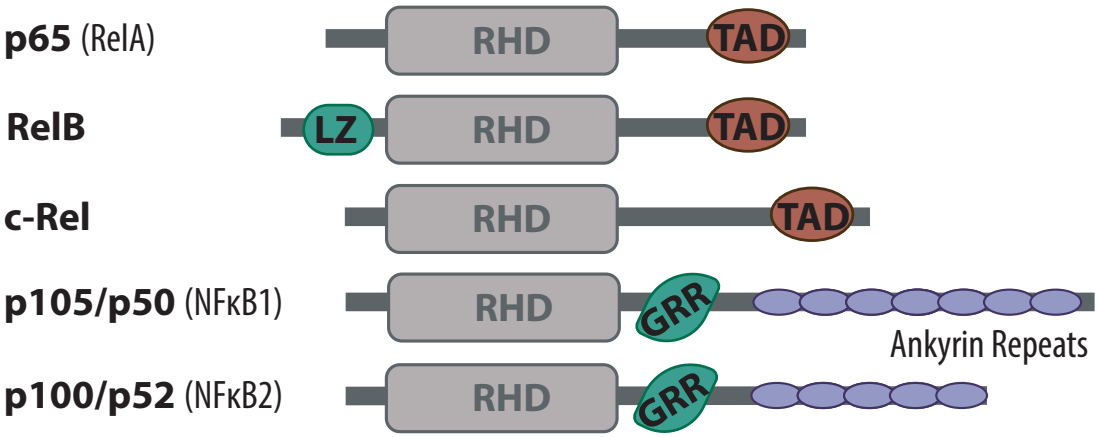

***Figure 4* Schematic representation of the NF-κB/Rel family**. The characteristic Rel homology domain (RHD) is found in all five family members. The p65, RelB and c-rel family members contain a Transactivation Domain (TAD) which confers positive regulation of gene expression. Only RelB contains an amino-terminal leucine zipper motif (LZ). The transcriptional suppressor family members p50 and p52 contain glycine-rich regions (GRR) required for their proteolytic cleavage and ankyrin repeats, also found on IκB proteins, acting as cytoplasmic inhibitors of NF-κB. (Fig. adapted from (*80*))

While there are at least 12 possible NF-κB subunit combinations that can bind to DNA and potentially regulate transcription, two superordinate signalling pathways have been characterised as the primary NF-κB signalling.

The canonical pathway is activated by a variety of cytokines (such as TNFα and IL-1) and PAMPS (such as LPS), which can signal through different pathways including TLR (cf. previous section) and NOD2 (cf. section 1.6). These pathways converge in the dissociation of canonical inhibitors of kB (IκB) IκBα, IκBβ and IκBε, which retain the transcription factors in the cytosol (*81, 82*).

The activated IKK has been shown to lead to the degradation of these inhibitory proteins.

Besides the classical, canonical NF-κB signalling, an alternative non-canonical route exists. It gets stimulated by a more restricted set of cytokines belonging to the TNF superfamily (such as lymphotoxin b). Signalling also differs from the classical pathway in that it does not utilise IκBs, but is held in an inactive state by the p52 precursor protein p100 which also contains the ARD domains found in IκB proteins (*83*). Phosphorylation and ubiquitination events lead to a degradation of the C-terminal structure on p100, resulting in the generation of the mature non-canonical NF-κB complex p52/RelB. Non-canonical NF-κB signalling solely requires IKKα, but not NEMO or IKKβ (*84-86*).

IKKα and IKKβ are ubiquitously expressed serine/threonine kinases that show high sequence homology (70%) and similarity in domain organisation and tertiary structure (*87-89*). In addition to their N-terminal kinase domain both contain a ULD (ubiquitin-like domain) as well as α helical scaffold/dimerisation domain (SDD) and a C-terminal NEMO-binding domain (NBD) (Figure 5). In the formation of the IKK complex, the regulatory subunit IKKγ (or NEMO) binds the kinases via their NBDs. Despite their high structural similarity, IKKα and IKKβ differ significantly from each other in their function due to different substrate specificities.

Activation of both kinases requires the phosphorylation of specific residues in the activation loop of their active sites: S176 and S180 for IKKα and S177, and S181 for IKKβ (*90, 91*). This activation is proposed to involve oligomerisation-mediated trans-autophosphorylation of the subunits (*89, 92*). In the case of IKKβ, it is first phosphorylated by the apical kinase TAK1 at S177 which enables autophosphorylation at S181 thus leading to an active IKK complex capable of phosphorylating IκB proteins and promoting their K48-linked ubiquitination, preparing them for degradation and initiating NF-κB signalling (*91-96*).

Besides the direct role in the NF-κB signalling, both IKKα and IKKβ phosphorylate 'non-classical' substrates are involved in diverse biological processes (*97*). Some substrates, such as FOXO3a and TSC1, are involved in proliferative and pro-survival pathways, thus suggesting a role of IKKs in tumorigenesis (*98, 99*).

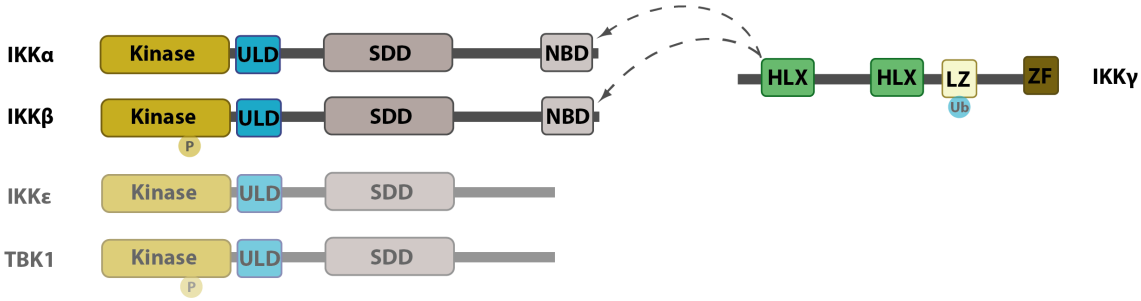

***Figure 5* Schematic representation of IKK proteins.** The IKK-family proteins (IKKα, IKKβ, IKKε and TBK1) all contain a C-terminal kinase domain, followed by a ULD (ubiquitin-like domain) and the central SDD (scaffold/dimerising domain). The regulatory IKKγ (NEMO) subunit is composed of two HLX (helix domains), a LZ (leucine zipper domain) responsible for ubiquitin-binding, and a ZF (zinc finger-binding domain) facilitating interaction with IκBs. Upon IKK complex formation, the HLX domain of IKKγ interacts with the c-terminal NBD (NEMO binding domain). (Fig. adapted from (*80*))

The activation of NF-κB transcription factors is not only accompanied by a rapid transcriptional upregulation of pro-inflammatory cytokines such as TNFα (tumour necrosis factor α), IL-6 (Interleukin-6) and IL-1β. However, it has also been shown to regulate the expression of cytosolic PRRs such as NLRP3, NLRP2 and NOD2 (*100, 101*).

1.6. Cytosolic PRRs

The cytosolic receptor families RLHs (RIG-I-Like Receptors), OLRs (OAS-Like Receptors), NLRs (Nod-Like Receptors) and ALRs (AIM2-Like Receptors) monitor the intracellular environment (*102-104*).

The RLHs such as RIG-I (retinoic-acid inducible gene I) and MDA5 (melanoma differentiation-associated protein 5) sense viral RNA inducing NF-κB and interferon signalling through MAVS (mitochondrial antiviral signalling protein) (*102*). The prominent OLR STING (Stimulator of interferon genes) together with its adapter cGAS (cyclic GMP-AMP synthase) is involved in the response to cytosolic DNA leading to a type I interferon response (*105, 106*).

NLRs form the largest family of intracellular PRRs, consisting of 22 known proteins that generally feature an N-terminal effector domain, a central nucleotide-binding domain (NACHT) and a C-terminal leucine-rich repeat (LRR) domain responsible for ligand recognition (*104, 107*). Depending on their N-terminal domain, NLRs are classified as

either NLRA (AD), NLRB (BIR), NLRC (CARD) or NLRP (PYD) proteins (Table 3). Among these, individual members of the NLRC and NLRP subfamily—that harbour the N-terminal death fold domains CARD or PYD, respectively—have been shown to act as PRRs. NLRCs and NLRPs can recruit CARD- and PYD- containing proteins and initiate the formation of multiprotein oligomers referred to as NODosomes or inflammasomes, respectively (Figure 6) (*108, 109*). While only conclusively shown for the NAIP/NLRC4 inflammasome, it is believed that ligand engagement by these NLRs results in the unfolding of an auto-inhibited receptor, which allows the central NACHT to bind ATP which promotes oligomerisation (*104, 110, 111*). Subsequently, ATP hydrolysis is believed to revert the active receptor complex to its ground state. Oligomerisation results in the formation of a wheel-like structure that serves as a seed-like structure to initiate signal transduction.

NLR family	N-terminal effector domain	Name
NLRA	acid transactivation domain (AD)	Class II transactivator (CIITA)
NLRBs	baculovirus inhibitor repeat (BIR)	NAIPs
NLRCs	caspase recruitment domain (CARD)	NODs
NLRPs	pyrin (PYD)	NALPs

***Table 3* NOD-like receptor family.** Varying N-terminal effector domains allow classification in sub-families. Modified from (*112*).

The NODosome is formed upon recognition of the cell wall component muramyl dipeptide (MDP), present in most Gram-negative and Gram-positive bacteria, by NOD2. This leads to the recruitment and ubiquitination of the adaptor kinase receptor-interacting protein kinase 2 (RIPK2) driving NF-κB and MAPK signalling (*113, 114*). The ubiquitin chains on RIPK2 serve as binding platforms for NF-κB activation similar to the TLR induced NF-κB signalling shown in Figure 3.

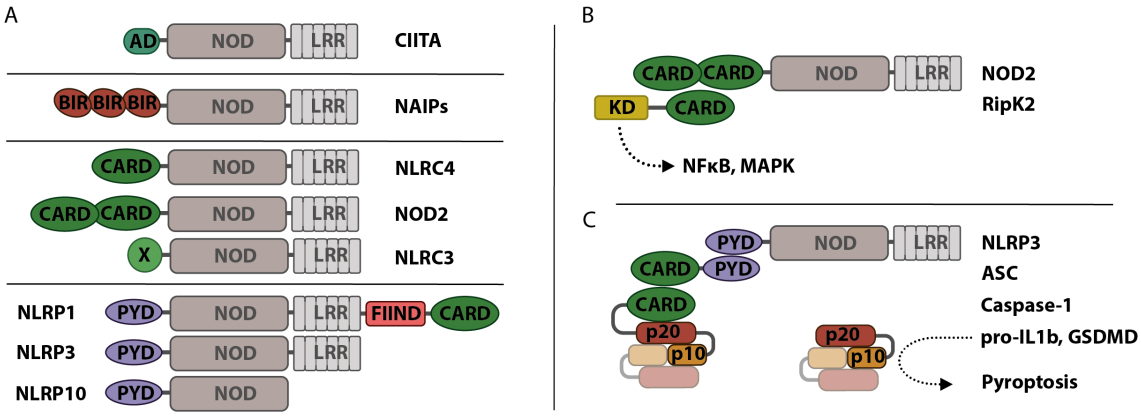

***Figure 6* NLR signalling proteins. (A)** Schematic representation of a subset of NLR family proteins. All human NLRs contain a central NACHT domain and a C-terminal ligand-sensing LRR domain (except NLRP10). **(B)** NOD2 oligomerisation recruits the adaptor protein RIPK2 via CARD–CARD interactions, which activate NF-κB and MAPK signalling. **(C)** Inflammasome forming receptors recruit the bipartite adaptor protein ASC via homotypic PYD–PYD (NLRP3) or CARD–CARD interactions (NLRP1B and NLRC4). CARD-CARD interactions lead to the recruitment of pro-caspase 1, leading to its proximity-induced autoproteolytic activation.

Inflammasome formation leads to the recruitment of the adaptor molecule ASC (an apoptosis-associated speck-like protein containing CARD) through pyrin-pyrin homotypic interactions resulting in the formation of ASC filaments (*115*). This facilitates the recruitment of the cysteine protease caspase-1, through CARD-CARD interactions (*116, 117*). Autocatalytically activated caspase-1 cleaves the pro-inflammatory cytokines pro-IL-1β and IL-18 into their mature forms, as well as the death effector molecule gasdermin D (GSDMS) (*108, 118, 119*). N-terminally cleaved GSDMD binds to phosphatidylinositol phosphates and phosphoserine of the plasma membrane forming pores that allow IL-1β secretion and rapid cell lysis (*120-122*). Lysis is evoked by a change of the ion gradient at the plasma membrane, driving an increase in osmotic pressure and characteristic swelling and rupturing of the cells (*120, 123*).

This lytic form of cell death is termed pyroptosis. In addition to releasing cytokines and destroying the potential habitat of intracellular bacteria, pyroptosis also releases cytosolic DAMPS, such as ATP, which further propagate the inflammatory response (*124, 125*). GSDMD maturation and pore formation can also precede and lead to inflammasome formation, as it is the case for non-canonical NLRP3 signalling.

1.7. NLRP3

Amongst all inflammasome sensors, NLRP3 is the most widely studied, as it is associated with multiple inflammatory diseases. Monogenetic autoinflammatory pathologies of NLRP3, summarised as CAPS (cryopyrin-associated periodic syndromes) include FCAS (familial cold autoinflammatory syndrome), MWS (Muckle-Wells syndrome) and NOMID (neonatal-onset multisystem inflammatory disorder) (*126-128*). They all show a systemic IL-1 mediated inflammation and fever, caused by spontaneous, stimulus-independent inflammasome activation (*129*). Furthermore, non-genetic dysregulation of NLRP3 has been implicated in diseases like type-2 diabetes, arteriosclerosis, Alzheimers and Parkinsons (*130-136*).

Inflammasome activation is often referred to as a two-step process: Signal 1 (Figure 7A) consists of the activation of the NF-κB signalling pathway (Chapter 1.3.2) by an independent PRR, typically TLR4 or TLR2 (*137, 138*). *In vitro,* this priming step is required for the transcriptional upregulation of the pro-IL-1ß precursor. In the absence of this first signal, the inflammasome can still be activated, inducing pyroptosis but no IL-1ß secretion. NLRP3 also relies on signal 1 for transcriptional upregulation and post-translational licensing (*137, 139*).

A wide range of activators are known for signal 2 of NLRP3 activation (Figure 7B), including extracellular adenosine triphosphate (ATP), pore-forming bacterial toxins, crystalline structures such as monosodium urate (MSU), asbestos or silica or drugs such as Nigericin (*108, 140-142*). These activators do not associate directly with NLRP3 but instead are thought to be activated by a generic pathway facilitated by other proteins (*143*).

In addition to these canonical stimuli, non-canonical inflammasome activation can occur through direct sensing of LPS by caspase 4/5 (human) or caspase 11 (mouse) (*144-146*). The activated caspases directly cleave GSDMD, thus activating pyroptotic cell death independent of caspase-1, which indirectly activates NLRP3 via potassium efflux through the formed pores (*121, 146, 147*).

While many models for activation have previously been reported including the mitochondrial release of reactive oxygen species (ROS), calcium (Ca^{2+}) signalling and

lysosomal disruption during incomplete phagocytosis, it was assumed for a long time that a drop in cytosolic potassium was necessary and for NLRP3 activation (*141, 145, 148-152*). Downstream of potassium efflux, Nek7 (never in mitosis gene a – related expressed kinase 7) was identified as an upstream protein required for murine NLRP3 activation (*153-155*).

However, in recent studies the dispersal of the trans-Golgi network (TGN) was identified as the common denominator of both potassium-dependent and -independent activation (*156-158*). In this model, the polybasic regions of NLRP3 are thought to interact with negatively charged phosphatidylinositol-4-phosphate (PtdIns4P) on the dispersed TGN leading to heptameric NLRP3 aggregation. This causes polymerisation of ASC and inflammasome formation, which leads to downstream signalling described in the previous section.

1.8. NLRC4

In contrast to NLRP3, NLRC4 (also known as IPAF) is not a direct sensor of PAMPs but acts as an adapter with NAIPs (neuronal apoptosis inhibitory protein) that serve as receptors for a variety of different bacterial components.

Among the seven NAIPs in mice, NAIP1 and NAIP2 detect components of the type III secretion system (T3SS), while NAIP5 and NAIP6 detect flagellin independent of TLR5 (*142, 160, 161*). The only human orthologue, hNAIP, detects both flagellin and T3SS proteins (*162, 163*).

NAIPs (NBD-domain-containing inhibitor of apoptosis proteins) are NLR proteins that contain baculoviral inhibitor of apoptosis protein repeat (BIR) domains at their N-termini. To date, the exact mechanism of ligand recognition remains unclear but is thought to involve interactions with the helical domains adjacent to the LRR. It was further suggested that, in contrast to Toll-like receptors, the LRR itself does not determine substrate specificity (*164*). More so, the expression of a truncated version lacking the C-terminus, but not full-length NLRC4, leads to spontaneous caspase-1 activation, suggesting a repressive role of the LRR (149). It is thought that NAIPs are released from an auto-inhibitory state upon ligand binding and allow interaction with NLRC4 (Figure 7C). This process then leads to a rotation of the LRR domain, causing the oligomerisation of 10-12 NLRC4 molecules in a disc-like structure (*165-167*). Instead of

a PYD domain, NLRC4 contains a CARD domain, which, upon oligomerisation, is capable of directly interacting with caspase-1, thus not requiring ASC for inflammasome assembly and downstream cell death. However, the production of IL-1β and IL-18 is dependent on ASC (*142, 168*).

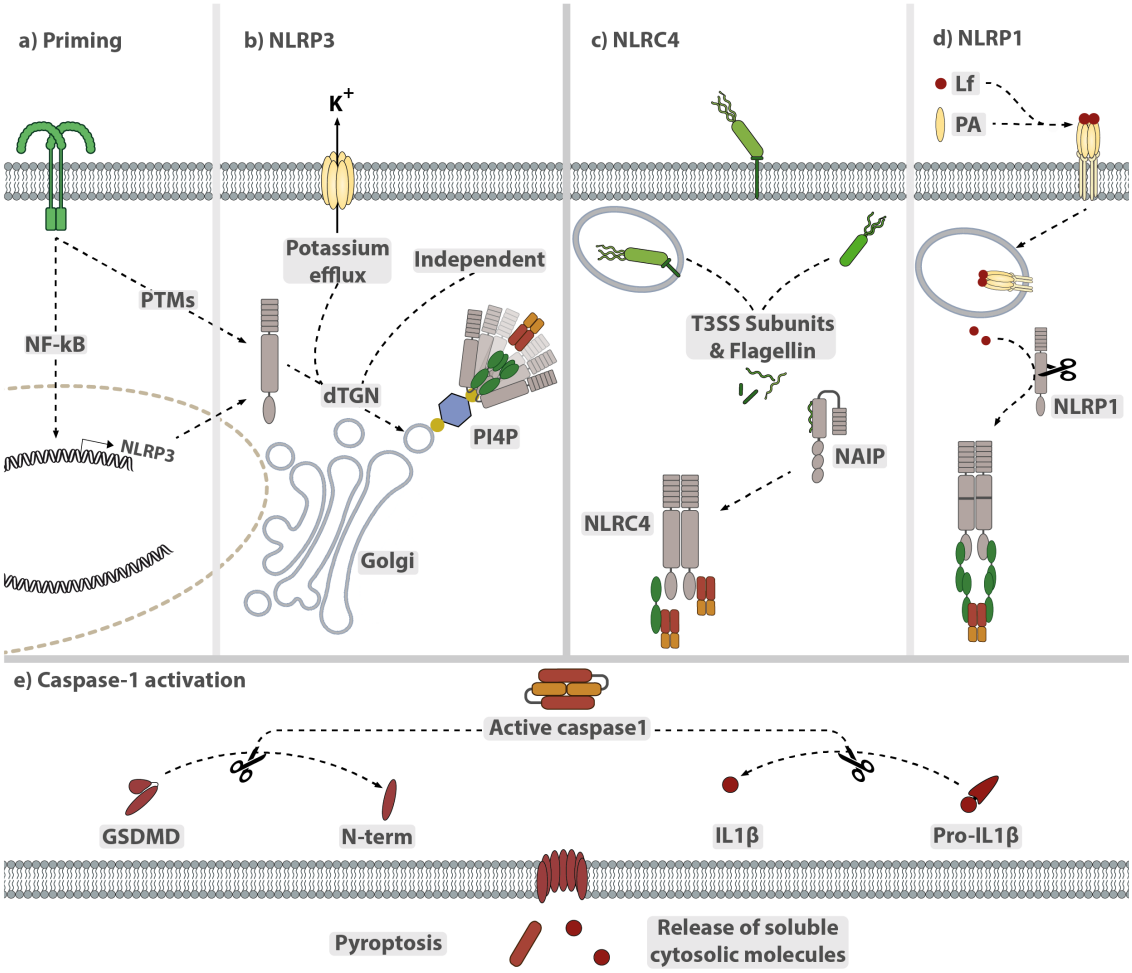

Figure 7 **Inflammasome dependent pyroptosis:** a) TLR dependent priming: NF-κB activation leads to transcriptional upregulation of Pro-IL-1β and NLRP3 and post-translational licensing of NLRP3. b) NLRP3 activation is mostly driven by stimuli leading to potassium efflux. These, as well as potassium-independent stimuli, can recruit NLRP3 to the dispersed TGN which serves as a scaffold for NLRP3 multimerisation. c) NAIP functions as a direct receptor for bacterial flagellin and the type 3 secretion system (T3SS) subunits. Binding results in NAIP activation, allowing it to recruit and activate NLRC4. d) Lethal factor (Lf) uptake is mediated via complex formation with protective antigen (PA) which binds to receptors on the cell leading to endocytic uptake. Internalised Lf leads to autolytic cleavage within the FIIND domain and removal of the auto-inhibitory PYD domain of NLRP1. E) Activation of the different receptors (b-d) leads to autoproteolytic activation of caspase-1, which can process pro-IL-1ß and GSDMD. The N-terminal fragment of GSDMD forms pores in the cell membrane driving pyroptosis. (Fig. adapted from (*159*))

NLRC4 expression was reported to be upregulated by pro-inflammatory stimuli such as TNFα, Type I interferons such as IRF8 as well as genotoxic stress-mediated P53 activation (*169-171*). However, numerous studies propose basal levels of NLRC4 to be sufficient for inflammasome signalling and suggest a regulation primarily at the post-transcriptional level (See chapter 1.9) (*172*). Activation of the NLRC4 in human cell-lines can be achieved using recombinant LFn-YscF protein (Needle Toxin protein). This protein contains the *Burkholderia* T3SS needle protein (YscF) that has been optimised to binding human NAIP and is fused to the anthrax lethal factor (LFn) transporter protein. LFn binds to Anthrax Protective Antigen (PA), which in turn binds to receptors on the cell surface (CMG2 or TEM8) leading to phosphorylation and ubiquitination events (*173-175*). These cause oligomerisation in lipid rafts and the internalisation of the receptor-toxin complex by endocytosis.

Bacillus anthracis, of which this cargo delivery system is derived, naturally encodes for anthrax toxin lethal factor (LF). LF is a metalloprotease that cleaves various host proteins (e.g. MAPKs) to subvert the innate immune response. At the same time, LF also cleaves murine NLRP1B in its N-region. This in turn results in the exposure of a neo N-terminus that is detected by the N-end rule machinery, which subjects this molecule to K48-linked ubiquitination. As a result of this process, NLRP1 gets degraded by the proteasome up to the pre-cleaved FIIND domain. This, in turn, liberates the C-terminal fragment that then oligomerises to form a seed-like signalosome, allowing the C-terminal CARD to trigger ASC filament formation (Figure 7D) (*176, 177*). This cleavage event is sufficient for Nlrp1b activation, emphasising the importance of post-translational modifications in inflammasome signalling, which will be discussed in the next section.

1.9. Control of inflammasome activation by post-translational modifications

As illustrated above, PTMs (post-translational modifications) are a central regulatory mechanism for inflammasome signalling. PTMs are covalent modifications of proteins to regulate their size, conformation, location, turnover and interaction with their target. Enzymes that catalyse these modifications can potentially be targeted pharmaceutically to fine-tune inflammatory signalling (*178, 179*).

The NF-κB pathway and its transcriptional regulation, as well as many NLRs, heavily rely on post-translational modifications throughout their signalling cascades. One PTM of particular importance in this context is ubiquitin modifications that can change activation states, lead to proteasomal degradation, and act as indispensable scaffolding for the signal components. Thus, tight regulation of the ubiquitin system, not only through ubiquitin ligases but also through deubiquitinases (DUBs), is critical. The DUBs A20 (*TNFAIP*) and CYLD negatively regulate NF-κB signalling by cleaving K63 linked polyubiquitin from RIPK1, TRAF2/6 and NEMO (*180, 181*). Notably, although A20 is characterised as a DUB, it can also add ubiquitin to its substrate proteins (*182*).

Besides the NF-κB priming step, the assembly and activation of inflammasomes are also directly controlled by PTMs. A variety of modifications of inflammasome components such as phosphorylation, ubiquitination, sumoylation and proteolytic processing are summarised in Figure 8.

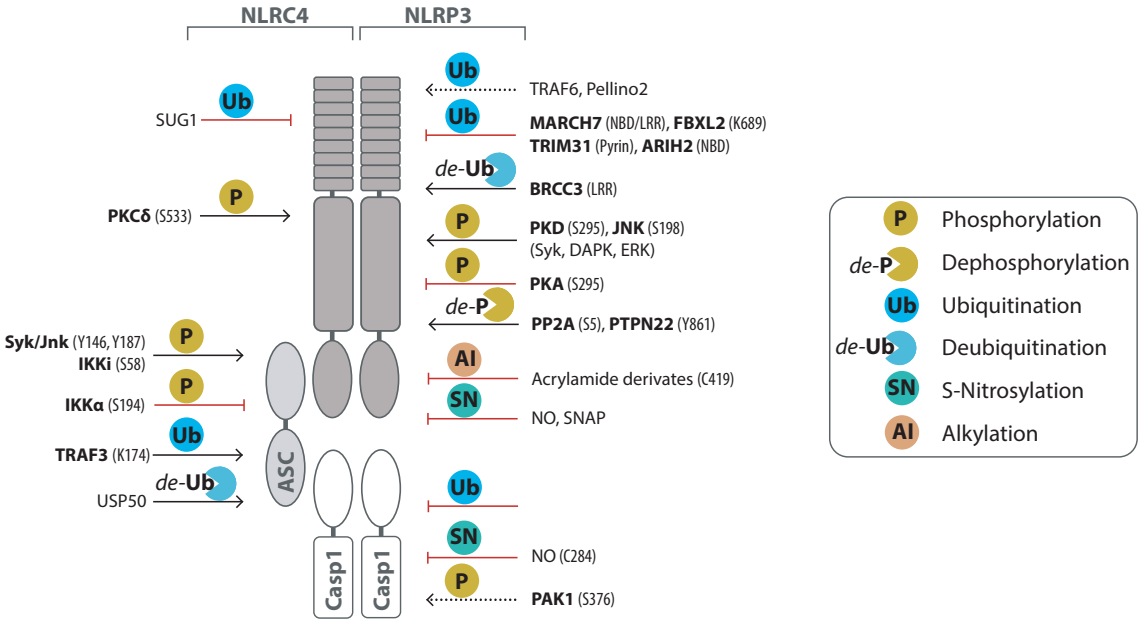

***Figure 8* Post-translational modifications (PTMs) regulate inflammasomes.** Schematic structure and PTMs on different inflammasome compartments. Modifying enzymes and target region are indicated. Modifications that promote activation are shown as black arrows, whereas those that suppress inflammasome activation are shown as red blocks. Modified from (*183, 184*).

Multiple E3 ligases have been shown to limit NLRP3 levels by targeting for proteasomal (TRIM3, FBXL2) or phagosomal (MARCH7) degradation. During priming, BRCC3, a Lys63-specific deubiquitinase is thought to remove ubiquitination, enabling a shift of NLRP3 from its inactive, monomeric state to an active form capable of multimerization. Recently, E3 ligases that positively regulate NLRP3 have also been discovered (Pellino2, TRAF6); however, their mechanism of NLRP3 activation still remains elusive.

Phosphorylation remains the most extensively studied PTM in inflammasome signalling, with over a dozen phosphorylation sites identified for NLRP3 alone (Table 5). Well-studied NLRP3 phosphorylation events include Ser198 by c-jun kinase (JNK) and Ser295 by protein kinase D (PKD) and protein kinase A (PKA). Phosphorylation by JNK1 was suggested to play a critical role in the deubiquitination of NLRP3 during priming, facilitating the molecular interaction of NLRP3 with BRCC3 (*185*).

The phosphorylation at Ser295 of NLRP3 has been extensively studied, with reports of both activation and inhibitory effects (*186, 187*).

cAMP-activated PKA was reported to directly interact with NLRP3 and drive the phosphorylation of Ser295, preventing inflammasome formation. In contrast, a different

study showed that in response to the inflammasome activators ATP and Nigericin, PKD was activated, leading to an activating phosphorylation of the same Ser295 site. It was proposed that this modification leads to the release of NLRP3 from Golgi-associated MAMs (Mitochondria-associated ER membranes) to the cytosol, where it assembled a fully mature inflammasome.

Human/Murine Residue	Effect of Phosphorylation	Kinase	Validation/Source
S5/S3	Inhibitory	*Unknown*	Yes (*188*)
Y13/Y11	*Unknown*	*Unknown*	Yes (*185*)
S161/S157	No effect	*Unknown*	Yes (*188*)
S163/D159	*Unknown*/No effect	*Unknown*	Yes (*185*)
S198/S194	Activation	JNK1	Yes (*185*)
T233/T229	*Unknown*	Unknown	No
S295/S291	Activating Inhibitory	PKD PKA	Yes (*186*) Yes (*187*)
S334/S330	No effect	*Unknown*	Yes (*185*)
S387/S383	*Unknown*	*Unknown*	No
S436/S432	*Unknown*	*Unknown*	No
S728/S725	*Unknown*	*Unknown*	No(*188*)
Y861/Y858	Inhibitory	*Unknown*	Yes (*189*)
S975/N972	No effect	*Unknown*	Yes (*185*)

Table 4 ***Phosphorylation Sites on NLRP3.*** *List of all phosphosites on NLRP3 published to date. Modified from (190).*

2. Aims of this work

As shown above, post-translational modifications play a significant role in inflammasome signalling. Nevertheless, the exact role and effects of PTMs are still poorly understood. In this study, we set out to analyse both the effect of ubiquitination and phosphorylation events in the context of different inflammasome signalling pathways.

Broadly, the objectives of the study were:

1. To determine the role of the deubiquitinase USP7 in NF-κB and inflammasome signalling.
2. To understand the NF-κB-independent role of the kinase IKKβ on NLRP3 signalling.

Aim 1 is relevant to Chapter 4, while aim 2 is explored in Chapter 5.

3. Materials and Methods

3.1. Materials

If materials or reagents are not listed in this section, the information on the origin or manufacturer can be found in the Methods section.

3.1.1. Consumables

The consumables for sterile and non-sterile laboratory work were purchased from the following manufacturers: Bioplastics, Bio-Rad, Biozym, Corning, Greiner, Labomedic, Neolab, Sarstedt and VWR.

Novex™ 8%/10%/12% Tris-Glycine Mini Gels, WedgeWell™ format, 12-well/15-well were obtained from Thermo Fisher Scientific

Whatman Cellulose Blotting Papers (Grade GB005) and Amersham Protran 0.45 NC nitrocellulose Western blotting membranes were obtained from GE Healthcare.

3.1.2. Chemicals and reagents

Chemical/reagent	**Supplier**
6x loading dye	Thermo Fisher Scientific
Acetic Acid	Carl Roth
Agarose ultrapure	Biozym
Ammonium acetate	Carl Roth
Ammonium persulfate	Carl Roth
BD Pharma Lyse™	BD Biosciences
Bromophenol blue	Carl Roth
ß-mercaptoethanol	Carl Roth
Bovine Serum Albumin	Carl Roth
$CaCl_2$	Carl Roth
Chloroform	Carl Roth
cOmplete™ Protease Inhibitor Cocktail	Roche
DMSO	Carl Roth
DNA Ladder	Fermentas
DNA stain G	Serva
dNTP-set	Genaxxon
Doxycycline hyclate	Sigma-Aldrich
DTT	Carl Roth

EDTA (0.5 M solution, pH = 8,0)	Life Technologies
EDTA (Sodium salt)	Carl Roth
Ethanol (ultra pure)	Carl Roth
Ethanol (denatured)	Carl Roth
Biocoll (density 1,077g/ml)	Merck Millipore
Gene Ruler 1kb and 100bp	Thermo Fisher Scientific
Glycerol	Carl Roth
Glycin	Carl Roth
Guanidinium chloride	Carl Roth
HEPES	Carl Roth
H_2O (sterile)	Braun
HCl	Carl Roth
Isopropanol	Carl Roth
Potassium acetate	Carl Roth
KCl	Carl Roth
LB	Carl Roth
LB agar	Carl Roth
Luminata Forte Western HRP substrate	Merck
Methanol	Carl Roth
$MgCl_2$	Carl Roth
Milk powder	Carl Roth
Na_2HPO_4	Carl Roth
Na_2Cl_2	Carl Roth
NaOH	Carl Roth
Nuclease-Free Water	Thermo Fisher Scientific
PageRuler™ Prestained Protein Ladder	Thermo Fisher Scientific
PhosSTOP™ Phosphatase Inhibitor	Roche
Pierce ECL WB substrate	Thermo Fisher Scientific
Ponceau S staining	Sigma-Albich
RNase A	Life Technologies
SDS	Carl Roth
Sodium acetate	Carl Roth
SYBR green	Thermo Fisher Scientific
Tetramethylethylenediamine	Carl Roth
TRIS-base	Carl Roth
TRIS-HCL	Carl Roth
Triton X-100	Carl Roth
Trypan blue	Thermo Fisher Scientific
Trypsin EDTA	Gibco
Tween 20	Carl Roth

3.1.3. Enzymes and enzyme buffers

Enzyme/buffer	**Supplier**
5x Phusion Hf/Gc Buffer	Thermo Fisher Scientific
10x Fastdigest Buffer	Thermo Fisher Scientific
10x Fastdigest Green Buffer	Thermo Fisher Scientific

DNase I	Thermo Fisher Scientific
FastAP (Alkalische Phosphatase)	Thermo Fisher Scientific
Fastdigest Restriction Enzymes	Thermo Fisher Scientific
NEB2 Buffer	NEB
Phusion high-fidelity DNA polymerase (2 u/µl)	Thermo Fisher Scientific
Powerup Sybr Master Mix	Thermo Fisher Scientific
Proteinase K	VWR
Revertaid Reverse Transcriptase 200 U/µl	Thermo Fisher Scientific
Ribolock Rnase Inhibitor (40 U/µl)	Thermo Fisher Scientific
T4 DNA Ligase and buffer	Fisher Scientific
T4 DNA polymerase	Enzymatics
Gibson Master Mix	Inhouse

3.1.4. Kits

Kit	**Supplier**
BCA Protein Assay Kit (Pierce™)	Thermo Fisher Scientific
ELISA kits (hIL-1, hIL-6, hTNF, mIL-1, mIL-6)	BD Biosciences
ELISA kit (hIL-18)	R&D Systems
ECL Western Blot substrate (Pierce™)	Thermo Fisher Scientific
Lineage Cell Depletion Kit	Milteny
LDH cytotoxicity assay kit (Pierce™)	Thermo Fisher Scientific
MiSeq Reagent Kit v2 (300 cycle)	Illumina
PureLink® HiPure Plasmid Filter Maxiprep Kit	Invitrogen™
QIAquick Gel Extraction Kit	Qiagen
QIAquick PCR purification Kit	Qiagen
RNeasy mini kit	Qiagen

3.1.5. Buffers and solutions

Buffer/Solution	**Components**
10X PBS	800g NaCl 20g KCl 142g Na_2HPO_4 add water to 10 L, pH 7.4
10X TBS	240 g Tris 880 g NaCl dissolved in 900 ml water Add water to final volume 10 L, pH 7.6
10X Tris-glycine buffer	290g Tris 1440g Glycine Add water to final volume 10 L
10X SDS Running buffer	290g Tris 1440g Glycine 100g SDS Add water to final volume 10 L
2X Laemmli Sample buffer	150 mM Tris-HCl pH 6.8

	200 mM DTT 4% SDS 20% Glycerol 0.01% Bromophenol Blue Add water to final volume 100 ml
6X Laemmli Sample buffer	450 mM Tris-HCl pH 6.8 600 mM DTT 12% SDS 60% Glycerol 0.03% Bromophenol Blue Add water to final volume 100 ml
50X TAE Buffer	242g Tris 57.1 ml Acetic acid 18.6g EDTA Add water to final volume 1L
Direct Lysis Buffer	0.2 mg/ml Proteinase K 1 mM $CaCl_2$ 3 mM $MgCl_2$ 1 mM EDTA 1 % Triton X-100 10 mM Tris pH 7.5
LB Agar	20 g LB 15 g Agar 1 L H_2O Autoclaved before use
LB medium	20 g LB 1 l H2O Autoclaved before use
MACS buffer	2mM EDTA 2% FCS in PBS
Miniprep buffer N3	4.2 M Guanidine hydrochloride 0.9 M Potassium acetate pH = 4.8
Miniprep buffer P1	50 mM Tris pH = 8.0 10 mM EDTA 100 µg/ml RNase A
Miniprep buffer P2	200 mM NaOH 1 % SDS
Miniprep buffer PE	10 mM Tris pH = 7.5 80 % ethanol
PBST	1L 10X PBS 9L Water 5 ml Tween-20
RLT buffer	4.5 M Guanidine hydrochloride 50mM Tris-HCl pH 6.6 2% TritonX-100
SDC Lysis buffer	1% SDC 100mM Tris pH 8.5

TBST	1 L 10X TBS 9 L Water 5 ml Tween-20
Western Blot transfer buffer	200 ml 10X Tris-Glycine buffer 400 ml Ethanol 1400 ml water

3.1.6. Cell culture reagents

Reagent	**Supplier**
Amino Acid Mixture (Complete)	Promega
β-estradiol	Sigma-Aldrich
BAY 11-7082 (IKKB inhibitor)	MedChemTronica
Blasticidin S HCl (10 mg/ml)	Thermo Fischer Scientific
DB2313 (PU.1 inhibitor)	Aobious
DMEM with glutamine	Gibco
CLI095	Invivogen
Cycloheximide	Carl Roth
Doxycycline hyclate	Sigma-Adrich
Fetal cow serum (FCS)	Gibco
GeneJuice	Merck
HEPES	Gibco
hIL-3	PeproTech
hM-CSF	PeproTech
Imiquimod	InvivoGen
L18-MDP	InvivoGen
LF-YscF	Own production
Lipofectamine-2000	Life technology
LPS-EB Ultrapure	Invivogen
MCC950 (CRID3)	Tocris bioscience
MG-132	Selleckchem
Nigericin	InvivoGen
Pam3CSK4	InvivoGen
Penicillin/Streptomycin	Gibco
Phorbol 12-myristate 13-acetate	ENZO Life Sciences
Protective antigen (pA)	Biotrend
Puromycin dihydrochloride	Carl Roth
R848	InvivoGen
RPMI with glutamine	Gibco
SP600125 (JNK inhibitor)	Cell signalling technologies
Sodium pyruvate	Gibco
Staurosporine	Santa Cruz
Takinib	Selleck Chemicals
TPCA-1 (IKKB inhibitor)	R&D Systems
Z-VAD-FMK	Peptanova
Z-YVAD-FMK	R&D Systems

3.1.7. Antibodies

Antibody	Supplier	Dilution
Anti-Caspase-1 (p20) (human), mAb (Bally-1)	AdipoGen	1:1000
Anti-Caspase-1 (p20) (mouse), mAb (Casper-1)	AdipoGen	1:1000
Anti-NLRP3/NALP3, mAb (Cryo2)	AdipoGen	1:1000
NLRC4	Cell Signaling Technology	1:500
Ubiquitin (P4D1)	Santa Cruz	1:1000
Rip2 (D10B11)	Cell Signaling Technology	1:1000
Anti-IL1 beta/IL-1F2 (human)	R&D Systems	1:500
Anti-ASC	Santa Cruz	1:500
Anti-GAPDH (D16H11) HRP	Cell Signaling Technology	1:2000
Anti-USP7	Biomol	1:1000
Anti-p53	Santa Cruz	1:500
Anti-IKKβ	Cell Signaling Technology	1:1000
Anti- IκBa (L35A5)	Cell Signaling Technology	1:1000
Anti-Phospho-iκBa	Cell Signaling Technology	1:1000
Anti-Phospho-NF-κB-P65 (Ser536)	Cell Signaling Technology	1:1000
Anti-FLAG® M2 HRP	Sigma-Aldrich	1:1000
Anti-goat IgG HRP	Santa Cruz	1:3000
Anti-mouse IgG HRP	Santa Cruz	1:3000
Anti-rabbit IgG HRP	Santa Cruz	1:3000
Anti-actin-HRP	Santa Cruz	1.2000

3.1.8. Plasmids

Plasmid	Usage	Source
pCMV-Gag-Pol	Retrovirus generation	AG Hornung
pCMV-VSVG	Lentivirus/ Retrovirus generation	AG Hornung
pFUGW_ev (empty vector)	Cloning	AG Hornung
pLI_mCherry	Transduction	AG Hornung
pLI_hNLRP3	Transduction	This study
pFUGW_NLRP3	Transduction	This study
pLI_ev (empty vector)	Cloning	AG Hornung
pMini_U6_gRNA_CMV_BFP_T2A_Cas9	KO generation	AG Hornung
pMini_U6_gRNA_CMV_mCherry_T2A_Cas9	KO generation	AG Hornung
pRP_ev (empty vector)	Cloning	AG Hornung
pRP_mCherry	Transduction	AG Hornung
pRZ_Cas9_BFP	KO generation	AG Hornung
pRZ_Cas9_mCherry	KO generation	AG Hornung
pMDLg/pRRE	Lentivirus generation	AG Hornung
pRSV-REV	Lentivirus generation	AG Hornung
LentiCas9-Blast	KO generation	Addgene #52962
LentiGUIDE-Puro	KO generation	Addgene #52963

pcDNA3.1_IKKβ	Cloning	Addgene #23298
pcDNA3.1_ IKKβ S177E	Cloning	This study
pFBD-LFn-YscF	Protein production / Cloning	R. Vance, UC Berkeley
pLI_ IKKβ	Transduction	This study
pLI_ IKKβ S177E	Transduction	This study
pRP_huNLRP3-flag, S161A	Transduction	This study
pRP_huNLRP3-flag, S163A	Transduction	This study
pRP_huNLRP3-flag, S161A, S163A	Transduction	This study
pLI_LFn-YscF	Transduction	This study

3.1.9. Primers and other oligonucleotides

DNA oligonucleotides were synthesized by Integrated DNA Technologies (IDT).

Primer	**Sequence**	**Usage**
CHUK_miseq_fwd	*ACACTCTTTCCCTACACGACGCTCTTCCGATCTGC AAAGACACCAAAGCTCAAGGA*	Genotyping (PCR1)
CHUK_miseq_rev	*TGACTGGAGTTCAGACGTGTGCTCTTCCGATCTG AGCATCAGAGTAGATTTGTACA*	Genotyping (PCR1)
IKBKB_miseq_fwd	*ACACTCTTTCCCTACACGACGCTCTTCCGATCTTTC AGGGGCATGCGGCATTTATC*	Genotyping (PCR1)
IKBKB_miseq_rev	*TGACTGGAGTTCAGACGTGTGCTCTTCCGATCTAT GCAGAGTGTGCTCCTTTCCTC*	Genotyping (PCR1)
IRF1_miseq_fwd	ACACTCTTTCCCTACACGACGctcttccgatctTTGTAGCC CATGCCAAGGATGAC	Genotyping (PCR1)
IRF1_miseq_rev	TGACTGGAGTTCAGACGTGTGctcttccgatctCATGAAT GTTTTGCAAGGGATAG	Genotyping (PCR1)
IRF3_miseq_fwd	ACACTCTTTCCCTACACGACGctcttccgatctCTGGTCCA TATGAAGTCTCCAGA	Genotyping (PCR1)
IRF3_miseq_rev	TGACTGGAGTTCAGACGTGTGctcttccgatctCAACAGC CGCTTCAGTGGGTTCT	Genotyping (PCR1)
IRF4_miseq_fwd	ACACTCTTTCCCTACACGACGctcttccgatctTTGTAGTC CTGCTTGCCCGCGTG	Genotyping (PCR1)
IRF4_miseq_rev	TGACTGGAGTTCAGACGTGTGctcttccgatctAGCTCTTC TCCCCGCAGTGCAGA	Genotyping (PCR1)
IRF5_miseq_fwd	ACACTCTTTCCCTACACGACGctcttccgatctGTTCTCTGT GGTCGGCTATTTC	Genotyping (PCR1)
IRF5_miseq_rev	TGACTGGAGTTCAGACGTGTGctcttccgatctCCTCGTA GATCTTGTAGGGCTG	Genotyping (PCR1)
IRF7_miseq_fwd	ACACTCTTTCCCTACACGACGctcttccgatctTGCTTCCA GGGCACGCGGAAACA	Genotyping (PCR1)

IRF7_miseq_rev	TGACTGGAGTTCAGACGTGTGctcttccgatctTAACACC TGACCGCCACCTAACT	Genotyping (PCR1)
IRF8_miseq_fwd	*ACACTCTTTCCCTACACGACGCTCTTCCGATCTAA AGGAGACACTGTGCCCACAGT*	Genotyping (PCR1)
IRF8_miseq_rev	*TGACTGGAGTTCAGACGTGTGCTCTTCCGATCTCT GTCTTTCCAAGGATGTGTGAC*	Genotyping (PCR1)
JUN_ miseq _fwd	*ACACTCTTTCCCTACACGACGCTCTTCCGATCTCCT TCTATGACGATGCCCTCAAC*	Genotyping (PCR1)
JUN_ miseq _rev	*TGACTGGAGTTCAGACGTGTGCTCTTCCGATCTCC CGTTGCTGGACTGGATTATCA*	Genotyping (PCR1)
JNK1_ miseq _fwd	*ACACTCTTTCCCTACACGACGctcttccgatctTTGTA GCCCATGCCAAGGATGAC*	Genotyping (PCR1)
JNK1_ miseq _fwd	*TGACTGGAGTTCAGACGTGTGctcttccgatctCATG AATGTTTTGCAAGGGATAG*	Genotyping (PCR1)
YY2_miseq_fwd	*ACACTCTTTCCCTACACGACGCTCTTCCGATCTACC ATCAATGGCGGATGGTTGTG*	Genotyping (PCR1)
YY2_miseq_rev	*TGACTGGAGTTCAGACGTGTGCTCTTCCGATCTC ACTCCCCTCAGCGTTCTTTTTC*	Genotyping (PCR1)
STAT5A_miseq_fwd	*ACACTCTTTCCCTACACGACGCTCTTCCGATCTTCA TCGTGTGTCTGTCCCTGTGT*	Genotyping (PCR1)
STAT5A_miseq_rev	*TGACTGGAGTTCAGACGTGTGCTCTTCCGATCTC ACAATTACTTGCGGGTGTTCTC*	Genotyping (PCR1)
MAF_miseq_fwd	*ACACTCTTTCCCTACACGACGCTCTTCCGATCTAG TCCCCTGGCCATGGAATATGT*	Genotyping (PCR1)
MAF _miseq_rev	*TGACTGGAGTTCAGACGTGTGCTCTTCCGATCTG TAGCCGGTCATCCAGTAGTAGT*	Genotyping (PCR1)
IKBKE_miseq_fwd	*ACACTCTTTCCCTACACGACGCTCTTCCGATCTCC GAGACGAACTTCTCATCATCA*	Genotyping (PCR1)
IKBKE_miseq_rev	*TGACTGGAGTTCAGACGTGTGCTCTTCCGATCTG AACTCCTGTCTCTCTGGATGCA*	Genotyping (PCR1)
MAP3K7_miseq_ fwd	*ACACTCTTTCCCTACACGACGCTCTTCCGATCTGT GCTTGCATTCACATTGTGTCT*	Genotyping (PCR1)
MAP3K7_miseq_ rev	*TGACTGGAGTTCAGACGTGTGCTCTTCCGATCTG TGAGAGTGAGAGAGAAGGAGGA*	Genotyping (PCR1)
NLRP3_miseq_fwd	*ACACTCTTTCCCTACACGACGCTCTTCCGATCTCCA CTTCGGCTCATCTCTTTTTG*	Genotyping (PCR1)
NLRP3_miseq_rev	*TGACTGGAGTTCAGACGTGTGCTCTTCCGATCTA CCTGGAGGATGTGGACTTGAAG*	Genotyping (PCR1)
NLRC4_miseq_fwd	*ACACTCTTTCCCTACACGACGCTCTTCCGATCTAT GGCAATTCGCTGCAGCAGAGT*	Genotyping (PCR1)
NLRC4_miseq_rev	*TGACTGGAGTTCAGACGTGTGCTCTTCCGATCTA GGACTTGTACCATACCCCATCT*	Genotyping (PCR1)
RELA_miseq_fwd	*ACACTCTTTCCCTACACGACGCTCTTCCGATCTTA ATGGGGCTGCGGTGTCCCCTG*	Genotyping (PCR1)
RELA _miseq_rev	*TGACTGGAGTTCAGACGTGTGCTCTTCCGATCTC AGACATCCAAACCTGACTCCCA*	Genotyping (PCR1)
RELB_miseq_fwd	*ACACTCTTTCCCTACACGACGCTCTTCCGATCTGT GGGGCTTCCTTGGGATATTCT*	Genotyping (PCR1)

RELB _miseq_rev	*TGACTGGAGTTCAGACGTGTGCTCTTCCGATCTT GTCAGGAGAAAGCTGAGGTGGA*	Genotyping (PCR1)
USP7_miseq_fwd	*ACACTCTTTCCCTACACGACGCTCTTCCGATCTTCA GATTCAGCATTGCACTGGAG*	Genotyping (PCR1)
USP7_miseq_rev	*TGACTGGAGTTCAGACGTGTGCTCTTCCGATCTA GGCTCTGTGACTGATGATGTGT*	Genotyping (PCR1)
TP53_miseq_fwd	*ACACTCTTTCCCTACACGACGCTCTTCCGATCTTG CAGCTGTGGGTTGATTCCACA*	Genotyping (PCR1)
TP53_miseq_rev	*TGACTGGAGTTCAGACGTGTGCTCTTCCGATCTCT CCACACGCAAATTTCCTTCCA*	Genotyping (PCR1)
LIColigo20mer	*GGAAAGGACGAAACACCGNNNNNNNNNNNNN NNNNNNGTTTTAGAGCTAGAAATAGCAAGTTAA AATAAGG*	LIC cloning
LIColigo18mer	*GGAAAGGACGAAACACCGNNNNNNNNNNNNN NNNNGTTTTAGAGCTAGAAATAGCAAGTTAAAA TAAGG*	LIC cloning
LICsgRNA_rev	*AACGGACTAGCCTTATTTTAACTTGCTATTTCTAG CTCTAAAAC*	LIC cloning
Illu fwd 1	*AATGATACGGCGACCACCGAGATCTACACTATAG CCTACACTCTTTCCCTACACGACGCT*	Genotyping (PCR2)
Illu fwd 2	*AATGATACGGCGACCACCGAGATCTACACATAGA GGCACACTCTTTCCCTACACGACGCT*	Genotyping (PCR2)
Illu fwd 3	*AATGATACGGCGACCACCGAGATCTACACCCTAT CCTACACTCTTTCCCTACACGACGCT*	Genotyping (PCR2)
Illu fwd 4	*AATGATACGGCGACCACCGAGATCTACACGGCTC TGAACACTCTTTCCCTACACGACGCT*	Genotyping (PCR2)
Illu fwd 5	*AATGATACGGCGACCACCGAGATCTACACAGGC GAAGACACTCTTTCCCTACACGACGCT*	Genotyping (PCR2)
Illu fwd 6	*AATGATACGGCGACCACCGAGATCTACACTAATC TTAACACTCTTTCCCTACACGACGCT*	Genotyping (PCR2)
Illu fwd 7	*AATGATACGGCGACCACCGAGATCTACACCAGGA CGTACACTCTTTCCCTACACGACGCT*	Genotyping (PCR2)
Illu fwd 8	*AATGATACGGCGACCACCGAGATCTACACGTACT GACACACTCTTTCCCTACACGACGCT*	Genotyping (PCR2)
Illu rev 1	*CAAGCAGAAGACGGCATACGAGATCGAGTAATG TGACTGGAGTTCAGACGTGTGCT*	Genotyping (PCR2)
Illu rev 2	*CAAGCAGAAGACGGCATACGAGATTCTCCGGAG TGACTGGAGTTCAGACGTGTGCT*	Genotyping (PCR2)
Illu rev 3	*CAAGCAGAAGACGGCATACGAGATAATGAGCGG TGACTGGAGTTCAGACGTGTGCT*	Genotyping (PCR2)
Illu rev 4	*CAAGCAGAAGACGGCATACGAGATGGAATCTCG TGACTGGAGTTCAGACGTGTGCT*	Genotyping (PCR2)
Illu rev 5	*CAAGCAGAAGACGGCATACGAGATTTCTGAATGT GACTGGAGTTCAGACGTGTGCT*	Genotyping (PCR2)
Illu rev 6	*CAAGCAGAAGACGGCATACGAGATACGAATTCG TGACTGGAGTTCAGACGTGTGCT*	Genotyping (PCR2)
Illu rev 7	*CAAGCAGAAGACGGCATACGAGATAGCTTCAGG TGACTGGAGTTCAGACGTGTGCT*	Genotyping (PCR2)

Illu rev 8	*CAAGCAGAAGACGGCATACGAGATGCGCATTAG TGACTGGAGTTCAGACGTGTGCT*	Genotyping (PCR2)
Illu rev 9	*CAAGCAGAAGACGGCATACGAGATCATAGCCGG TGACTGGAGTTCAGACGTGTGCT*	Genotyping (PCR2)
Illu rev 10	*CAAGCAGAAGACGGCATACGAGATTTCGCGGAG TGACTGGAGTTCAGACGTGTGCT*	Genotyping (PCR2)
Illu rev 11	*CAAGCAGAAGACGGCATACGAGATGCGCGAGAG TGACTGGAGTTCAGACGTGTGCT*	Genotyping (PCR2)
Illu rev 12	*CAAGCAGAAGACGGCATACGAGATCTATCGCTGT GACTGGAGTTCAGACGTGTGCT*	Genotyping (PCR2)
NLRP3_S161A_S163A_fwd	*GTCTGGGTGAGGCTGTGGCACTCAACAAACGCTA CACACGACTGCGT*	Mutagenesis
NLRP3_S161A_S163A_rev	*CGTTTGTTGAGTGCCACAGCCTCACCCAGACGGG CAT*	Mutagenesis
NLRP3_S161A_fwd	*GTCTGGGTGAGGCTGTGAGCCTCAACAAACGC*	Mutagenesis
NLRP3_S161A_rew	*CGTTTGTTGAGGCTCACAGCCTCACCCAGACGGG CAT*	Mutagenesis
NLRP3_S163A_fwd	*AGAGTGTGGCACTCAACAAACGCTACACACGACT GCGT*	Mutagenesis
NLRP3_S163A_rew	*CGTTTGTTGAGTGCCACACTCTCACCCAGACGGG CAT*	Mutagenesis
Gibson_NLRP3_pRP_fwd	*ACCGGGACCGATCCAGCCTCCGCGGCCCCAATTA GCTAGCATGAAGATGGCAAGC*	Cloning
Gibson_NLRP3_pRP_rew	*TCCATGCCTTGCAAAATGGCGTTACTTAAGATTA GGATCCCTACTTGTCATCGTCAT*	Cloning
LFn-YscF_fwd	*CCGTCCCACCATCGG*	Cloning
LFn-YscF-NHEI_rew	*ATGATGCTAGCAAGATACATTGATGAGTTTGGAC AA*	Cloning
BclI_IKKβ	*ATGTGATCAGGTCGAGTCCCCCCACA*	Cloning
Nhe_Flag_IKKβ	*ATGGCTAGCTGAACCGTCAGAATTGATCTACCAT G*	Cloning
IL1B_fwd	*CGAGGCACAAGGCACAAC*	qPCR
IL1B_ rew	*CTGTTTAGGGCCATCAGCTTC*	qPCR
IL6_fwd	*AGTGAGGAACAAGCCAGAGC*	qPCR
IL6_ rew	*TGAGATGAGTTGTCATGTCCTG*	qPCR
NLRC4_set1_fwd	*TCAGAAGGAGACTTGGACGAT*	qPCR
NLRC4_set1_rew	*GGAGGCCATTCAGGGTCAG*	qPCR
NLRC4_set2_fwd	*TGCATCATTGAAGGGGAATCTG*	qPCR
NLRC4_set2_rew	*GATTGTGCCAGGTATATCCAGG*	qPCR
GAPDH_fwd	*CTTTGTCAAGCTCATTTCCTGG*	qPCR
GAPDH_rew	*TCTTCCTCTTGTGCTCTTGC*	qPCR

3.1.10. sgRNAs

sgRNAs oligos consist of flanking sequence necessary for LIC cloning: 5'-GGAAAGGACGAAACACCG-3 ', followed by the specific target site (Protospacer without PAM), followed by 5' GTTTAGAGCTAGAAATAGCAAGTTAAAATAAGG-3' as second flanking sequence. The PAM sequence is highlighted in bold.

Target Gene	**Proteospacer**
IRF1	CTCATGCGCATCCGAGTGAT**GGG**
IRF3	GGGGTCCCGGATCTGGGAGT**GGG**
IRF4	CTGATCGACCAGATCGACAG**CGG**
IRF5	ATGAAGCCGATCCGGCCAAG**TGG**
IRF7	GCAGCCCCACGCGTGCTGTT**CGG**
IRF8	AGAGCATGTTCCGGATCCCT**TGG**
TP53	GCACAAAACACGGAGGGCTA**AGG**
USP7	GAGCGCTGCTCAGATAGCGA**TGG**
RelA	GCGCTTCCGCTACAAGTGCG**AGG**
RelB	GGAAACGGCGAGCGAGAGTG**AGG**
NLRP3	GCTAATGATCGACTTCAATG**GGG**
NLRC4	GGACCAACACCATCACCGCG**TGG**
MYD88	GCTGCAGGAGGTCCCGGCGC**GGG**
TRIF	GGCCCGCTTGTACCACCTGC**TGG**
TBK1	TTCAGATTCTGGTAGTCCAT**AGG**
IKBKE	GCATCGCGACATCAAGCC**GGG**
MAP3K7	GTAAACACCAACTCATTGCG**TGG**
CHUK	TAGTTTAGTAGTAGAACCCA**TGG**
IKBKB	GAAGGTATCTAAGCGCAG**AGG**
YY2	GGAGCTCCACGACATCAATG**TGG**
STAT5A	GCCACCGTACGCCTGCTGGT**GGG**
MAF	GTGCGGCCGTCTCATCGCCG**GGG**
SPI1	TTGGTATAGATCCGTGTCAT**AGG**
TBK1	TTCAGATTCTGGTAGTCCAT**AGG**
JUN	GGCTCCCCACTGGGTCGGCC**AGG**
JNK1	GAAGATTCTTGACTTCGGTC**TGG**
FOS	GGGCTCGCCTGTCAACGCGC**AGG**
SYK	GCGCCAGAGCCGCAACTACC**TGG**

3.1.11. Laboratory equipment and instruments

Sequence	**Usage**
Biomek® FXp liquid handler	Beckman Coulter
C1000 Touch Thermal Cycler	Bio-Rad
CFX384 Touch Real-Time PCR Detection System	Bio-Rad
Centrifuge 5430	Eppendorf
Centrifuge 5810	Eppendorf
Epoch Microplate Spectrophotometer	BioTek

Fusion SL	Vilber Lourmat (PEQLAB)
Gene Pulser Xcel	Bio-Rad
HydroSpeed™ Microplate Washer	TECAN
MACS-Separators	Miltenyi Biotec
Microscopes	Leica
Mini Gel Tank	Thermo Fisher Scientific
Mini Trans-Blot®	Bio-Rad
NanoDrop™	Thermo Fisher Scientific
Optima XPN-80 Ultracentrifuge	Beckman Coulter
SH800Z Cell Sorter	Sony
Spark® 20m multimode Reader	Tecan
TC-20™ Automated Cell Counter	Bio-Rad
Thermomixer® C	Eppendorf

3.2. Molecular biology methods

3.2.1. Production of competent *E. coli* bacteria

DH5a chemically competent bacteria were generated according to the protocol described in the brochure “Subcloning Notebooks” (Promega).

3.2.2. Restriction cloning

The desired DNA insert was either directly cut out of the original plasmid with suitable restriction enzymes or first amplified by PCR, whereby the corresponding restriction sites were added via primers and digested after purification using PCR purification columns with appropriate restriction enzyme. Tags or modifications were added in the PCR step by the use of modified primers wherever necessary. The target plasmid was digested with compatible restriction enzymes and dephosphorylated using FastAP (Fast alkaline phosphatase, Fermentas) according to the manufacturer´s instructions. Both DNA preparations were purified by agarose gel electrophoresis. For the ligation, 100 ng of the linearized vector was mixed with a 3-fold molar excess of insert DNA.

Ligation occurred using 1 µl of T4 DNA ligase (Promega) and suitable buffers in a final volume of 10 µl according to the manufacturer's instructions. The ligation mixture was

incubated at 16°C overnight. The product of the ligation was subsequently transformed into competent bacteria (DH5α *E. coli*).

3.2.3. Gibson cloning

For sequence independent cloning, Gibson assembly was employed. The master mix containing the 5´exonuclease, DNA polymerase and DNA ligase was produced inhouse. While the target plasmid was linearized as described in 2.2.2., insert DNA were amplified using primers designed with the Snapgene® Gibson Assembly primer design tool generating overlapping ends. Both DNA preparations were purified by agarose gel electrophoresis. For the ligation, 75 ng digested vector mixed with a 3-fold molar excess of insert DNA was added to 15 µl of Gibson master mix and filled up to 20 µl with H_2O. The mixture was incubated for one hour at 50 °C. The product of the ligation was subsequently transformed into competent bacteria (DH5α *E. coli*).

3.2.4. Production of sgRNA expression plasmids by LIC

If possible, plasmids expressing sgRNA targeting the gene of interest were obtained directly from the laboratory's sgRNA library (*191*). If no sgRNA was available in the library, the existing sgRNA was inactive or did not cover all the isoforms of the gene, an expression construct was designed and cloned *de novo*. To do so, synthesized DNA oligos (IDT- Integrated DNA Technologies) were cloned into prepared target vectors using LIC (ligation independent cloning) (*191*). sgRNAs were designed with the public sgRNA finder CHOPCHOP (https://chopchop.rc.fas.harvard.edu/) (*192, 193*). sgRNAs targeting early coding exons and all splice variants were preferred. For the LIC procedure, 10 µl of the sgRNA target vector (200ng/µl in H_2O) were digested with ApaI and SpeI and purified via agarose gel. To generate long overhangs the vector was digested with T4 DNA-Polymerase in the presence of dTTP:

10x NEB2 buffer	10 µL
Vector (70 ng/µl)	10 µL
BSA (10 mg/ml)	1 µL
dTTP (100 mM)	1 µL
H_2O	74.66 µl
T4 DNA-Polymerase (3 U/µl)	3.33 µl

The reaction mix was incubated for five minutes at 27 °C and inactivated for 20 minutes at 75 °C. The vector was then mixed with the universal reverse oligonucleotide LICsgRNA_rev (PAGE purified):

20 µl	10x NEB2 buffer
10 µl	Chewed Vector
0.5 µl	LICsgRNA_rev
69.5 µl	H_2O

The LIC target vector obtained this way was stored at 4 °C and used for LIC cloning by mixing 2.5 µl of the vector mix with 2.5 µl of a 0.25 µM solution of the specific sgRNA oligonucleotide. Hybridization occurred under the following conditions:

70 °C	1 min
65 °C	1 min
60 °C	30 min
55 °C	2.5 min
29 Cycles, Δ = -1 °C per cycle	

Finally, the hybridization mix was used to transform competent E.coli. Colonies bearing the vector were validated via Sanger sequencing and expanded for plasmid DNA isolation.

3.2.5. Transformation of *E. coli*

Chemically competent *E. coli* DH5a were used for transformation according to the following protocol: 50 µL of bacteria suspension were thawed on ice, mixed with the DNA and incubated on ice for 10 minutes. After a heat shock at 42 °C for 45 seconds, bacteria were incubated 5 minutes on ice, topped up with approximately 1ml of LB medium and shaken for 30-60 minutes at 32 °C. Finally, bacteria were plated on LB- agar plates containing 100 µg/ml ampicillin (Roth) and incubated at 32 °C overnight. Single colonies were inoculated in LB liquid cultures (100 µg/ml ampicillin) and incubated at 37 °C for between 8 and 16 h.

3.2.6. Isolation of plasmid DNA from bacteria cultures

Plasmid DNA was isolated according to the protocol from QIAprep Spin Miniprep Kits (Qiagen) using buffers prepared in-house and EconoSpin columns (Epoch Life Science).

Correct sequence of the insert was confirmed by Sanger sequencing (performed by Eurofins) and/or appropriate restriction digestion. If higher yields were required, larger overnight cultures were prepared and plasmid DNA was isolated with commercial midi-prep or maxi-prep kits (Life Technologies).

3.2.7. RNA isolation and c-DNA Synthesis

For the isolation of RNA monocyte cell culture cells, 300.000 cells per analysis condition were lysed in 60 µl RLT buffer (RLT + 40 mM DTT) and stored at -80 °C until further processing. The lysate was thawed on ice and protein digestion was performed at 50 °C for 10 min followed by an inactivation step at 80 °C for 10 min. Nucleic acids were isolated from the lysate using magnetic beads. For this purpose, 2 volume pooling beads (30 % PEG) were added to the lysate and incubated for 5 min at room temperature. After magnetic separation the supernatant was removed and washed 3 times with 180 µl ethanol (80 % in nuclease-free water). After the final washing step, the pellet was dried at RT. Purified nucleic acids were eluted with 15 µl nuclease-free water and adjusted to 100 ng/µl.

DNA was digested by adding 1 µL of DNase I (Thermo Fisher Scientific) and 1 µL of 10x DNase I buffer to 8 µL of eluate and incubation at 37 °C for 30 min. Subsequently 1 µL of 25 mM EDTA was added and DNaseI was inactivated by incubation at 70 °C for 10 min. DNaseI-treated RNA samples were reverse transcribed using the RevertAid First Strand cDNA synthesis kit (Thermo Fisher Scientific) with oligoDT primers according to the manufacturer's protocol:

RT-Puffer	2.1 µL
dNTPs	1 µL
oligoDT-Primer	0.25 µL
RevertAid	0.25 µL
Ribolock	0.25 µL
H_2O	1.15 µl

The reverse transcription mix incubated at 42 °C for one hour. Enzyme was inactivated by final incubation at 70°C for 10 min.

3.2.8. PCR

For polymerase chain reactions (PCR) for genotyping of gene-deficient cell clones and for cloning, Phusion polymerase (Thermo Scientific) was used according to the manufacturer's specifications. In case of amplification from cDNA, 10 µl of cDNA was used for a 50 µl PCR reaction, while plasmid DNA was used in the final amount of 10 ng/reaction. The optimal annealing temperature for primer pairs was assessed by the TM-calculator tool (New England Biolabs*)*. Generated PCR products were analysed by agarose gel electrophoresis and compared with a DNA ladder of known size (Fermentas). PCR fragments of correct size were purified from the gel using the agarose gel extraction kit (Qiagen) or the QIAquick PCR purification kit (Qiagen) following the manufacturer's instructions.

3.2.9. Mutagenesis PCR

In order to specifically modify individual amino acids in overexpressed proteins, their DNA sequence on the coding plasmid was modified by mutagenic PCR.

For nucleotide changes in short vector systems this was done by QuickChange PCR. Primer pair was created with the "QuickChange Primer Design" software (Agilent), in QuikChange® II mode. The obtained primers containing the corresponding mutation were used for a PCR amplification of the complete plasmid. The PCR was performed with native Pfu DNA polymerase (Thermo Fisher Scientific) according to the manufacturer's protocol and 10ng plasmid template under the following conditions:

95 °C	30 sec	
95 °C	30 sec	16 Cycles
55 °C	1 min	
68 °C	2.5 min	
25 °C	∞	

The PCR was purified using the QIAquick PCR purification kit (Qiagen) and the non-mutagenized original plasmid was digested with Dpn-I (Thermo Fisher Scientific) according to the manufacturer's protocol. After heat inactivation of the enzyme, the cloning mix was used in a transformation.

For the mutagenesis of large vectors, a fusion PCR was used to generate a DNA product from two partially overlapping sequences. As this method does not perform a PCR reaction over the whole vector, PCR errors are minimized. For this purpose, the fragments of interest were amplified separately with primers containing the desired mutation. After PCR purification, 50 ng of the longer product and the same molecular concentration of the second product were mixed in a PCR reaction without addition of primers. This mixture was amplified for 10 cycles to enable the synthesis of the fused complete sequence. The obtained PCR product was diluted to 1 ng/µl and used for a second round of PCR (25 cycles), in which forward and reverse primers were added to the extremities of the complete sequence.

3.2.10. QPCR

To determine the gene expression of selected genes cDNA was quantified by real-time PCR using PowerUp SYBR™ master mix:

cDNA	2 µl
PowerUp SYBR™	2.5 µl
gene specific forward primer	0.25 µl (10 µM)
gene specific reverse primer	0.25 µl (10 µM)

Relative expression of target genes was normalized to GAPDH expression (ΔCt) and fold induction (ΔΔCt) was calculated according to the following equations:

$$\Delta Ct = Ct_{(target\ gene)} - Ct_{(GAPDH)}$$

$$\Delta\Delta Ct = 2^{(\Delta Ct(unstimulated) - \Delta Ct(stimulated)}$$

3.2.11. Agarose gel electrophoresis

DNA fragments obtained by PCR or digested plasmids were analysed via agarose gel electrophoresis. Unless otherwise specified, 1-2 % (w/v) agarose (Biozym) was dissolved by heating in 1x TAE buffer until a homogeneous solution was obtained. After addition

of SYBR™ Green, at a final concentration of 0,1 mg/ml, the solution was cooled in a casting device until complete polymerization. DNA samples to be investigated were mixed with DNA loading buffer (Thermo Scientific™) and loaded on the gel. The running chamber was filled with TAE buffer and electrophoresis was performed at 5 V/cm for 30-60 min. A size marker (GeneRuler 1kb or 100bp, Thermo Scientific) was used to estimate the weight of the fragments of interest. Imaging of DNA gels was performed on a ChemiDoc imaging system (Bio-Rad).

3.2.12. Precipitation of nucleic acids

To precipitate nucleic acids, samples were mixed with 10 % of their volume of sodium acetate (Roth; 3 M, pH = 5.2). Subsequently, 110 % of its volume of isopropanol (Roth) was added and the mixture was incubated for 30 minutes at -20 °C. After a centrifugation step at 14.000 g and 4°C for 15 minutes, the nucleic acid pellet was washed with 70% (v/v) ethanol (Roth), precooled to -20°C and centrifuged at 14.000 g and 4°C for 5 minutes. The pellet was then air dried and resuspended in H_2O.

3.2.13. Quantification of nucleic acids

Nucleic acids were quantified by measurement of absorbance at 260 nm (A_{260}) using a Nanodrop™ (Thermo Fisher Scientific). The concentration of 50 µg/µl for dsDNA samples and 40 µg/µl for RNA per A260 unit was used for calculations. The purity of the nucleic acid samples was estimated using the ratio of the absorption of 260 nm to 280 nm and was aimed to correspond to a quality standard of ≥ 1.5.

3.3. Cell biology methods

3.3.1. Cell lines

BLaER1 (*194*): a subclone of a human B cell-lymphoma cell line expressing the transdifferentiation construct CEBPa-ER-GFP. BLaER1 monocytes showed remarkable similarity in reactivity and strength as well as sensitivity to primary monocytes (*156*). Since genetic perturbations can occur at the proliferative immunologically rather insensitive B-cell stage, CRIPSR/Cas9-mediated genome editing is technically easy to perform.

In the course of these studies it was found that BLaER1 cells express transcripts of SMRV (Squirrel Monkey Retrovirus). A comprehensive characterization of BLaER1 monocytes in comparison to other human myeloid cells has not provided evidence that SMRV-positivity would affect the functionality of these cells as myeloid cells.

THP1 (ATCC® TIB-202TM): monocytic cell line from human myeloid lymphoma

HEK 293T (ATCC®CRL-3216TM): human embryonal kidney cells stably expressing SV40 Large T antigen.

hiPSC (*195*): Human induced pluripotent stem cells (hiPSCs) were kindly provided by F. Ginhoux. The expression of pluripotency markers, teratoma formation and normal karyotype were verified.

J774 (ATCC®TIB-67^{TM}): immortalized mouse macrophage cell line from ascites.

3.3.2. Cell culture conditions

All cells were cultivated at 37°C, 5% CO_2. FCS was heat-inactivated at 55°C for one hour and filtered before use. Splitting of all cell lines was performed every 3-4 days depending on cell confluence. If the supernatants of a cell culture were to be used in a protein precipitation, the cells were stimulated in a medium containing 3% FCS.

Primary human monocytes, BLaER1 and THP1 cells were cultivated in RPMI supplemented with 10 % FCS, 1 mM Pyruvate, 100 U/ml Penicillin and 100 µg/ml Streptomycin (all Gibco). Primary murine bone marrow macrophages, J774

macrophages and HEK293T cells were cultured in DMEM supplemented with 10% FCS, 1% sodium pyruvate, 100 U/ml penicillin-streptomycin.

For transdifferentiation of BLaER1 cells into macrophages, 7 x 10^5cells per ml were plated out in 96-well plates (7 x 10^4 cells) or in 10 cm dishes (7 x 10^6 cells) in differentiation medium containing 10 ng/ml IL-3, 10 ng/ml M-CSF (both Peprotech) and 100 nM β-estradiol (Sigma-Aldrich). After 5 days, the cells were stimulated in fresh regular RPMI medium according to experimental needs.

THP1 cells were differentiated overnight in the presence of 100 ng/ml PMA (Sigma-Aldrich), washed three times with cold PBS (Life Technologies) and seeded at a density of 7 x 10^4 cells per well in 96-well plates.

3.3.3. Isolation of PBMCs and primary monocytes

Peripheral blood mononuclear cells (PBMCs) of informed, consenting and healthy donors were obtained from Leukoreduction systems chambers (LRSCs). These were obtained from the cell separation unit of the Department of Transfusion Medicine, Cell Therapeutics and Haemostaseology (ATMZH), University Hospital Munich. The contained blood was rinsed out of the LRSCs with 70 ml 0.9 % isotonic NaCl solution, 30 ml of each diluted blood solution was layered over 15 ml Biocoll solution and centrifuged at 800 g for 15 min at RT (speed-up/break ramp at 9/1). The PBMCs were removed from the interphase, diluted in NaCl solution and centrifuged at 450 g for 7 min at 4 °C. The PBMC pellet was resuspended in 10 ml of 1x BD Pharm erythrocyte lysis buffer and incubated on ice for 5 min. Lysis was stopped by adding PBS and cells were centrifuged at 450 g for 7 minutes at 4°C. For subsequent isolation of primary human monocytes cells were resuspended in cold MACS Buffer (0.5% FCS, 2mM EDTA in PBS) and enriched using CD14 MACS kit (Miltenyi), according to the manufacturer´s instructions. Purified monocytes were plated as desired (8 x 10^4 cells/well for 96-well plate; 1 x 10^6 cells /well for 24-well plate). For differentiation into monocytes-derived macrophages, cells were cultured in the presence of M-CSF (Peprotech) at the final concentration of 100 ng/ml for 4-6 days of.

3.3.4. Generation of bone marrow macrophages

Wild type (WT) C57BL/6 mice kept under SPF conditions were used as source of murine primary bone marrow derived macrophages (BMDMs). Mice were euthanized according to the FELASA guidelines by cervical dislocation. Femurs and tibias of 8-12 weeks old mice were removed, cleaned from tissue, washed with 70 % ethanol for 1-2 min and put in 50 ml falcon full of ice-cold PBS. Bones were cut under sterile laminar hood and bone marrow was flushed with PBS through a 70 µM Nylon cell strainer into a falcon tube. Cells were centrifuged at 400 g for 10 min at RT. The pellet was resuspended in 2 ml of 1X BD Pharm erythrocyte lysis buffer for 2 min. Lysis was stopped by adding PBS and cells were centrifuged at 400 g for 10 min at RT. For differentiation into macrophages cells transferred to sterile (non-coated) 10 cm petri dishes in media containing 30 % L929 supernatant (prepared and filtered inhouse) for at least 6-7 days at 37 °C. One day before the experiment, cells were washed with PBS and adherent cells were detached by using 2 mM EDTA in PBS for 10 min at 37 °C. BMDMs were plated as desired (1 x 10^5 cells/well for 96-well plate; 1 x 10^6 cells /well for 24-well plate).

3.3.5. Cell stimulation

Unless otherwise noted, the specified cells were stimulated with 200 ng/ml ultrapure LPS from *E. coli* (Invivogen) for two hours. Primary monocytes or PBMCs were stimulated with 2 µg/ml Pam3CSK4 (Invivogen), while BLaER1 monocytes were stimulated with 20 µg/ml Pam3CSK4 for two hours. After priming with the indicated stimulus, the cells were stimulated with 6.5 µM Nigericin (Sigma-Aldrich) for two hours to activate the NLRP3 inflammasome. For stimulation of NLRC4 inflammasome cells were stimulated with 4 µg/ml Protective Antigen (List) and 0.2 µg/ml LFn-YscF (in house production). For activation of NOD2 signalling cells were stimulated with 200 ng/ml L18-MDP (InvivoGen) for different timepoints.

To inhibit signalling pathways with appropriate inhibitors, these were given to the cells one hour before stimulation in the following stimulations unless otherwise noted: 20 µM Z-VAD-FMK (Peptide Institute, Inc); 20 µM Z-YVAD-FMK (R&D Systems); 5 µM MCC950;

Unless otherwise noted cells transduced with pLI plasmids were treated with 1 ug/ml doxycycline for six hours to induce the expression of encoded proteins.

3.3.6. Production of viral particles and transduction of target cells

For the production of viral particles, a transient second generation expression system (three constructs: transfer vector, packaging plasmid and virus envelope plasmid) was used for the production of pseudotyped γ retroviral particles and a third generation system for pseudotyped lentiviral particles (four constructs: transfer vector) (*196*).

3.5 x 10^6 HEK293T cells were seeded in 10 cm dishes and transfected a few hours later after a media change. For lentiviral constructs (pFUGW,pLi) 8 µg of transfer vector, 12 µg of pMDLg/pRRE, 4 µg of pRSV-REV, and 8 µg of pCMV-VSVG were used for transfection. For retroviral constructs 20 µg of transfer vector, 15 µg of pCMV-Gag-Pol, and 6 µg of pCMV-VSVG were used.

The DNA mixture was resuspended in 500 µl H_2O, mixed with 500 µl of 2X HBS buffer and 50 µl of 2.5M $CaCl_2$, and incubated at RT for 20 minutes. The transfection suspension was then added dropwise to the HEK293T cells. After 12 h, fresh medium with 30% FCS was added to the cells for virus production. After 24 h the virus was harvested, cellular components were separated by centrifugation at 1000 g for 10 minutes and filtration through a 0.45 µm filter. If necessary, the resulting cell-free supernatant was centrifuged at 22800 rpm for two hours to concentrate the virus.

For transduction, 2 x 10^5 cells were incubated for 24 h with 2 ml of virus containing supernatant mixed with 2ml of regular medium containing 16 µg/ml polybrene (Sigma Aldrich). After 48 h the medium was replaced by fresh medium. 48 h – 72 h after transduction cells were selected with either 1.25 µg/ml Puromycin (Roth) for 48 h or sorted for expression of fluorescent selection markers. Unless otherwise noted Surviving cells were experimentally investigated in a polyclonal approach.

3.3.7. Quantification of cytokine and lactate dehydrogenase (LDH)

Cytokine and LDH release was quantified from cell-free supernatants with Triton X 100 added to an final concentration of 0.5% for inactivation of potential pathogens.

LDH assays were done on supernatants immediately after experiments using the PierceTM LDH Cytotoxicity Assay Kit (Life Technologies) according to the manufacturer's specifications using flat-bottom 384 well plate and incubated in the dark at RT for 15-20 minutes. The relative amount of LDH release was calculated according to the following formula:

$$LDH\ release\ (\%) = 100 \times \frac{Experimental\ condition - unstimulated\ control}{Lysis\ control - unstimulated\ control}$$

Absolute quantification of cytokines were measured by Enzyme-linked immunosorbent assays (ELISAs) of supernatants previously stored at -20 °C. Human TNF, human IL-6, human IL-1 β, murine IL-1β, murine IL-6 (all OptEIA, BD Bioscience) and human IL-18 (R&D) were performed according to manufacturer's instructions. For all OptEIA kits, sample volumes were reduced to 50 µL and all the antibodies were used at half the recommended concentration. ELISA high binding plates (Greiner Bio One) were coated with coating antibody diluted in appropriate coating buffer overnight at 4°C.

Plates were washed with ELISA wash buffer and blocked and blocked with 10% FCS in PBS for one hour at RT. After samples and standard were incubated for two hours at RT plates were washed again and detection antibody was loaded on plates for one hour. Following another wash, streptavidin conjugated HRP enzyme was added for 30 min. Final thorough washing was performed and ELISAs were developed for 30 min in dark using TMB substrate (BD Bioscience). The reaction was stopped by addition of 2N sulfuric acid. Absorbance was read at 450 nm and 570nm by Gen5-Epoch microplate reader (BioTek).

3.4. Biochemical methods

3.4.1. Cell lysis, sample collection and bicinchoninic acid assay (BCA)

Depending on the experiment, cells were either lysed directly or detached from the plate using PBS with 2 mM EDTA and lysis of the pellet after centrifugation. Unless otherwise noted, cells were lysed using 40 µl DISC buffer (containing cOmplete™ and, when necessary, PhosSTOP™ and/or 5 mM NEM) at approximately $5x10^6$ cells/ml. After centrifugation at 24000 g for 10 min, the protein concentration was determined using a BCA kit (Thermo Fisher Scientific) according to manufacturer's instructions:
Reagent A and B from the kit were mixed 1:50 and 200 µl of the solution was added to 10 µl of sample or BSA standard. The reaction was incubated at 37 °C for 20 minutes followed by absorbance measurement at 562 nm using Gen5-Epoch microplate reader (BioTek).

3.4.2. Protein precipitation from cell supernatant

Proteins from cell-free supernatant of $1\text{-}3x10^6$ cells were precipitated by chloroform/methanol precipitation. To this end 700 µL of the supernatant was mixed with 700 µL methanol (Roth) and 210 µL chloroform (Roth) was added. The mixture was vortexed for a few seconds and the phases separated by centrifugation at 16000 rpm for 1 minute at RT. The upper aqueous phase was discarded and 700µL methanol was added to the lower organic phase and the interphase. Samples were vortexed and centrifuged as above and the supernatant was discarded. The protein pellet was air-dried for 7 minutes under a fume hood before addition of 40-80ul 1X SDS laemmli buffer. Samples were dissolved and denatured for 10 minutes at 95 °C and 1500 rpm and stored at -80 °C until use.

3.4.3. Ubiquitin Immunoprecipitation

Lysates from at least $10x10^6$ cells were enriched for ubiquitinated proteins using glutathione S-transferase (GST)-ubiquitin associated domain (UBA) bound to Sepharose beads. Lysates were adjusted to equal protein levels in 500µl DISC (containing cOmplete™ and 5 mM NEM) and 20 µl packed glutathione sepharose beads pre-bound with 100 µg GST-UBA were added to each condition. Beads were incubated on a rotating

wheel at 4 °C for at least two hours, washed 5 times with IP buffer and eluted in 30-60 µL 1x SDS sample buffer. Initial untreated Lysates were kept as input controls.

3.4.4. SDS-Page and Immunoblotting

Samples in 1X SDS laemmli buffer, prepared as described above, were subjected to SDS-PAGE under denaturing conditions. For supernatant precipitation samles, 12% self-cast gels were prepared in Bio-Rad casting devices using the following recipe:

	12% separating gel (8ml)	5% stacking gel (4 ml)
Water	2.64 ml	2.72 ml
Acrylamide Rotiophorese 30	3.2 ml	0.68 ml
1.5M Tris-HCl, pH 8,8	2 ml	-
1 M Tris-HCL, pH 6,8	-	0.52 ml
10% SDS	80 µl	40 µl
10% APS	80 µl	40 µl
TEMED	8 µl	4 µl

Sample were loaded on self-cast or commercially available SDS gel (tris-glycine), and runat 100-120 V until the required separation was achieved. The samples were then transferred from the gel to a nitrocellulose membrane (0.2 µm or 0.5µm, GE Healthcare) in a wet system at 100 V for 90 min.

Proteins were transferred to nitrocellulose membrane in a wet western blot transfer system (Bio-Rad) for 70 minutes at 4 °C. Ponceau S staining (Sigma-Aldrich) was performed to control for transfer quality. After washing in PBST, membranes were blocked with 3% milk in PBST for one hour at RT. Blots were incubated overnight at 4 °C with primary antibodies in TBST containing 3 % BSA and 0.1 % sodium azide. After three washing steps with TBST for 5-10 min each, the membrane was incubated in corresponding secondary antibodies conjugated with for one hour at RT. before one hour incubation at RT with the required HRP-conjugated secondary antibody diluted in 5% milk in PBST. After 3-4 final washing steps, membranes were developed using Pierce ECL WB substrate (Thermo Fisher Scientific, or Merck Luminata Forte for weaker signals) in a Fusion Fx device (Vilber). If required, whole image was contrast-enhanced in a linear fashion.

3.5. Genome editing using CRISPR-Cas9 technology

Gene-deficient monoclonal cell lines were generated largely following a published protocol (*197*).

3.5.1. Electroporation of BLaER1 and THP1 cells

Cas9 and sgRNA plasmids were introduced into cells by electroporation. The required gRNA expression plasmids were generated as described in 3.2.4. For each electroporation 2.5 x 10^6 cells were pelleted and resuspended in 250 µL of pre-warmed OptiMEM and incubated with 2.5 µg of Cas9 and 2.5 µg of sgRNA plasmid (or 5 µg of Cas9-sgRNA double plasmid) for 10 min at RT. BLaER1 were electroporated in a 4 mm cuvette using the following conditions: 265 V, 975 µF, 700 Ω. For THP1 the following settings were used: 250 V, 950 µF, ∞ Ω. Electroporated cells were directly transferred to a 6-well plate with pre-warmed RPMI medium.

3.5.2. Transduction of J774 cells

J774 murine macrophages were transduced with viral particles driving expression of Cas9 (pRZ_Cas9_mCherry or Lenti-Cas9-Blast) and sgRNA (pLenti-gRNA-GFP or LentiGUIDE-Puro). Transduction was carried out as described in 3.3.6.

3.5.3. Selection and generation of monoclones

24-48 h after electroporation or transduction cells were sorted for positivity to the fluorescent protein expressed in the Cas9 containing vector (BFP or mCherry from pRZ_Cas9_BFP or from pMini_U6_gRNA_CMV_BFP_T2A_Cas9). 2-10% highest positive cells were sorted on a Sony sorter SH800Z into 15 ml tubes containing 3 ml of fresh medium.

Selection using antibiotics was carried out as described in 3.3.6.

For generation of monoclonal cell lines, selected cells were plated in 96-well plates (U-Bottom for BLaER1/THP1 and F-Bottom for J774) with a dilution of 4 cells/well, 2 cells/well and 1 cell/well. After about 3 weeks of expansion, single cell clones were

identified by absorption at 600 nm using Spark20M microplate reader (Tecan) and thereupon picked and duplicated using a Beckman Coulter Biomek FX.

3.5.4. Genotyping of gene-deficient cell clones

Gene editing and monoclonality was analysed by PCR-based next generation deep sequencing on a MiSeq system. Cells lysed in 30 µL of direct lysis buffer per well by incubation at 65 ◦C for 10 min. Proteinase K was inactivated by incubation at 95 °C for 10 min. Using a nested PCR approach, the potentially edited locus was amplified and barcode sequences as well as Illumina sequencing adapters were added. For the first PRC a sequence fragment of about 250 bp surrounding the targeted gene locus was amplified using 1 µl of the generated lysate. The target site specific primer pairs (cf. section 3.1.9) contained adaptor sequences for binding of barcode primers used in the second PCR (cf. section 3.1.9). The PCR reactions were prepared in a total of 6 ul, with 5 µl of PCR mix and 1 µl from the previous reaction, as follows:

	PCR1	PCR2
Buffer (HF or GC)	1.2 µl	1.2 µl
dNTPs (10 mM)	0.12 µl	0.12 µl
fwd primer	0.06 µl	-
Rev primer	0.06 µl	-
Barcode primer mix (2.5 µM)	-	1.2 µl
Phusion polymerase	0.06 µl	0.06 µl
H_2O	3.5 µl	3.92 µl
Lysate	1 µl	-
PCR1	-	1 µl

Both PCR reactions were performed in 384 well plates (Bioplastics) as follows:

95 °C	3 min	
95 °C	30 sec	16 Cycles
62 °C	30 sec	
72 °C	30 sec	
72 °C	3 min	
25 °C	∞	

The orthogonal mixing of 8 different forward primers and 12 different reverse primers (see chapter 3.1.9) and the thus resulting barcode primer mixes with a 96 unique

barcode combination enabled mixing of all PCR reactions. The DNA was purified by agarose gel electrophoresis, precipitated and quantified. DNA sequencing was performed on Illumina's MiSeq Platform with a 300 base single read run using v2 chemistry. Sequencing files were analysed for all-allelic frameshift mutations using the OutKnocker.org software. To exclude clonal effects 3-6 different KO clones were tested per target gene. If possible, single cell clones with two differently edited alleles were chosen.

3.6. Data analysis and software

3.6.1. Data analysis

FACS raw data was analysed using Flowjo. ELISA and LDH raw data were analysed using Excel and R.

If not otherwise stated, statistical significance was determined by two-way ANOVA when the response was affected by two factors (e.g. genotype and stimulus) with Sidak's correction for multiple comparison. If only one factor influenced the results, a one-way ANOVA was employed. If not otherwise stated, the results were examined for significant differences compared to the values of the corresponding wild type clone. n.s. = not significant, * $p<0.05$, ** $p<0.01$, *** $p<0.001$. The exact number of replicates (n) is indicated within figure legends. Data are represented as mean + SEM if at least three independent experiments were performed or as mean + SD if two independent experiments or one representative experiment is shown. All statistical analyses, except the analysis of proteomic and transcriptomic data, were performed using Prism.

RNA sequencing was performed on an Illumina 1500 HiSeq machine in cooperation with the Laboratory for Functional Genome Analysis (Gene Center, LMU Munich). Analysis of the obtained data was conducted by G. Kuut.
In brief, data was demultiplexed from the Illumina barcoded reads using JE demultiplexer (*198*). Read quality was checked by FastQC and RSeQC and low quality samples were removed (*199*). Transcript abundances were quantified using Salmon and gene level count matrices generated through tximport (*200, 201*). Normalization, exploratory analysis and differential

expression analysis was performed using DESeq2 (*202*). Genes were considered significantly differentially expressed if FDR was less than 5% and log fold change was greater than 2.5. The List of significant genes was imported to Cytoscape and TF analysis was performed using iRegulon and Trrust (*203*). Raw proteomics data was analysed using MaxQuant (*204*) by M. Tanzer as described in (*205*).

3.6.2. Software and algorithms

Adobe Illustrator	Adobe Systems
CHOPCHOP v3	https://chopchop.rc.fas.harvard.edu (*193*)
EMBL-EBI analysis tools (Clustal Omega, BLAST)	https://www.ebi.ac.uk/services (*206*)
FastQC	http://www.bioinformatics.babraham.ac.uk/projects/fastqc
Flowjo V10.0.5	Tree star, Inc.
Galaxy	blum-galaxy.genzentrum.lmu.de/galaxy/ (*207*)
Gen5 2.09	BioTec
GPS 5.0	http://gps.biocuckoo.cn (*208*)
IRegulon	http://iregulon.aertslab.org (*209*)
PANTHER 14	http://geneontology.org (*210*)
PHOSIDA	http://141.61.102.18/phosida/index.aspx (*211*)
PhosphoNET Kinase Predictor	http://www.phosphonet.ca/kinasepredictor.aspx
Graphpad Prism 8.3.1	GraphPad Software, Inc.
Microsoft Office 16.16.11	Microsoft
Nano Drop 1000 3.8.1	Thermo Fisher Scientific
OutKnocker	http://www.outknocker.org (*197*)
QuikChange Primer Design	http://www.genomics.agilent.com/primerDesignProgram.jsp
RStudio	RStudio, Inc.
SnapGene 4.3.11	Insightful Science
Tm Calculator v 1.12.0	https://tmcalculator.neb.com
Trrust v2	https://www.grnpedia.org/trrust/ (*212*)

4. Investigating the Role of USP7 in NLRC4 signalling

4.1. Introduction

The modification of signalling components through ubiquitination is a widespread method to modulate their activity (cf. Chapter 1.4.3). DUBs, which are tightly regulated ubiquitin proteases, play an essential role in this regulation. There are approximately 100 known DUBs, which can be grouped into five subclasses based on their protease domains. With approximately 50 members, the ubiquitin-specific proteases (USP) family is the largest of all subfamilies (*213*). Ubiquitin-specific-processing protease 7 (USP7), also known as Herpesvirus-associated ubiquitin-specific protease (HAUSP) is a USP family deubiquitinase that was first identified to interact with the ICP0 ubiquitin E3 ligase herpes simplex virus (HSV). USP7 can also interact with other viral proteins, including the Viral Interferon Regulatory Factors 1 and 4 (vIRF1 and vIRF4) of Kaposi sarcoma herpesvirus (*214, 215*).

Besides viral proteins, multiple other targets of USP7 have been identified (Figure 9). Of particular interest for pharmacological applications, is USP7´s ability to regulate p53 and MDM2, which leads to cell growth repression and the activation of apoptotic pathways, which has understandably placed this gene in the focus of cancer research and therapy (*216*).

One signalling pathway which heavily relies on ubiquitination control is NF-κB (cf. chapter 1.5 and 1.9). While CYLD, OTULIN and TNFAIP3 (A20) have been consistently reported as negative regulators, contradicting reports can be found for USP7 stating both negative and positive regulation(*217, 218*)(*219, 220*)(*181, 221*)(*222, 223*)(*224*).

Due to embryonically lethality of *USP7*$^{-/-}$ mice, there is a lack of *in vivo* studies characterising the role of USP7 in immune responses and associated pathologies (*225*).

It is therefore of interest to further investigate the role of USP7 in the context of NF-κB signalling and other immune-related signalling pathways.

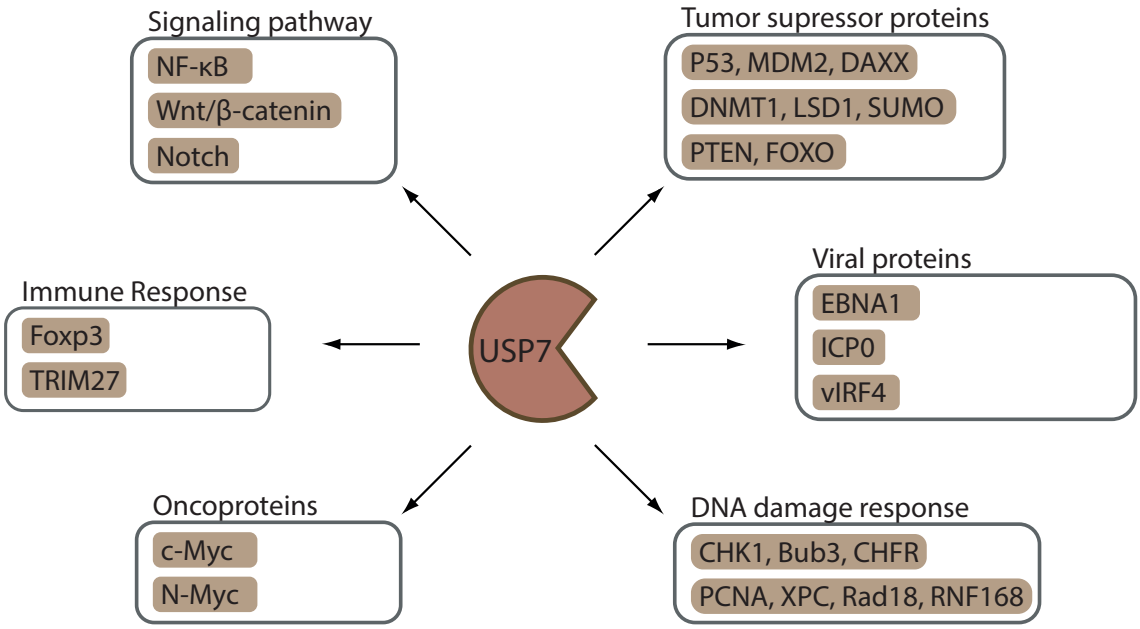

Figure 9 Overview of USP7 functions. Published potential substrates and binding partners of USP7. Most substrates play important roles in tumour suppression, immune response, viral replication, epigenetic control, and DNA repair. (Fig. adapted from (*226*))

4.2. Chapter overview

As discussed above, contradicting reports surrounding the role of USP7 in NF-κB signalling exist. Furthermore, unpublished data from our group suggest involvement in NLRP3 inflammasome activation.

In order to identify the role of USP7 both in NF-κB and inflammasome signalling, we generated BLaER1 knockout cell lines. Utilising these cells, we could demonstrate a dependence of NF-κB and NLRC4 signalling on USP7. We further studied the mechanism of NLRC4 inhibition and found a strong transcriptional regulation dependent on USP7. In the course of this study, we discovered additional immune regulatory proteins, which were downregulated in the knockout cells and displayed a reduction of signalling in follow up experiments. Finally, we set out to identify the common transcription factor responsible for the regulation of the genes we observed to be affected by USP7.

4.3. Results

4.3.1. P53 is responsible for USP7 KO lethality

In a genome-wide CRISPR/Cas9 screen in immortalised mouse macrophages, which was previously conducted in our research group (J.L. Schmid-Burgk, unpublished, follow up to (*155*)), USP7 appeared to play a role in the regulation of the NLRP3 inflammasome. We thus aimed to generate USP7 deficient cells to further study its mechanism in NLRP3 inflammasome signalling in the previously described transgenic B-cell line BLaER1 (cf. section 3.3). For this purpose, BLaER1 cells were electroporated with a Cas9 containing plasmids and a CRISPR gRNAs targeting USP7. While USP7 knockouts have previously been shown to be lethal in mice, leading to growth arrest and embryonic lethality within 6.5–7.5 days, there is scare data on the depletion *in vitro* (*225, 227*).

Single-cell clones generated were analysed by deep sequencing to obtain all-allelic frame-shift mutations (Figure 10 A). Only clones bearing heterozygous frame-shift with WT (grey) or in-frame mutations (blue) were obtained. More than 300 clones were screened, all showing the same pattern as shown in Figure 10 A. These cells still contain an allele encoding for the functional protein, therefore these cells were not considered to be a knockout. Three different gRNAs were tested and all showed high editing activity, as nearly all alleles displayer editing, thus ensuring that the gRNAs were functional and the method was conducted correctly. Previous knockout attempts on essential genes had produced similar patterns of editing, as a full knockout is lethal. In line with previous *in vivo* studies, USP7 seems to also be an essential gene *in vitro*.

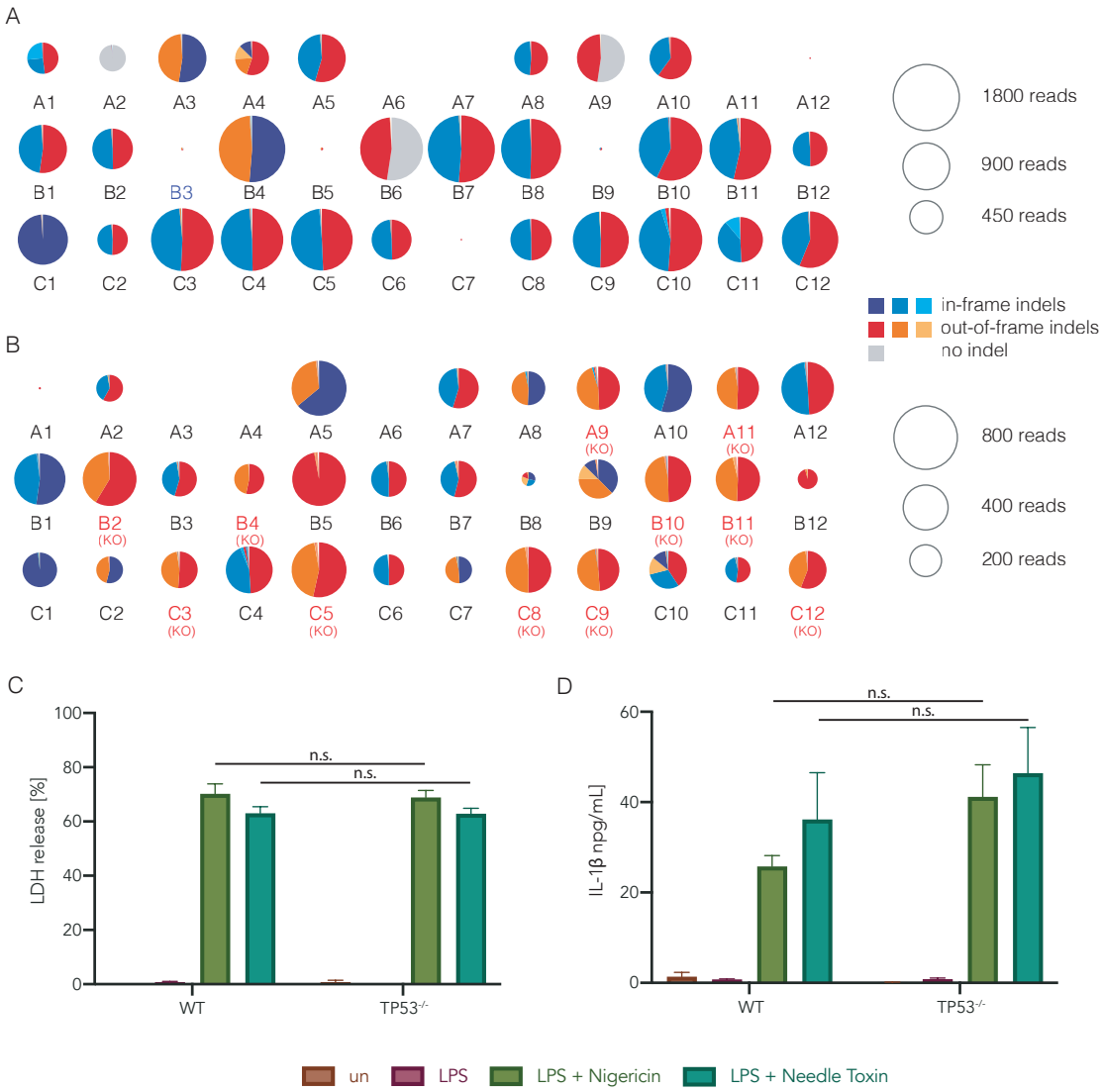

Figure 10 **Example of USP7 editing observed in deep sequencing genotyping.** BLaER1 cells were electroporated with Cas9-BFP plasmid and CRISPR gRNA targeting USP7 and sorted for BFP positive cells. Single-cell clones generated by limiting dilution were analysed by deep sequencing to bear all-allelic frame-shift mutations. Visualisation of a representative fraction of analysed single-cell clone genotypes using the OutKnocker.org software. Grey colour indicates WT reads, red to orange colours KO alleles (reads with frame-shift indels) and blue colours in-frame mutation reads. **(A) WT** cells show robust editing, but no homozygote out-of-frame indel clones could be obtained. (**B)** In P53 deficient cells, clones with homozygote out-of-frame indels were frequently found. **(C,D)** BLaER1 monocytes of the indicated genotype were stimulated for 2 h with LPS and subsequently stimulated with Nigericin or pA and Needle Toxin (LF-YscF). LDH release (C) and IL-1β secretion (D) are depicted as mean + SEM of three independent experiments.

Under basal conditions, USP7 binds to and deubiquitinates the E3 ubiquitin ligase MDM2, protecting it from degradation. MDM2, in turn, ubiquitinates p53, resulting in its proteasomal degradation, thus limiting apoptosis and cell cycle arrest (*228*). Through these mechanisms USP7 indirectly drives survival and proliferation (Figure 11).

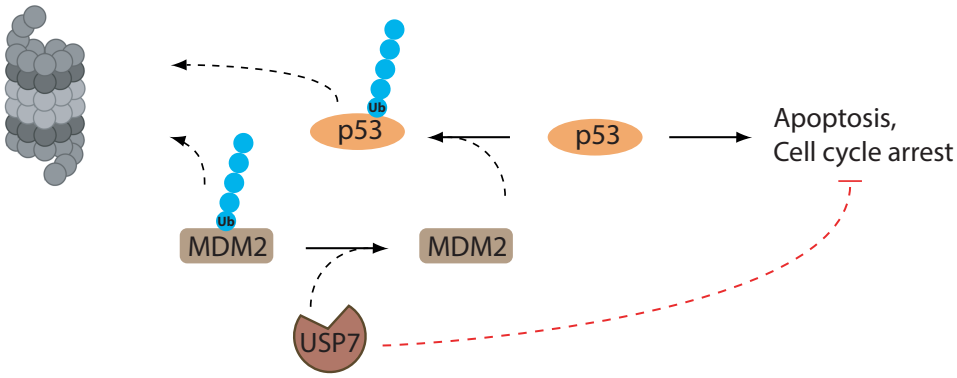

***Figure 11* Function of USP7 in cell cycle and growth regulation.** Schematic representation of the role of USP7 in the stabilisation of the tumour suppressor p53. Modified from (*229*)

USP7 knockouts have previously been shown to be lethal in mice (*225, 227*). In these studies, the embryonic lethality was explained by a dramatic reduction in proliferation partly due to p53 activation. Moreover, several publications using highly specific USP7 inhibitors all reported elevated p53 levels (*230-232*). *TP53*$^{-/-}$ x *USP7*$^{-/-}$ animals, albeit not being fully protected against embryonic lethality, showed extended development compared to the single knockouts.

In light of this, we generated p53-deficient cells (gene name: *TP53*) in an attempt to bypass the presumed USP7 dependence. Using the newly generated p53 knockout cells, we were successful in acquiring several viable *USP7*$^{-/-}$ clones. To determine if the *TP53*$^{-/-}$ background would influence the differentiation or inflammasome signalling, cells were differentiated for five days, treated with 200 ng/ml LPS for two hours following stimulation with 6.5 µM nigericin or 4 µg/ml pA and 0.2 µg/ml Needle Toxin (LF-YscF) for additional two hours to activate the NLRP3 and NLRC4 inflammasome respectively. Compared to WT cells, p53 deficiency neither impacted on macrophage differentiation, nor did it affect inflammasome signalling (Figure 10 C, D).

In summary, our findings confirmed that USP7 deficient cells are not viable, but could be rescued *in vitro* by additionally depleting p53. Moreover, these studies showed that p53 deficiency does not impact on macrophage differentiation and NLRP3 and NLRC4 inflammasome signalling.

4.3.2. NF-κB dependent gene expression is dependent on USP7

Ubiquitination and proteasomal degradation are essential processes of NF-κB transcription activity (cf. chapter 1.5 and 1.9). However, the role of deubiquitinases in this pathway are not fully understood yet. While CYLD, OTULIN and A20 have been consistently reported as negative regulators, contradictory reports can be found for USP7 stating both negative and positive regulation (*181, 217-224*). To date, no study has been carried out using full knockouts.

Since this project focused on the inflammasome signalling pathway, which can be modulated by NF-κB signalling, we first wished to determine the role of USP7 in this signalling pathway. For this, we treated BLaER1 with LPS for different timepoints and measured transcriptional changes by qPCR and secretion of cytokines by ELISA. While the TP53 single knockouts showed the same levels of *IL1B* and *IL6* expression as the WT, the *TP53*$^{-/-}$ x *USP7*$^{-/-}$ cells showed an almost complete reduction (Figure 12 A). This reduction was also observed in the secretion of IL-6 and IL-1β (Figure 12 B). This data demonstrates that USP7 is necessary for LPS-induced gene expression in human monocytes.

To further dissect the role of USP7 in the NF-κB pathway, we performed immunoblotting to detect the phosphorylation and degradation of IκBα after stimulation with LPS (Figure 12 C). While phosphorylation can be detected after one hour of LPS treatment in both WT and *TP53*$^{-/-}$, it cannot be detected in *TP53*$^{-/-}$ x *USP7*$^{-/-}$.

DUBs known to be negative regulators for NF-κB, such as TNFAIP3 and CYLD, are reported to act as negative feedback regulators. When analysing transcription levels via RNA sequencing, we observed these DUBs to be upregulated upon LPS treatment (Figure 12 D). For USP7, no such LPS dependent regulation could be observed.

Overall our results show a requirement of USP7 for NF-κB, which appears to be upstream of IκBα phosphorylation. However, the lack of IκBα phosphorylation could still be explained through the mechanism proposed by Colleran *et al.*, with the loss of USP7 leading to proteasomal loss of p65 and thus leading to a negative feedback loop resulting in a loss of IκBα phosphorylation that we also observed in p65 KO cells (*233*).

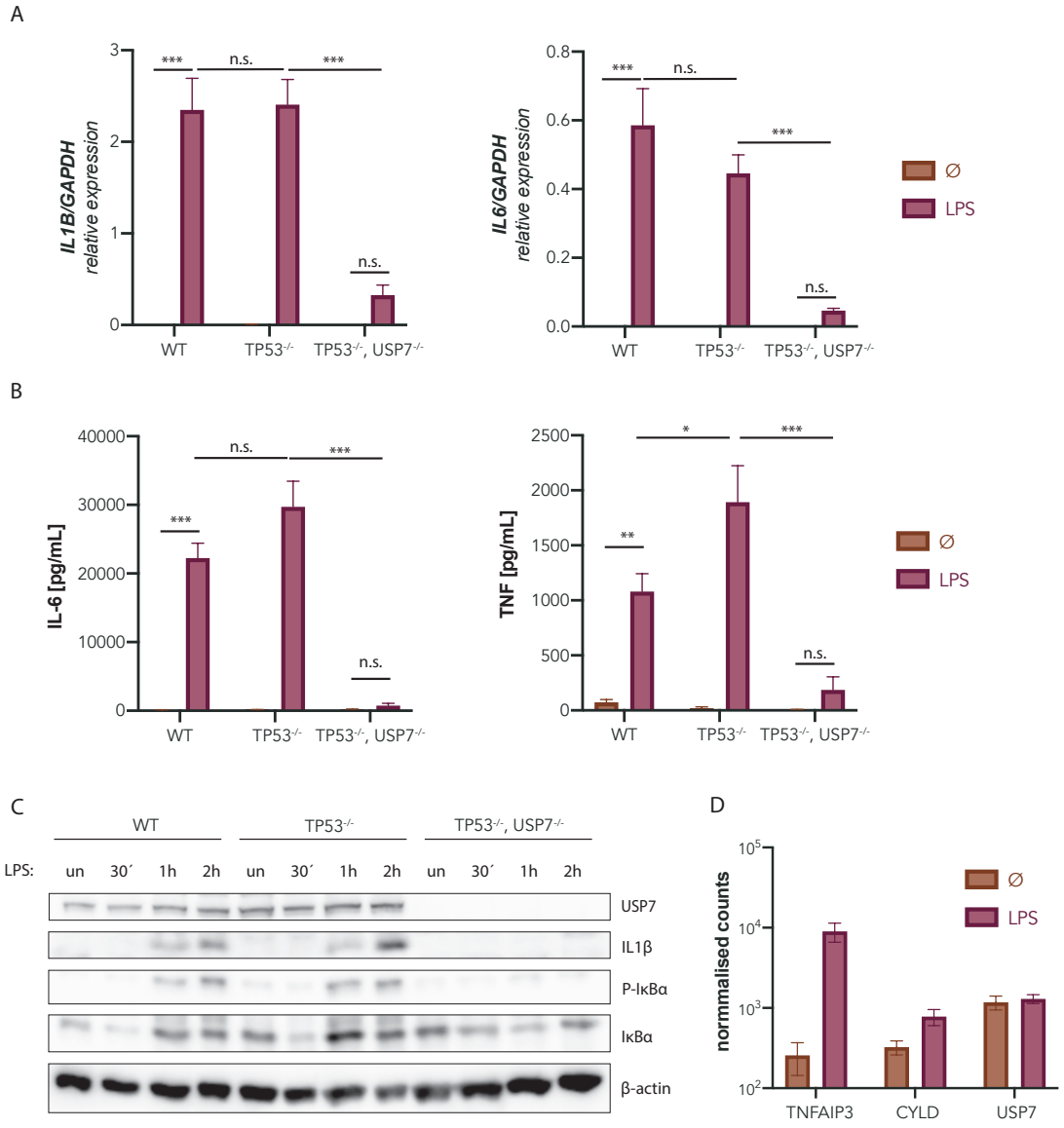

Figure 12 **NF-κB induction after LPS treatment. (A)** BLaER1 monocytes of the indicated genotype were stimulated for 2 h with LPS or left untreated. Expression of *IL1B* and *IL6* was quantified by qRT-PCR. Shown are mean values + SEM of three independent experiments. **(B)** BLaER1 monocytes of the indicated genotype were stimulated for 4 h with LPS or left untreated. Cytokine secretion is depicted as mean + SEM of three independent experiments. **(C)** BLaER1 monocytes of indicated genotype were treated with LPS for the indicated time. Immunoblot of P- IκBα and IκBα were performed as markers of NF-κB activation. One representative of two independent experiments. un = unstimulated control. **(D)** RNA-seq comparison of BLaER1 transcription level changes upon LPS stimulation. Shown are mean values + SEM of three independent sequencing samples. Counts are normalised using quantile normalisation.

4.3.3. Inflammasome activation

After establishing that USP7 indeed is required for NF-κB signalling, we then sought to further investigate the effect of USP7 deficiency upon inflammasome activation. For this, we primed BLaER1 monocytes with LPS for two hours and subsequently stimulated with Nigericin for two hours to activate the NLRP3 inflammasome or with Needle Toxin to stimulate NLRC4 as a control.

Upon NLRP3 activation, we did not see a strong effect of USP7 deficiency, the small reduction that was observed mimicked the response in the NF-κB-deficient RelA, RelB double knockout cells (Figure 13 A). NLRP3 levels in BLaER1 cells are upregulated after LPS treatment in a NF-κB dependent manner; therefore the slight reduction of LDH release could be attributed to the NF-κB signalling defect described in *3.2.1*.

In contrast to the minor change in LDH release observed after nigericin treatment, we unexpectedly observed a full inhibition of NLRC4 dependent pyroptotic cell death, in *TP53*$^{-/-}$ x *USP7*$^{-/-}$ following Needle Toxin stimulation (Figure 13 A*)*. The IL-1β release was completely abolished in both NLRP3 and NLRC4 stimulations (Figure 13 B), which again could be linked to the loss of NF-κB signalling (*3.2.1*.). This is further supported by the fact that the levels of pro-IL-1β were abolished entirely in lysates of USP7 deficient cells analysed via immunoblot (Figure 13 C).
Immunoblotting of mature caspase-1 demonstrated the dependence of USP7 upstream of caspase-1 autoproteolysis. The mature p20 fragment of caspase-1 was observed in WT and p53 deficient cells both after Nigericin and Needle Toxin treatment. For USP7 deficient cells, the p20 fragment can only be detected after NLRP3 activation and is not detectable after Needle Toxin stimulation (Figure 13 C).

No reduction in cell death was observed in NF-κB deficient cells, suggesting this phenotype to be independent of the discussed NF-κB deficiency. Besides, as NLRC4 does not require LPS priming for lytic death induction, we repeated the experiments in the absence of LPS, resulting in the same outcome (Figure 13 D). In all experiments, the parental *TP53*$^{-/-}$ mimicked the WT.

Some studies suggest functional redundancies between USP7 and USP47 (*234, 235*). For our observed phenotype we could not observe this: the single *USP47* knockout did not show any inflammasome related phenotype and the additional depletion of *USP47* in *USP7* knockouts did not show any additional effect (Figure 13 E).

In summary, we were able to show that USP7 deficiency leads to a loss of pyroptotic cell death after NLRC4 activation due to the loss of caspase-1 cleavage independent of NF-κB signalling.

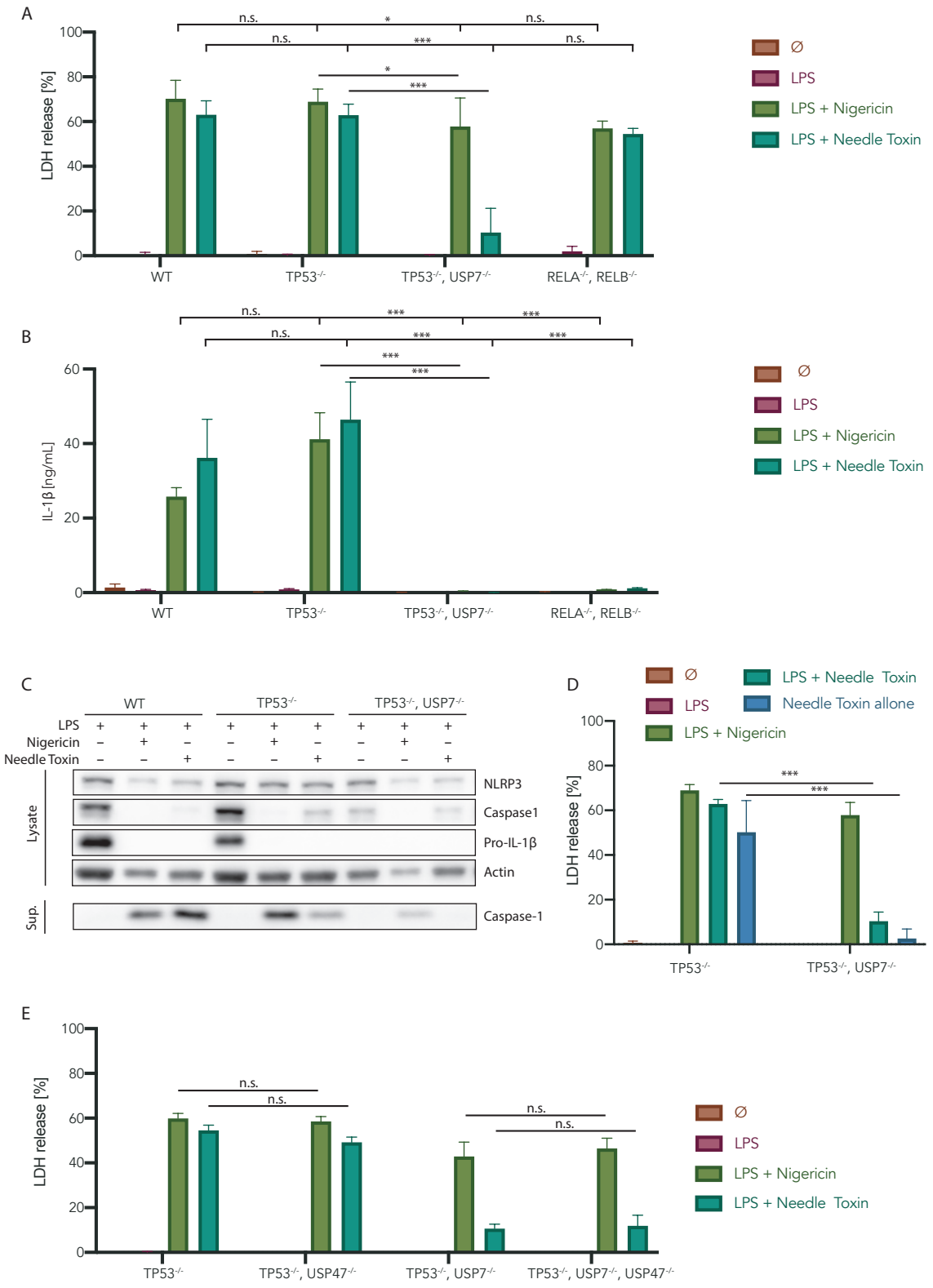

***Figure 13* USP7 dependence in Inflammasome activation. (A-C, E)** BLaER1 monocytes of the indicated genotype were stimulated for 2 h with LPS subsequently stimulated with Nigericin or pA and Needle Toxin (LF-YscF). LDH release **(A, E)** and IL-1β secretion **(B)** are depicted as mean + SEM of three independent experiments. **(C)** Immunoblot analysis of BLaER1 monocytes lysates and precipitated supernatant of indicated genotype. One representative experiment of two is depicted. **(D)** Un-primed BLaER1 show similar LDH response to Needle Toxin as LPS primed cells.

4.3.4. Cytosolically expressed Needle Toxin triggers NLRC4 activation in an USP7-dependent fashion

The uptake of Needle Toxin, described in 1.8, has also been shown to require receptor ubiquitination (*236*). Therefore we wanted to investigate if USP7 is involved in the toxin uptake or the downstream cytosolic signalling. To this end, we created cell lines which could express the toxin in a doxycycline dependent manner, thus bypassing the uptake mechanism. For this, USP7 deficient cells and the parental p53 deficient cells were transduced with a doxycycline-inducible lentiviral construct additionally constitutively expressing BFP. Cells with equal expression levels were stringently selected through FACS sorting of BFP expression (Figure 14 A). The thus-obtained cells were treated with doxycycline for six hours or left untreated, and supernatants were analysed for LDH release (Figure 14 B). While the induction of Needle Toxin led to proptosis mediated LDH release in the control cells, this was absent in the USP7 deficient cells. In summary, our data suggest USP7 to interfere with intracellular NLRC4 signalling rather than toxin uptake.

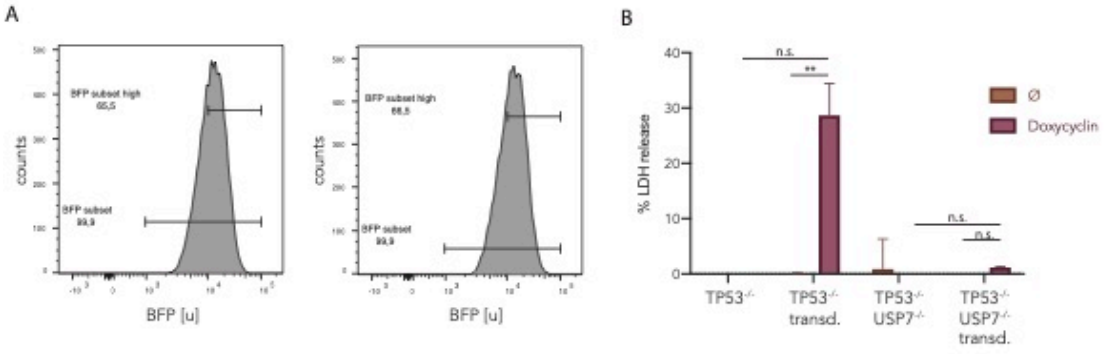

Figure 14 **BLaER1 cell line with stable expression of doxycycline-inducible Needle Toxin.** BLaER1 monocytes were transduced with lentivirus construct expressing pLI_BFP_Lfn-scF. **(A)** Comparison of the BFP expression of the inducible construct in *TP53*$^{-/-}$ (left) and the *TP53*$^{-/-}$ *x USP7*$^{-/-}$ (right) show even expression in both genotypes. **(B)** Cells of the indicated genotype were treated with Doxycyclin for 6 h or left untreated. LDH release is depicted as mean + SEM of three independent experiments.

4.3.5. NLRC4 levels are strongly reduced in USP7 deficient cells

After establishing that USP7 plays a role in cytosolic signalling, we focused on the proteins involved in NLRC4 activation (cf. section 1.8).

When analysing protein levels in BLaER1 monocytes via immunoblotting, we observed a strong reduction of NLRC4 expression itself in USP7 deficient cells (Figure 15 A). This had also been observed in previous experiments (Figure 13 C). Of note, the loss of p53 did not affect the NLRC4 levels.

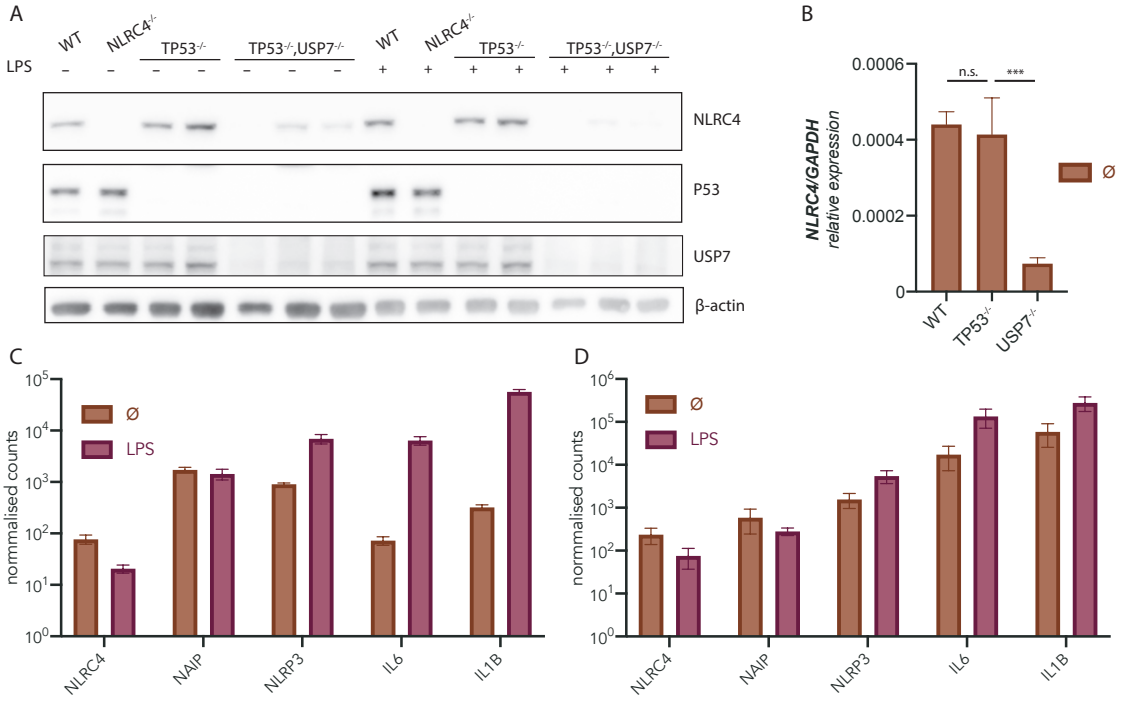

***Figure 15* Reduction of NLRC4 levels in USP7 knockout. (A)** Immunoblot analysis of BLaER1 monocytes lysates of indicated genotype stimulated for 4 h with LPS or left untreated. Multiple clones are shown in this experiment to highlight subtle differences between the individual USP7 knockout clones. One representative experiment of two is depicted. **(B)** Expression of NLRC4 was quantified by qRT-PCR. Shown are mean values + SEM of three independent experiments. **(C,D)** RNA-seq comparison of BLaER1 **(C)** and primary monocyte **(D)** transcription level changes upon LPS stimulation. NLRC4 inflammasome components compared to inflammasome components known to be upregulated by priming.

As in our previous experiments, we asked if this phenotype was due to NF-κB deficiency. We analysed transcription levels of BLaER1 monocytes (Figure 15 C) as well as primary human monocytes (Figure 15 D) after two hours of LPS treatment via RNA sequencing. As expected, NLRP3, as well as cytokines such as *IL1B* and *IL6*, showed induction upon LPS as a result of NF-κB priming. However, components of the NLRC4 inflammasome did not show an induction but even indicated a small decrease. This is in line with the fact that we had also observed, that NF-κB deficient RelA KO cells did not show any reduction in NLRC4 signalling (Figure 13). Our data thus indicates that it is not the loss of NF-κB signalling which is responsible for the decreased NLRC4 levels.

As USP7 is predominantly reported to function in the nucleus, we examined if the reduction of NLRC4 on the protein level was due to transcriptional regulation (*216, 237*). In line with this hypothesis, mRNA levels of NLRC4 were strongly reduced in USP7 deficient cells (Figure 15 B). Altogether, these results suggested that USP7-deficiency impacted on NLRC4 functionality by regulating its expression.

4.3.6. Multiple immune genes are regulated by USP7

To form a better understanding of the USP7 dependent transcriptional regulation we analysed the whole transcriptome of BLaER1 cells of *TP53*$^{-/-}$ x *USP7*$^{-/-}$ cells in comparison to WT and *TP53*$^{-/-}$ controls. For each genotype, several different BLaER1 knockout clones were analysed to ensure valid biological interpretation of the results. Euclidian distance analysis of the gene expression data showed the *TP53*$^{-/-}$ clones to cluster together with the WT sample, while the *USP7*-deficient cells clustered separately (Figure 16 A). This indicates that the p53 deficient cells have a similar transcriptional profile as the WT, while the USP7 depletion leads to big changes in gene expression. This is in line with our previous data, in which p53 deficient cells mimic the WT situation. For further analysis, if not stated otherwise, *USP7*$^{-/-}$ x *TP53*$^{-/-}$ cells were compared with control data from the cluster containing WT and *TP53*$^{-/-}$ cells. Analysing differential gene expression between these two cell populations showed that a total of 1,940 genes were significantly downregulated in USP7-deficient cells compared to the control cells (Figure 16 B and Figure 17A).

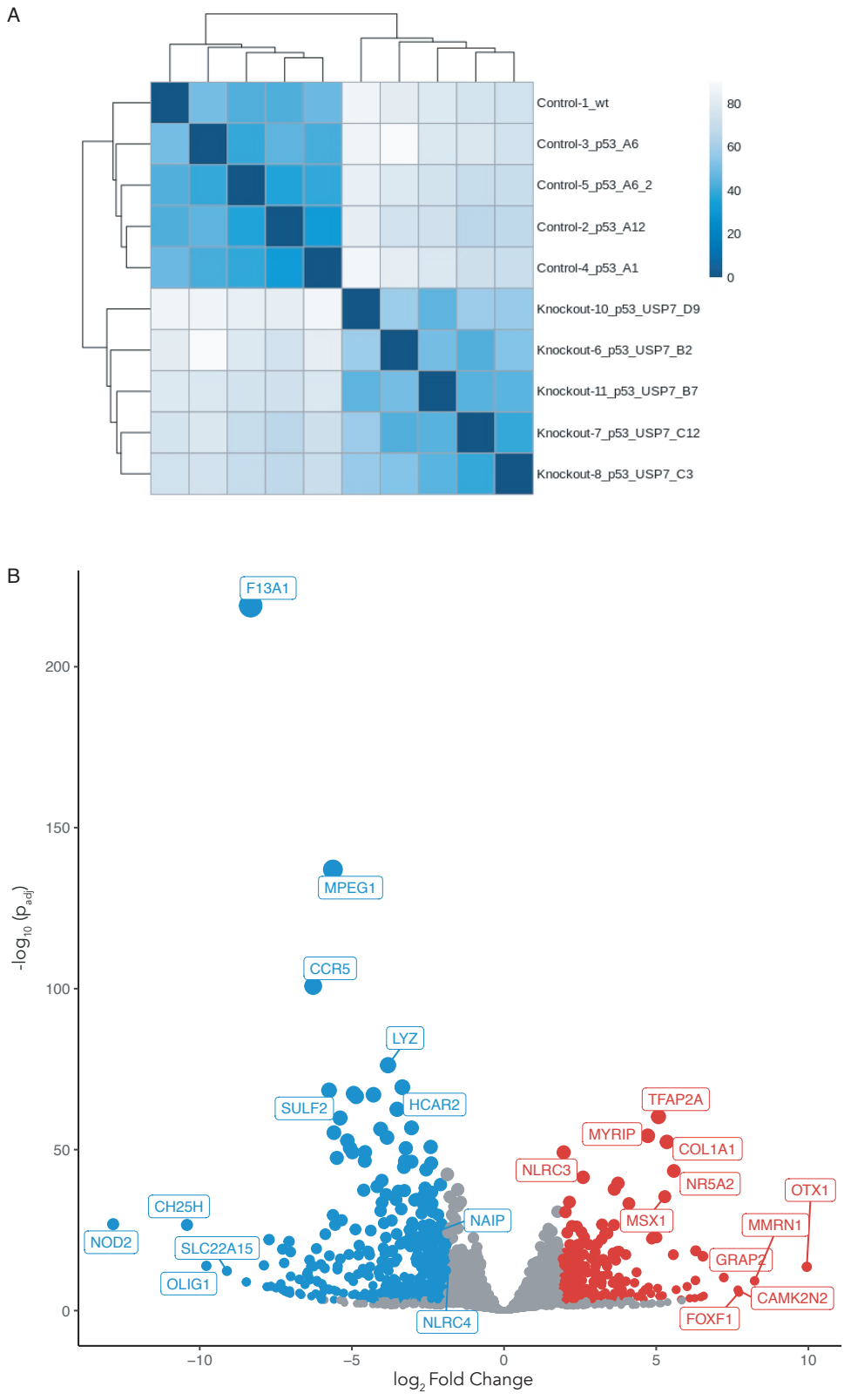

Figure 16 **RNA seq of BLaER1 monocytes with or without USP7 deficiency.** 3x10^6 differentiated, unstimulated BLaER1 cells were lysed in 1ml Trizol, frozen at -80 °C and handed over to the sequencing facility (LAFUGA, LMU, Munich) for and sequencing **(A)** Euclidean distance of all samples shows a strong similarity between the WT sample and P53 knockouts, while USP7 deficient cells cluster separately. **(B)** Volcano plot showing differential gene expression between double knockouts compared to control samples. Genes in red are upregulated and genes in blue are down-regulated in *TP53*$^{-/-}$ x *USP7*$^{-/-}$.

These genes also showed strong enrichment of GO terms linked to immune system processes (Figure 17 B) while the set of genes which were upregulated in the USP7 deficient cells did not show any significant accumulation of GO terms (data not shown). Interestingly, genes that did appear as significantly upregulated included inhibitory proteins such as CDKN2A (CDK-Inhibitor 2A), NLRC3 (Disruption of STING-dependent activation) and ZIC2 (Wnt/β-catenin signalling inhibitor). Despite these cells not having exposure to LPS prior to gene expression analysis, some NF-κB target genes were found to be downregulated in the knockouts, as cells also activate NF-κB under steady-state conditions. It is to be expected that after TLR induction a much bigger number of NF-κB target genes would have been picked up due to the effect of USP7 on this signalling cascade (ct. section 4.3.2). However, as we showed in the previous section, that NLRC4 activation is independent of priming we decided to analyse un-primed cells and thus be able to analyse a dataset that is not confounded by additional immune stimulation.
When focusing on the top 500 most significantly downregulated genes (Figure 16A), we found that both NLRC4, as well as NAIP, were among them. The downregulation of both components of this signalling pathway explains our previously observed phenotypes and suggests a role of USP7 in transcriptional regulation of immune sensors.

Many other members of the innate immune response to bacteria (TLR2, TLR4, TLR5, IRAK3) or viruses (TLR8, RNASE1, RNASE6) were also found in the top 500 downregulated genes, indicating profound immunomodulatory dependency for USP7. Detailed expression profiles, with an additional comparison between WT and $TP53^{-/-}$ for selected genes are shown in figure 17 C. For most of these genes, except for TLR2 and TLR5, the depletion of p53 alone did not have any effect on their expression levels. The TLR2 levels are increased in p53 deficient cells compared to the WT, but additional depletion of USP7 leads to a reduction that is well under initial WT levels.

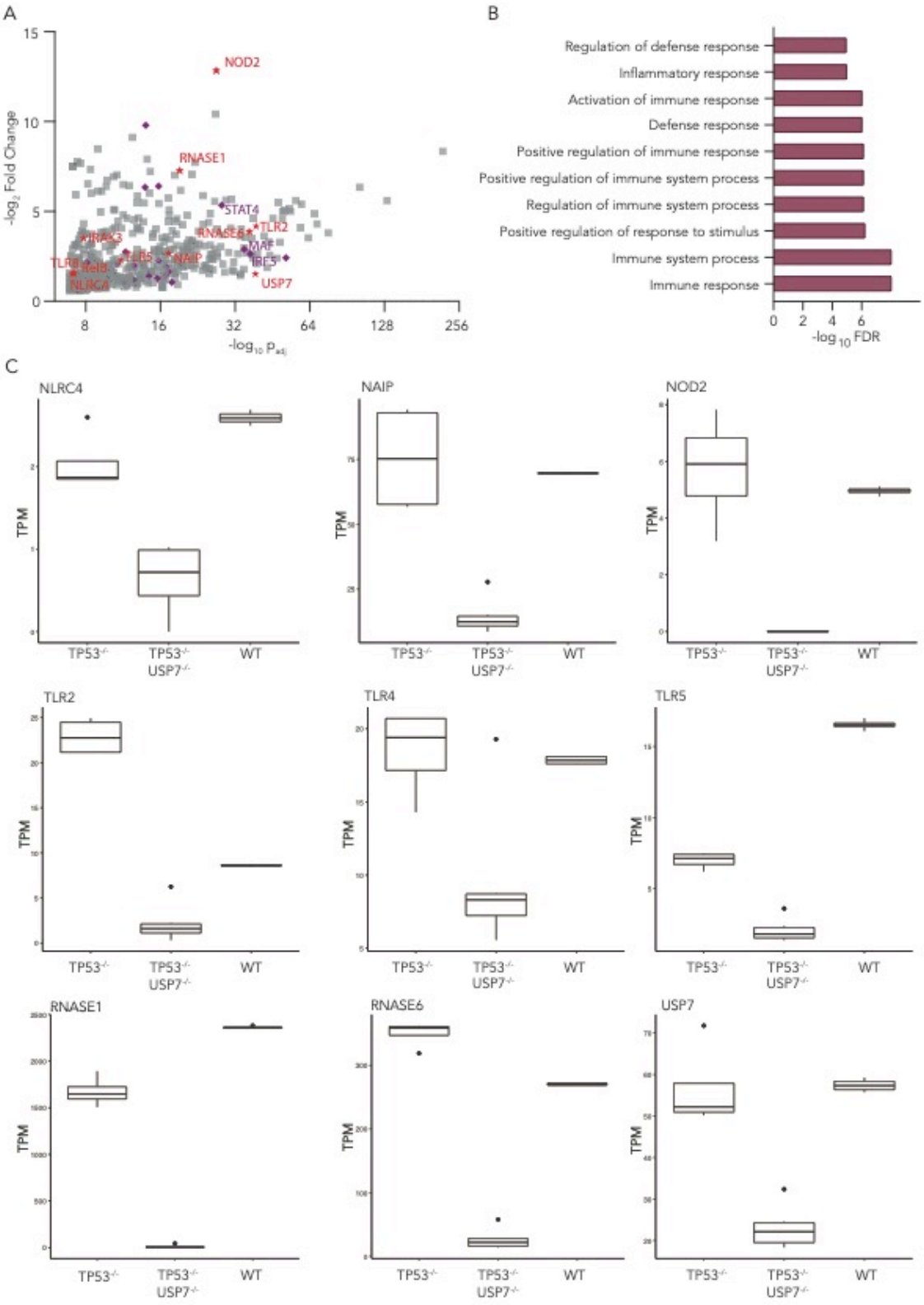

Figure 17 **Analysis of the top 500 downregulated genes in USP7 knockout. (A)** Dot blot with relevant immune signalling components highlighted in red and transcription factors highlighted in purple. **(B)** GO-Term analysis of these genes shows strong enrichment of immune regulating proteins. **(C)** Detailed overview of mRNA levels of selected relevant hits in three different genetic backgrounds. For better statistical analysis, subsampling was used for the WT sample, as no biological duplicates were available.

Of all transcripts downregulated in USP7 knockouts, NOD2 showed the highest reduction in mRNA levels (Figure 17 A).

To assess the impact of USP7 knockouts on the NOD2 pathway, we utilised our BLaER1 knockout cells treated with the membrane-permeable MDP (L18-MBP). We measured IL-6 secretion at different timepoints (Figure 18 A). We found that in USP7 deficient cells, IL-6 secretion was completely blunted. As expected, this was also the case in NF-κB deficient *RelA*$^{-/-}$ x *RelB*$^{-/-}$ cells. To dissect whether the effect on the IL-6 levels was solely due to the role of USP7 on NF-κB signalling described in chapter 4.3.2, we analysed RIPK2 ubiquitylation by western blot (Figure 18 B). We stimulated BLaER1 cells for one hour with L18-MDP and purified ubiquitylated proteins using glutathione S-transferase (GST)-ubiquitin associated domain (UBA) bound to Sepharose beads (*238*). Following MDP treatment, strong RIPK2 ubiquitination was observed in the WT and *TP53*$^{-/-}$ controls, as indicated by higher molecular weight species of RIPK2 by Western blot (Figure 18 B). When analysing *RelA*$^{-/-}$ x *RelB*$^{-/-}$ only a slight reduction of RIPK2 ubiquitination was observed. This is in line with previous studies hinting towards a positive feedback regulation between NF-κB and NOD2 leading to a reduction, but not a full loss, of RIPosome formation after RelA silencing (*239, 240*). In USP7 deficient cells, the ubiquitination of RIPK2 was completely absent. Input control lysates showed no difference in the protein levels of ubiquitinated RIPK2 (Figure 18 C).

In summary, these findings indicate that USP7 plays a role upstream of RIPK2 ubiquitination. This is consistent with the fact that NOD2 levels were found to be almost completely abolished in the RNA sequencing (Figure 17 C), and demonstrates that the transcriptional regulation is required for functional NOD2 signalling.

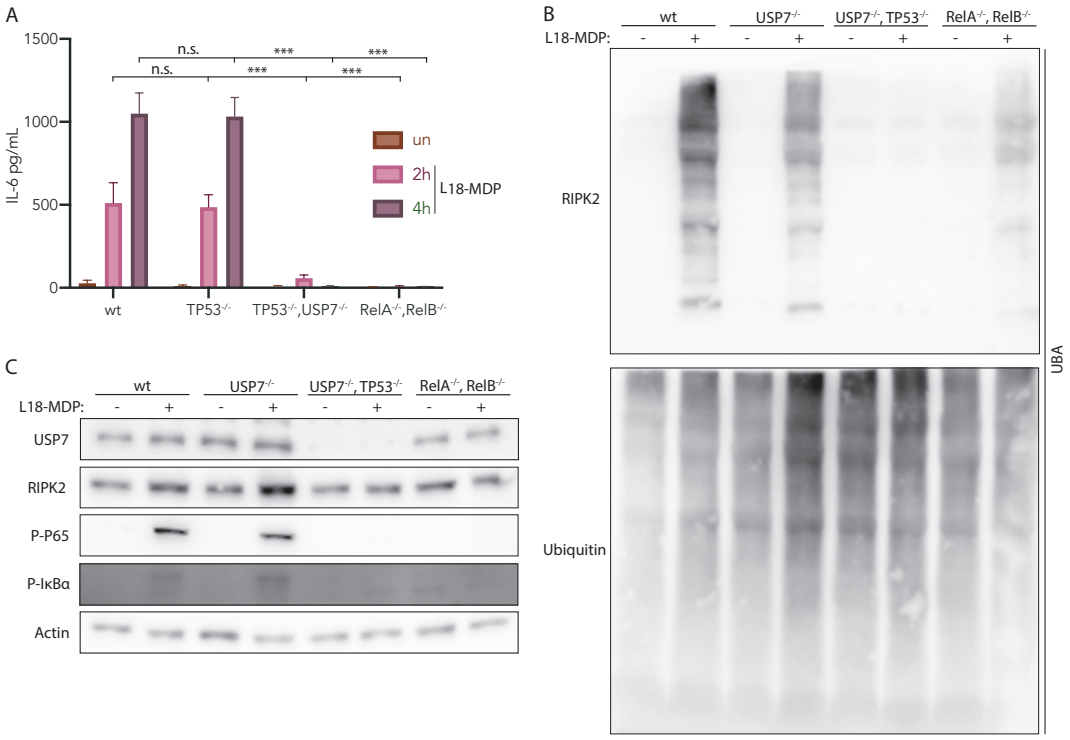

Figure 18 Analysis of NOD2 signalling. **(A-C)** BLaER1 monocytes of indicated genotype stimulated with L18-MDP. **(A)** IL-6 secretion after 2 h and 4 h stimulation. Immunoblot of lysates **(B)** and UBA enriched fraction **(C)** after 1h stimulation.

Another immune-related gene that we found to be strongly downregulated in the USP7 deficient cells was TLR2 (Figure 17). We therefore set out to investigate the phenotypical changes in the knockout after TLR2 stimulation. For this, we compared NLRP3 inflammasome activation under different priming conditions. To exclude an impact of TLR4 mediated inflammasome activation on Nigericin stimulation, we used TLR2 priming by Pam3CSK4. While there was only a weak reduction of cell death in the USP7 deficient cells after Nigericin treatment following TLR4 dependent LPS priming (as already described in 4.3.3), there was a substantial decrease of cell death when using Pam3CSK4 priming (Figure 19). In this condition, the WT showed lower levels of cell death than the *TP53* knockout. This is in line with the transcriptomics data, that showed an upregulation of TLR2 in the *TP53* KO compared to the WT (Figure 16C). Not only did the loss of *USP7* revert the increased cell death observed in *TP53* KO cells, it even showed a substantial reduction compared to the WT, thus mimicking the observed transcriptional regulation of TLR2.

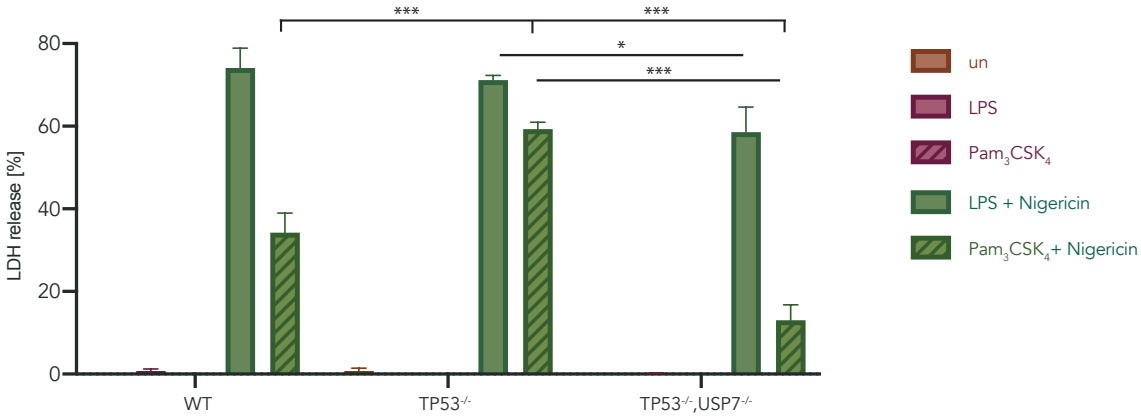

***Figure 19* LDH release upon NLRP3 activation after specific TLR2 priming.** BLaER1 monocytes of the indicated genotype were treated with LPS or Pam3CSK4 for 2 h and subsequently stimulated with Nigericin for 2 h. LDH release is depicted as mean + SEM of three independent experiments.

In summary, the analysis of the total transcriptome showed a downregulation of the two main components of the NLRC4 inflammasome in USP7 deficient cells. Multiple other innate immune components were shown to be regulated in a USP7 dependent manner. For two additional signalling molecules revealed by the transcriptomic analysis, NOD2 and TLR2, it was additionally shown that the observed transcriptional regulation shows an effect on the signalling capability.

4.3.7. USP7 regulated genes correlate with IRF4/8 dependent transcription

After experimentally validating selected gene hits from the RNA-seq dataset and showing that in the USP7 KO the respective pathways were impaired, we sought to find the responsible common transcription factor or mechanism of regulation affected by USP7. To find such a common regulation mechanism leading to the discussed phenotypes, the RNA-seq data were employed the iRegulon algorithms, highlighting common transcription factors of the down-regulated transcripts. iRegulon uses a genome-wide ranking-and-recovery approach utilising databases of 10.000 TF motifs and 1000 ChIP-seq data sets to detect enriched transcription factor motifs (*209*). Figure 20 shows the topmost enriched TF obtained by analysing genes downregulated in the knockout compared to the control cells. First, we analysed the list of genes

downregulated in p53 deficient cells, compared to the WT sample (Figure 20 A). As expected, p53 was among the top 10 transcription factors, that the analysis predicted to be responsible for the regulation of the genes, albeit not being the top hit. We thus proceeded to use this analysis on the list of genes downregulated in USP7 deficient cells (Figure 20 B).

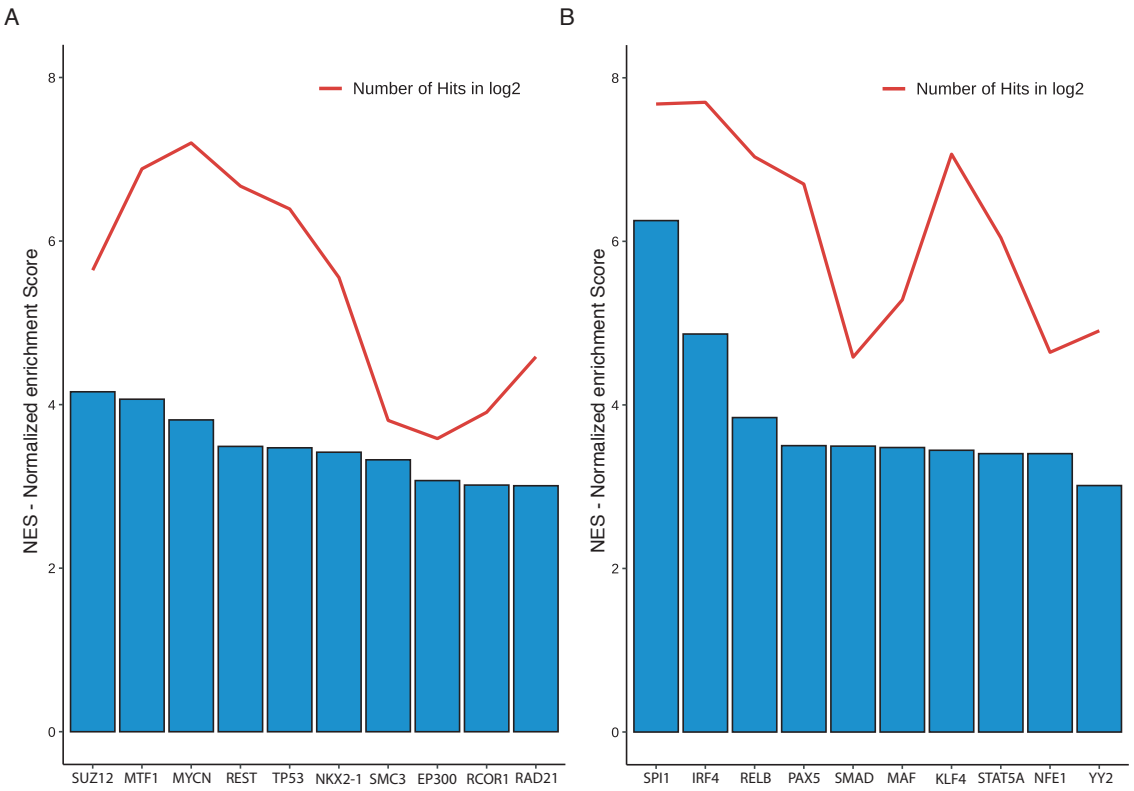

Figure 20 **Transcription factors analysis. (A-B)** Top 10 TFs identified by iRegulon analysis of most prominently downregulated genes (*209*). Bars represented normalised enrichment score and the red line indicates the number of hits. **(A)** Proof of concept TF analysis of transcripts downregulated in *TP53*$^{-/-}$ compared to WT. **(B)** TF analysis of transcripts downregulated in *TP53*$^{-/-}$ x *USP7*$^{-/-}$.

All of the transcription factors obtained from the analysis were knocked out, but none of the knockouts phenocopied the USP7 deficient cells (data not shown). The highest number of genes was found to be regulated by SPI1 (also known as PU.1) and IRF4. SPI1 KO resulted in cells that showed both a morphological defect in differentiating to macrophages and were unresponsive to both NLRP3 and NLRC4 stimuli (data not shown).

IRF4 has remarkable sequence homology with IRF8 and multiple studies show the cooperation of SPI1 and IRF4 as well as SPI1 and IRF8 in transcriptional programming (*241, 242*). We thus conducted a comparison of the transcription factor binding profiles

deposited in the JASPAR database, which show high sequence similarity of IRF4 and IRF8 binding sequences (Figure 21).

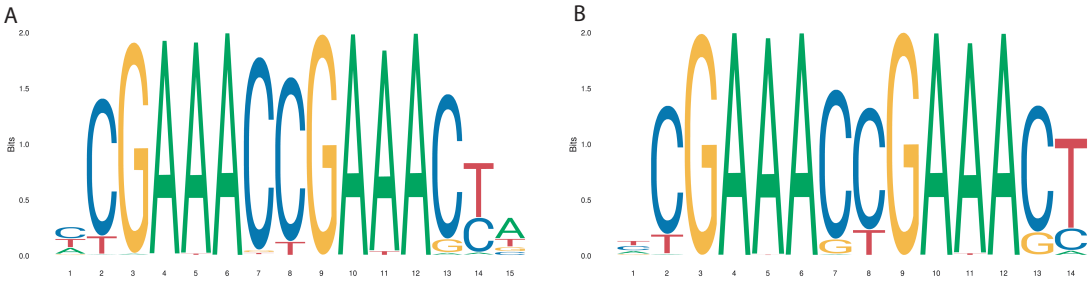

***Figure 21* Transcription factor (TF) binding profiles of IRF4 (A) and IRF8 (B).** Visualisation of the position weight matrices (PWMs) of the TF binding profile obtained from *JASPAR (243)*.

The transcriptional regulation of murine NAIPs in an IRF8 dependent manner has recently been shown in a study by Karki *et al.* (*170*). While analysing NAIP promoter binding in mice, this study also finds an enrichment of IRF4 and SPI1 binding but focuses mostly on the effect of IRF8.

In human macrophages, *IRF8*$^{-/-}$ cells showed a reduction of cell death upon NLRC4 stimulation, similar to the USP7 KO when stimulated with Needle Toxin without prior LPS priming (Figure 22 A). *IRF1*$^{-/-}$ x *IRF3*$^{-/-}$ x *IRF4*$^{-/-}$ x *IRF5*$^{-/-}$ x *IRF7*$^{-/-}$ cells did not show any reduction, suggesting no involvement of other IRFs. However, the *IRF8*$^{-/-}$ phenotype was not as strong as the phenotype of USP7-deficient cells after Needle Toxin treatment following LPS priming. A second LPS driven transcription factor could lead to this partial redundancy after LPS treatment. Moreover, *IRF8*$^{-/-}$ cells also showed a reduction in pyroptosis after NLRP3 induction following TLR2 priming, thus also resembling the phenotype observed in the USP7 knockouts.

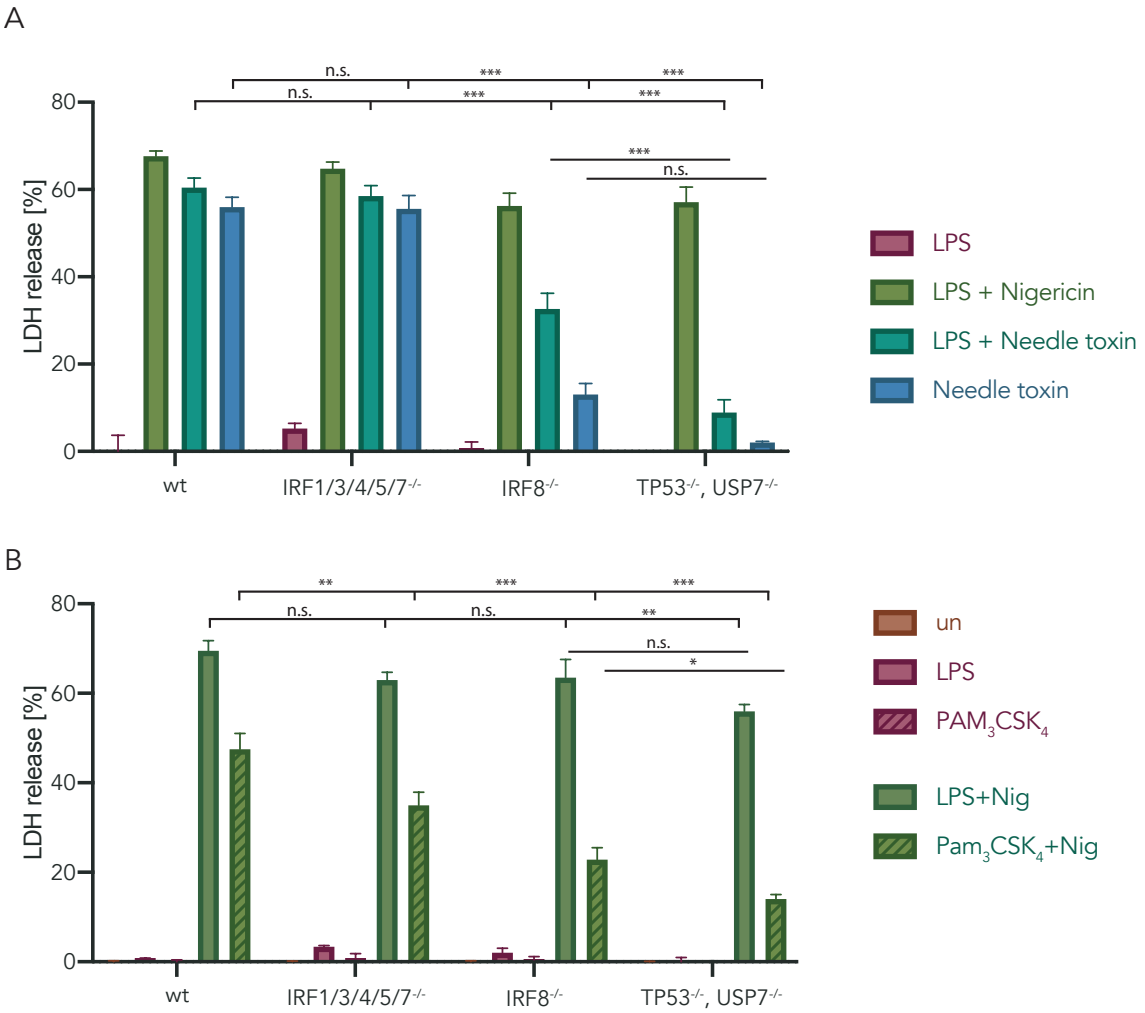

Figure 22 **Role of IRFs in NLRP3 signalling.** BLaER1 monocytes of the indicated genotype were treated with LPS or Pam3CSK4 for 2 h and subsequently stimulated with Nigericin or Needle Toxin for 2 h. LDH release is depicted as mean + SEM of three independent experiments. The depletion of IRF8 shows a similar impact on NLRC4 activation **(A)** and TLR2 priming **(B)** as the depletion of USP7.

4.4. Discussion

The role of ubiquitin as an important regulator of inflammasomes has become increasingly evident in recent years, with DUBs contributing significantly to this process (*244*). The priming step necessary for transcriptional upregulation of some inflammasome components and cytokines, mediated mainly by the NF-κB pathway, is regulated by DUBs such as A20 or CYLD and a role for USP7 has previously been suggested (ct. section 1.9). To date, most DUBs are described to act as negative regulators (Figure 23 A) and are upregulated in response to TLR activation in order to regulate and terminate NF-κB signalling (*245*). We found that unlike these DUBs, USP7 is a positive regulator of NF-κB. Additionally, unlike A20, the levels of USP7 are not upregulated by TLR4 activation. These findings contradict studies that describe USP7 as a negative regulator of the NF-κB by deubiquitination of NEMO (Figure 23 B) (*222, 223*) but support more recent research, showing USP7 to regulate NF-κB transcriptional activity in the nucleus, by increasing NF-κB stability as depicted in Figure 23 C (*224*).

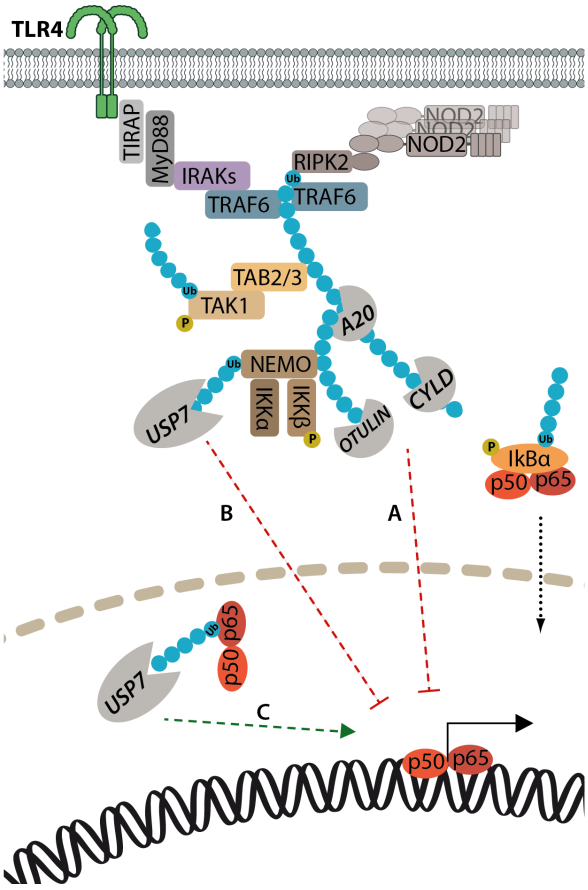

***Figure 23* The Role of DUBs in regulation of TLR4 signalling.** In MyD88-dependent signalling, TRAF6 synthesizes K63 poly-Ub chains, which act as a scaffold for TAK1 and IKK complexes, TAB2/3 and NEMO. This is facilitated by LUBAC, which leads to the linear ubiquitination of NEMO required for the recruitment of the IKK complex. Thus TAK1 phosphorylates IKKβ, which in turn phosphorylates IκB and subsequently undergoes ubiquitination and proteasomal degradation (See also Figure 3). **(A)** Several DUBs remove ubiquitin chains from TRAF6, NEMO negatively regulating this signalling pathway. **(B)** A similar mechanism proposed for USP7 would have the opposite phenotype of what we observed. **(C)** A different mechanism proposes that USP7 to prevents NF-κB degradation hence positively regulating transcription. This theory is in line with our findings.

Our data further showed that the loss of USP7 leads to an impaired NLRC4 response while only marginally affecting NLRP3. The weak effect on NLRP3 can be attributed to the NF-κB deficiency of the knockouts. Previous studies had suggested functional redundancies between USP7 and USP47 in some distinct settings (*234, 235*). While we were conducting our study, Palazón-Riquelme *et al.* published their findings that USP7 and USP47 regulate NLRP3 inflammasome activation based mostly on the inhibitor P22077, which targets both DUBs. We could recreate their data using the inhibitor (data not shown), but genetic depletion of USP47 did not show any inflammasome related phenotype and the additional depletion of USP47 in USP7 knockouts did not show any additional effect when compared to the USP7 deficient cells. Due to structural and mechanistic similarities of DUBs, there is the possibility that the observed effect on NLRP3 signalling is thus due to the inhibition of additional DUBs. This is in line with finding, that state a low activity and selectivity for P22077, showing it to inhibit multiple other USPs (such as USP9, 10, 20, 36) but also, for instance, the E3 ligase BRCC3, previously shown to be involved in NLRP3 activation (*246*).

Our observed phenotype on NLRC4 signalling was independent of TLR priming and was also present in un-primed conditions. While there are studies suggesting regulation of NLRC4 through a ubiquitin ligase (*206*), no direct endogenous ubiquitination has yet been described. While our efforts to detect USP7 dependent changes of NLRC4 ubiquitination could likewise not determine clear endogenous ubiquitination, we could, however, detect a strong reduction of total NLRC4 protein in the USP7 deficient cells.

In line with the previous finding of USP7 acting on transcription factors and its described predominant localisation in the nucleus, we found a substantial change in transcription profiles between parental cells and USP7 knockouts (*247*). Amongst others, both NLRC4 and its adapter NAIP were downregulated in the knockout cells, which serves as a conclusive explanation for the observed phenotype.

TP53$^{-/-}$ cells reacted liked WT cells in all of our experiments. NLRC4 RNA and protein levels were never reduced in these knockouts and also our transcriptome analysis did not indicate any role of p53 in the regulation of NLRC4. These data are in contrast to a study suggesting NLRC4 to be a p53 inducible gene (*171*).

The transcription factor analysis conducted with our transcriptome data had found SPI1 and IRF4 to be key transcription factors. A previous study by Karki *et al.* analysed NAIP promoter binding in mice and found an enrichment of IRF4 and SPI1 together with IRF8 (*170*). In this study, the authors emphasised the sequence homology between IRF4 and IRF8. They suggest that SPI1 might work in conjunction with IRF8 for the transcriptional regulation of Naips. The analysis of published ChIP-seq datasets further indicated IRF8 binding to the promoter regions of Naip2, Naip5, and Naip6 and to the intronic region of Nlrc4. Since this study, others have also identified IRF8 and IRF4 binding sites in the intronic regions of Nlrc4 (*248*).

While IRF8 knockouts showed a strong reduction of pyroptosis upon NLRC4 activation, it was not a full inhibition and LPS primed cells showed a weaker phenotype than un-primed cells. This is in line with Karki *et al.* that also could detect NLRC4 inflammasome activity in the absence of IRF8. This could be due to other factors that contribute to the transcription of the inflammasome components. Due to its weak DNA-binding activity IRF8 is often recruited together with other transcription factors. Other IRFs, AP-1 and Ets family TF (of which SPI-1 is a member) have been shown to interact with IRF8 allowing combinatorial control over numerous genes (*249, 250*). Our data would suggest the involved other TF to be inducible through LPS, as LPS priming dampens the phenotype of the IRF8 deficiency. AP-1 and some IRFs (IRF3, IRF7) have been shown to be induced by LPS (*251-253*).
Moreover, NF-κB also binds to the promoters of IRF1, IRF2, IRF5, and IRF8, thus linking TLR and IFN signalling (*254*). Figure 24 shows an overview of the proposed transcriptional regulation. Repeating the RNA-sequencing experiments with additional LPS treatment could help for a full understanding of involved transcription factors.

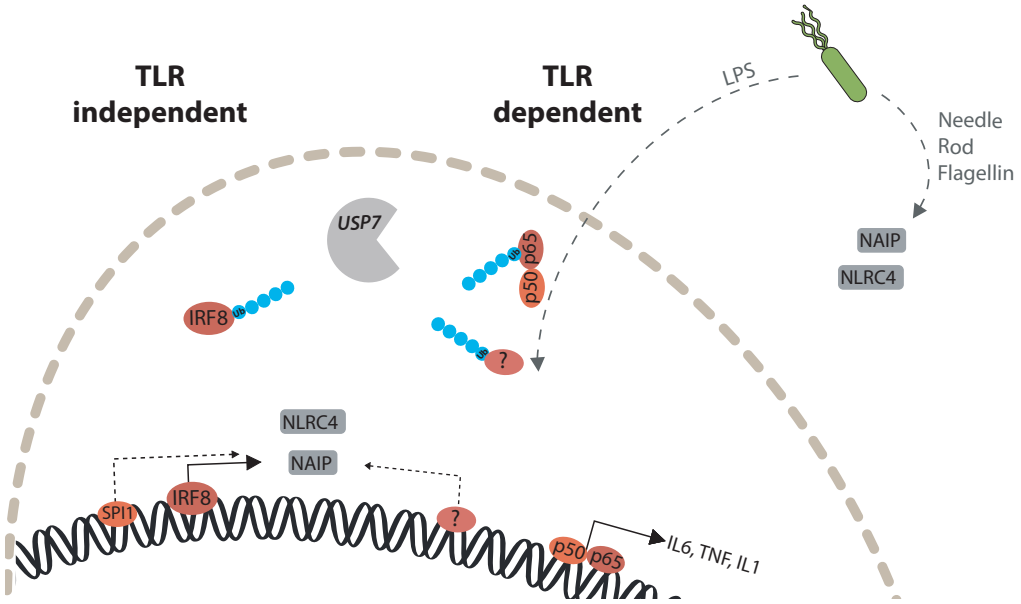

***Figure 24* Overview of the proposed transcriptional regulation of NLRC4 inflammasome.** The cytosolic receptor NAIP senses bacterial proteins such as type III secretion system (needle and rod) and flagellin and activates NLRC4. IRF8 seems to be required for the transcription of the NLRC4 inflammasome components, and SPI1 might have an assisting role in this process. In the presence of LPS, a TLR dependent TF appears to also regulate transcription of the inflammasome components. Both IRF8 and the unknown TLR dependent TF are likely to be stabilised through USP7.

NAIPs are the cytosolic receptors that sense bacterial proteins, specifically the type III secretion system (T3SS) needle, the T3SS inner rod, and flagellin. IRF8 is required for the transcription of genes encoding NAIPs, and SPI1 may also have a role in that process. The detection of bacterial proteins via NAIPs activates the NLRC4 inflammasome, leading to cell death and IL-1β/IL-18 secretion.

In the USP family, the catalytic site is strongly conserved throughout all members and noncatalytic domain confer substrate specificity. For USP7 this is through its ubiquitin-like domain (UBL). Of the over 50 USP family DUBs only 7 contain multiple of these UBLs: USP4, USP7, USP11, USP14, USP32, USP40 and USP47 (Figure 25) (*255*).

USP4, in turn, has been shown to acts as a deubiquitinase for IRF8, stabilising it by removing K48-linked polyubiquitin (*256*). The study further showed that a deficiency in USP4 resulted in decreased IRF8 levels.

With USP4, a DUB was shown to regulate IRF8 with similarities to USP7 (crystal structures are shown in Figure 25 B). Of note, like USP7, also USP4 was shown to regulate p53 (*257, 258*). Further experiments are needed to determine whether also USP7 can interact and directly deubiquitinate IRF8. The fact that past studies have shown USP7 to

interact with viral IRFs such as vIRF1 and vIRF4 does indicate USP7 to be able to directly interact with IRFs (*214, 215*). Some studies analysing the interaction of USP7 with its targets, have shown the importance of the TRAF domain and have characterised its interaction with a consensus sequence of P/AXXS on most of the known USP7 targets (Figure 25 A, E). It is worth noting that also IRF8 contains five of these motifs.

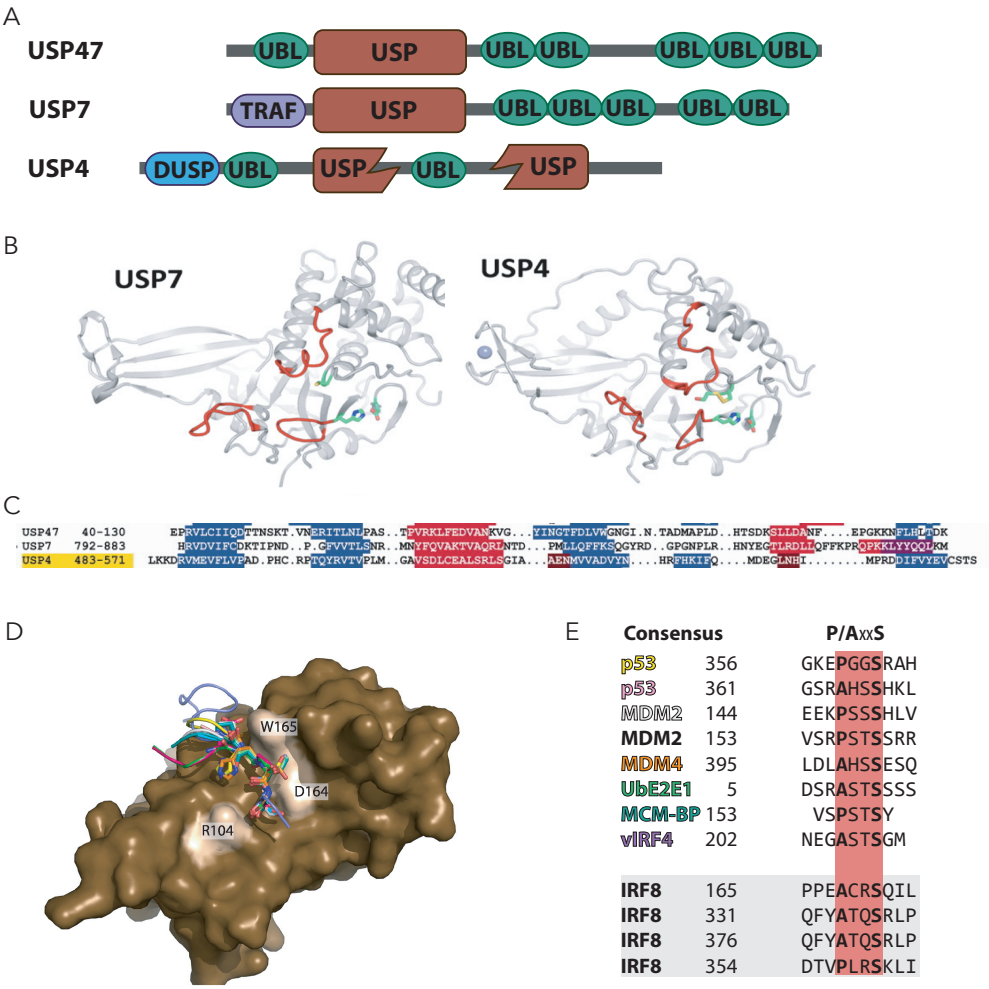

Figure 25 Similarities of different DUBs. **(A)** *Domain representation of USP47, USP7 and USP4 showing multiple UBL domains.* **(B)** Cristal structure of USP7 and USP4. **(C)** Sequence and secondary structure alignment between UBL domains of *USP47, USP7 and USP4.* ***(D)*** *Interaction between TRAF Domain of USP7 and target Proteins (in colours corresponding to E).* ***(E)*** *TRAF recognition motif is found upon the alignment of interacting peptides found in crystal structures (top) and can also be found in IRF8 (bottom). (Fig. adapted from (259-261))*

In future experiments, the ubiquitination state of IRF8 in WT and *USP7*$^{-/-}$ need to be studied to further investigate if a direct modification of the ubiquitination of IRF8 leads to the observed phenotypes. Additionally, co-immunoprecipitation experiments could show if an interaction of USP7 and IRF8 can be detected. However, previous co-immunoprecipitation attempts of deubiquitinases with their targets have turned out to be difficult, due to the very weak and transient interactions of DUBS.

A range of autoinflammatory diseases caused by NLRC4 mutations, commonly known as NLRC4-associated autoinflammatory diseases (NLRC4-AID), are known today (Table 5).

Variant	Origin of mutation	Phenotype	Source
p.S171F	somatic mosaicism	MAS/AIFEC	(*262*)
p.T177A	somatic mosaicism	CAPS-like	(*263*)
p.T337S	*de novo*	MAS/AIFEC	(*264*)
p.T337N	*de novo*	MAS/AIFEC	(*265*)
p.V341A	*de novo*	MAS/AIFEC	(*266*)
p.V341A	inherited	MAS/AIFEC	(*267*)
p.H443P	inherited	CAPS-like	(*268*)
p.S445P	inherited	CAPS-like	(*269*)

Table 5 *NLRC4 mutations and associated diseases observed in patients.*

The mutations are found on the NBD the, HD1, WHD and even on the LRR. NLRC4 crystal structure analysis suggests that the mutations in the NBD and HD1 acids are required for ADP binding or inflammasome formation (Figure 26 A-D).

The clinical manifestations range from Cryopyrin-Associated Periodic Syndrome (CAPS) like diseases to life-threatening macrophage activation syndrome (MAS), also known as autoinflammation with infantile enterocolitis (AIFEC). Affected individuals showed increased levels of IL-1b, IL-18 and pyroptosis (*262-264, 267, 268, 270*). Patients can also develop secondary organ-specific symptoms as well as central nervous system dysfunction (*262, 267*).

The observed CAPS-like disease diseases are characterised by recurrent episodes of fever, rash and arthralgia after exposure to cold stimuli and previously were only associated with mutations in NLRP3 and NLRP12 (*127, 271*).

MAS and accompanying hemophagocytic lymphohistiocytosis (HLH) are life-threatening systemic conditions associated with uncontrolled macrophage activation and hemophagocytosis (*272, 273*). If left untreated, ongoing flares can progress to organ failure and death.

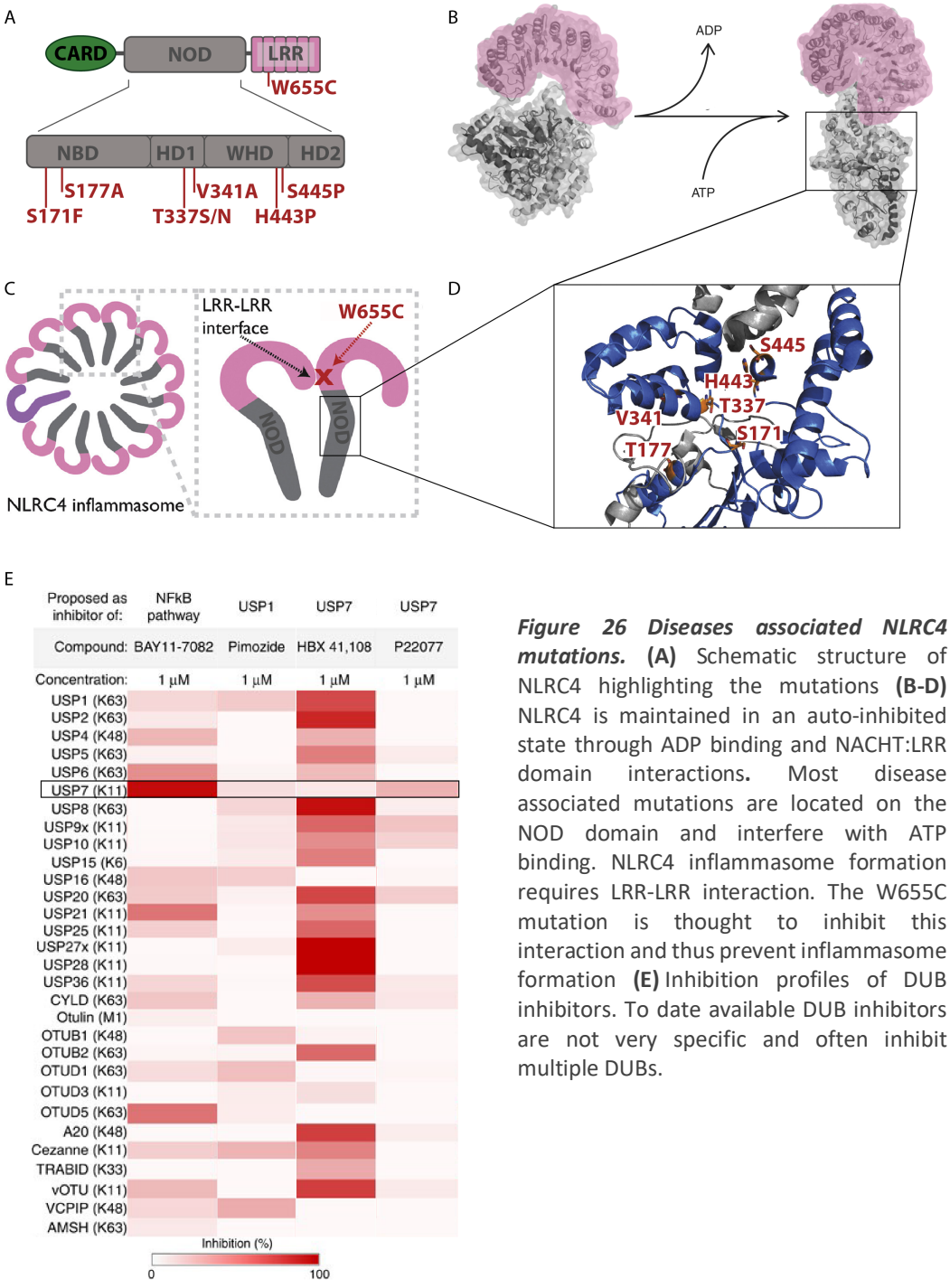

Figure 26 Diseases associated NLRC4 mutations. **(A)** Schematic structure of NLRC4 highlighting the mutations **(B-D)** NLRC4 is maintained in an auto-inhibited state through ADP binding and NACHT:LRR domain interactions**.** Most disease associated mutations are located on the NOD domain and interfere with ATP binding. NLRC4 inflammasome formation requires LRR-LRR interaction. The W655C mutation is thought to inhibit this interaction and thus prevent inflammasome formation **(E)** Inhibition profiles of DUB inhibitors. To date available DUB inhibitors are not very specific and often inhibit multiple DUBs.

With no NLRC4-specific therapy available, to date patients are treated with drugs targeting downstream inflammatory mediators in a broad and unspecific fashion: While non-steroidal anti-inflammatory drugs, corticosteroids recombinant IL-1RA (anakinra) and cyclosporine are often used effectively, some patients still succumb to the disease, suggesting that early diagnosis and more specific drugs are critical for effective intervention (*263, 267, 274*).

The ability to be able to potentially inhibit NLRC4 selectively is thus an interesting option for treating these patients. Our data suggest that the inhibition of USP7 could be used as an upstream inhibition of NLRC4 activity.

Therapeutic DUB inhibitor development is still in its early stages. With VLX1570, the first USP inhibitor (USP14) entered clinical trials in 2015 (*275*). Since then, multiple other DUB trials have been initiated. USP7 is being studied as a drug target in a wide range of malignancies, including multiple myeloma, breast cancer, neuroblastoma, glioma, and ovarian cancer (*276-280*). Several small molecular inhibitors of USP7 have been developed and tested in preclinical studies and are soon thought to enter clinical trials (*213, 281*). Pimozide, an FDA approved antipsychotic drug, has been shown to suppress cell growth of cancer cells in vitro. While this was mostly attributed to its inhibition of USP1, it is worth noting that Pimozide also inhibits USP7 (Figure 26 E) (*246, 282*).

5. Investigating the role of IKKβ in NLRP3 signalling

5.1. Introduction

IKKβ (IKBKB) has predominantly been studied with regard to its impact on NF-κB signalling (see chapter 1.5), as early mouse studies suggested that IKKβ and NEMO (IKBKG) are essential for its activation, while Ikkα is not (*283, 284*). It was found that *IKBKB*$^{-/-}$ mice exhibit embryonic lethality due to severe liver apoptosis (*285, 286*). Strikingly the lack of IKKβ in humans is not embryonically lethal, albeit leading to early infections (*287-289*).

Some studies show an anti-inflammatory effect observed by genetic ablation or small-molecule inhibition of IKKβ *in vivo* and explain this through and inhibition of the NF-κB pathway (*290-292*). However, others have shown that IKKβ inhibition can lead to spontaneous inflammatory conditions, thus arguing a role for NF-κB in the negative regulation of caspase-1 activation and IL-1β secretion. Intriguingly, studies on kinase inhibitors showed that inhibition of IKKβ or the upstream kinase TAK1 inhibits NLRP3 inflammasome activity independent of inhibitory effects on NF-κB (*293, 294*). As mentioned in section 1.5, both IKKα and IKKβ have been shown to phosphorylate a growing number of 'non-classical' substrates and exert multiple NF-κB independent functions. It was shown previously, for instance, that in the context of TNF signalling, the IKK complex phosphorylates RIPK1 at TNFR1 complex I (*295*). The NF-κB independent role of IKKα/IKKβ protected the cells from RIPK1-dependent death downstream of TNFR1. Other research studying the inhibition or loss of upstream kinase TAK1 also show a RIPK1 dependent cell death, describing it as apoptosis, necroptosis and pyroptosis (*296, 297*).

5.2. Chapter overview

As discussed above, the loss of IKKβ has been described to interfere with NF-κB signalling, while at the same time, conflicting data reports show both anti-inflammatory as well as spontaneous inflammation. To further understand the role of IKKβ both in NF-κB dependent and independent inflammasome signalling, we first set out to analyse the effect of IKKβ inhibition in mouse macrophages, as most of the previous studies focus on this model organism. While early inhibition of IKKβ leads to LPS induced pyroptosis

in mouse macrophages, late-stage inhibition has an inhibitory effect even on Nigericin induced pyroptosis. In human macrophages no LPS induced proptosis was detectable in IKKβ deficient cells, highlighting a key difference between mice and man. Moreover, we could observe a striking reduction of pyroptosis in the knockouts after Nigericin stimulation. We could show that this effect was independent of NF-κB and upstream of caspase-1 activation.

In order to identify the catalytic IKKβ target responsible for NLRP3 activation, we conducted phosphoproteomics, which led us to further study direct phosphorylation of NLRP3.

5.3. Results

5.3.1. Loss of IKKβ in mouse macrophages leads to pyroptosis after LPS treatment

As described above, the seemingly conflicting findings have been reported on the effect of the loss of IKKβ. To readdress and clarify the role of IKKβ in mice, we went on to generate *IKBKB*$^{-/-}$ J774 immortalised macrophages as an *in vitro* model system for murine macrophages. We were able to generate viable knockout clones, demonstrating that previously observed lethality *in vivo* dos not affect *in vitro* cell systems. To assess inflammasome activation, we subjected these macrophages to four hours of LPS priming and subsequently stimulated the cells with Nigericin. The *IKBKB* deficiency showed pyroptotic cell death already upon LPS treatment alone (Figure 27 A). IL-1β and IL-6 secretion, however, were completely absent in these knockouts (Figure 27 B-C). We also analysed the effect of the inhibitor TPCA1 on the J774 cells since the use of an inhibitor would allow us to study primary cells. This potent, selective inhibitor of IKKβ (IC_{50} = 17.9 nM) displays high selectivity over IKKα and other kinases (*298*). J774 cells were treated with 4 µM TPCA1 for 30 minutes prior to priming and stimulated with LPS for two hours and subsequently stimulated with Nigericin for two hours. The inhibitor showed a comparable effect on both LDH release and IL-1β secretion (Figure 27 D-E), thus making the inhibitor a useful tool for further experiments.

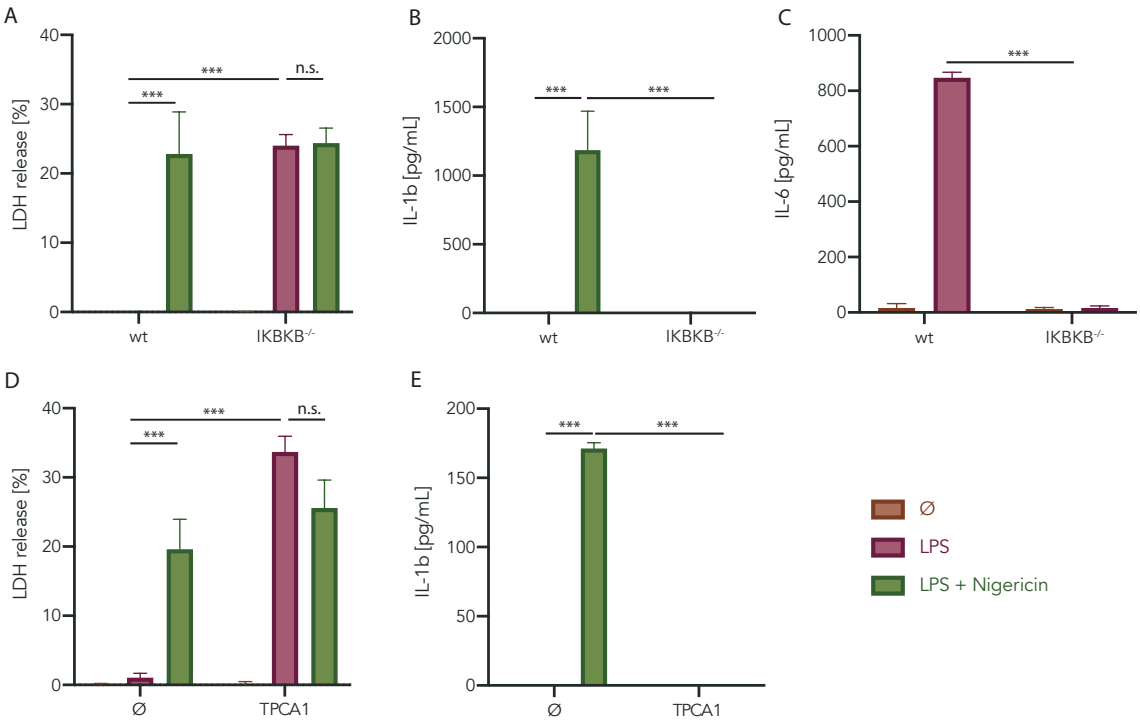

Figure 27 **Role of IKKβ in LPS induced cell death in J774 immortalised mouse macrophages. (A-C) WT** or IKKβ KO J774 macrophages were treated with LPS for 4 h and subsequently stimulated with Nigericin for 2 h. **(D-E) WT** J774 macrophages were treated with 4 µM TPCA1 or left untreated prior to treatment with LPS for 2 h and subsequently stimulated with Nigericin for 2 h. Cytokine and LDH release are depicted as mean + SEM of three independent experiments.

We next conducted an experiment using murine bone marrow-derived macrophages treated with TPCA1 at different timepoints of stimulation. As observed in the immortalised cell line, the untreated cells showed cell death only after Nigericin treatment, whereas the inhibition of IKKβ prior to LPS treatment lead to cell death without the need of a second signal (Figure 28 A). Again, IL-1β secretion could only be observed after stimulation of both LPS and Nigericin (Figure 28 B) and was absent in all TPCA1 treated conditions. As both IL-6 and TNF levels are similarly reduced after treatment, this suggested that the loss of NFK-B dependent cytokine induction was responsible for the observed loss of interleukin production.

In cells treated with TPCA1 two hours after LPS treatment (labelled “with Nigericin” in Figure 28), the LPS-dependent cell death observed in the case of early IKKβ inhibition was strongly reduced. Interestingly, the classical Nigericin induced NLRP3 dependent cell death was also blocked. By immunoblot, we could show that the observed cell death was driven by the maturation of caspase-1 in all conditions leading to LDH release

(Figure 28 E). While the protein levels of NLRP3 were not affected by TPCA1 treatment, this did not explain the observed phenotype: functional levels of NLRP3 were present in all conditions and in the late TPCA1 treated conditions that show the strong reduction in pyroptosis levels NLRP3 levels are higher than in the early TPCA1 treat conditions, which show proptosis induction.

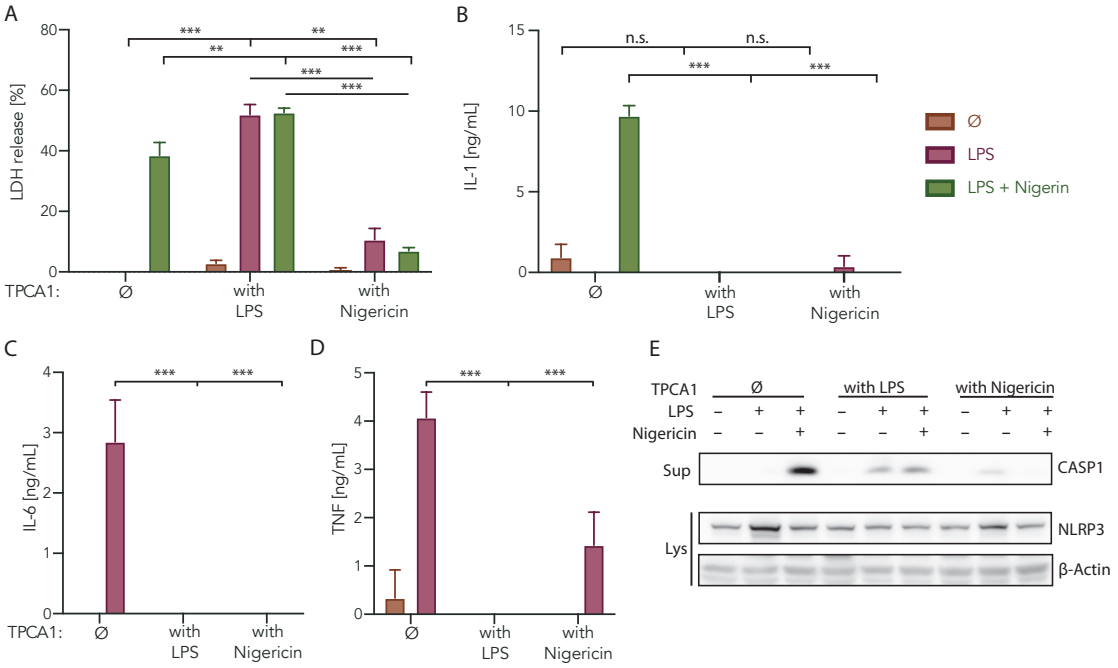

***Figure 28* Role of IKKβ in LPS induced cell death in murine bone marrow-derived macrophages.** 4 µM TPCA1 was added either together with LPS or Nigericin. BMDMs were treated with LPS for 2 h and subsequently stimulated with Nigericin for 2 h. **(A-D)** Cytokine and LDH release are depicted as mean + SEM of three independent experiments. **(E)** Immunoblot analysis of lysates and precipitated supernatant. One representative experiment of two is depicted.

In summary, our data show that the loss of IKKβ in mouse macrophages leads to pyroptotic cell death mediated through caspase-1 cleavage upon LPS treatment. At the same time, classical NLRP3 inflammasome signalling seems to be dependent on IKKβ. In mouse cells, this can only be studied when IKKβ gets pharmacologically inhibited shortly before NLRP3 stimulation, as the LPS mediated pyroptosis observed in the IKBKB deficient cells otherwise masks this effect.

Spontaneous IL-1β release after IKKβ inhibition, which was previously published, could not be detected in our stimulation conditions (*299*).

5.3.2. Loss of IKKβ in human macrophages does not lead to pyroptosis after LPS treatment

To study the underlying mechanisms in human macrophages, BLaER1 and THP1 cells deficient in *IKBKB* were generated. Cells were treated with LPS for two hours and subsequently stimulated with Nigericin or pA and Needle Toxin (LF-YscF) for additional two hours. In contrast to the data obtained in mice, LPS treatment on its own did not lead to pyroptosis in these cells (Figure 29 A, F). On the other hand, the inhibitory effect after additional Nigericin treatment was strongly present. As NLRC4 stimulation through Needle Toxin treatment showed no difference in LDH release between WT and *IKBKB*$^{-/-}$, it appears that the IKKβ requirement is specific to the NLRP3 inflammasome (Figure 29 A, F).

In IKBKB knockouts, IL-1β secretion was strongly reduced after stimulation of both inflammasomes, though showing a stronger phenotype after NLRP3 signalling (Figure 29 B, G). The fact that other NF-κB dependent cytokines were also blunted in *IKBKB*$^{-/-}$ both in THP1 and BLaER1 cells, this strongly suggested the loss of IL-1β release is also mainly due to a loss of NF-κB signalling in these cells (Figure 29 C-E). This observation is in line with multiple previous studies (*90*) that have implied the role of IKKβ in NF-κB dependent regulation of cytokines.

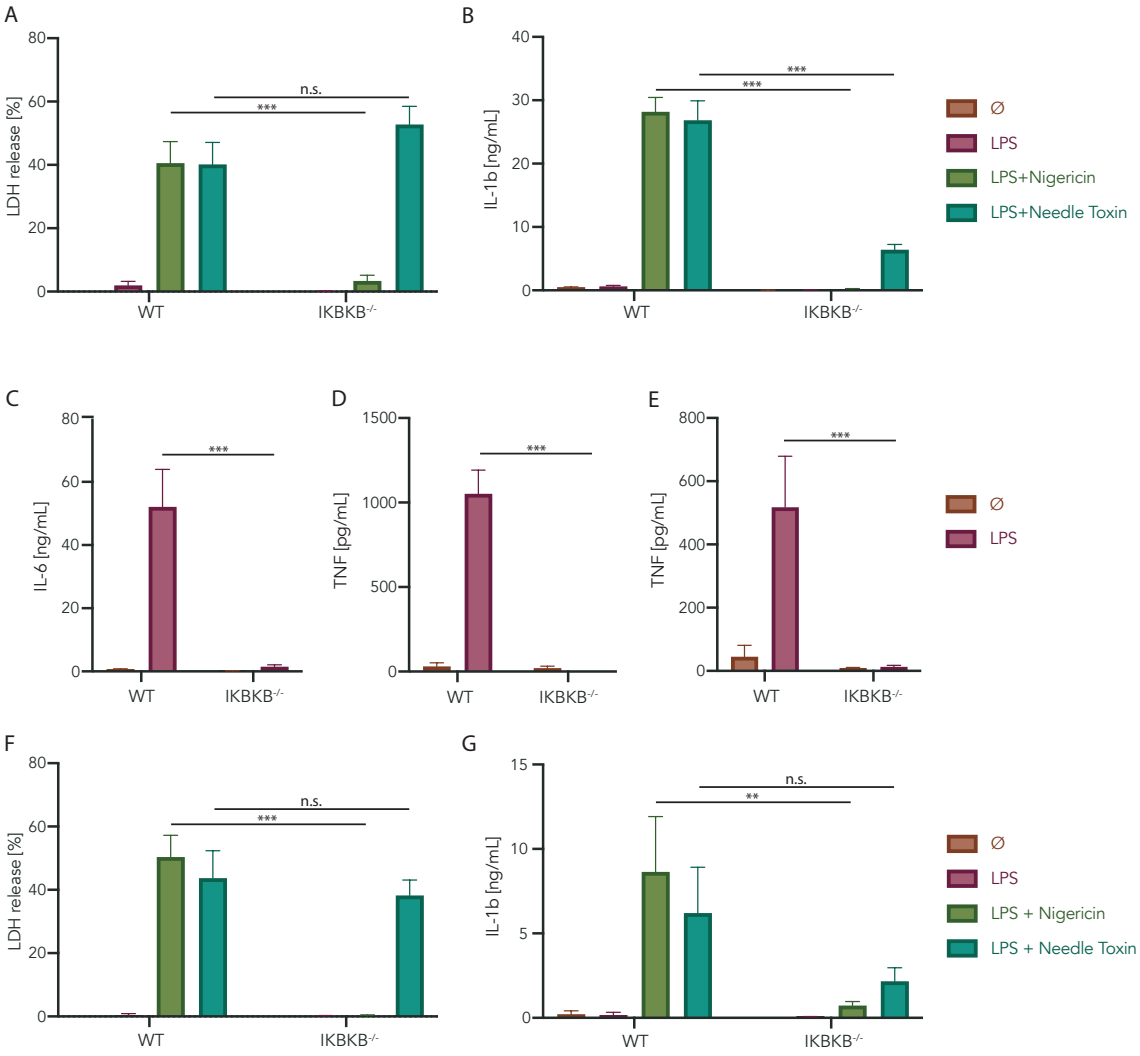

Figure 29 **Role of IKKβ in inflammasome activation in human monocytes. (A-D)** BLaER1 and **(E-G)** THP1 cells of the indicated genotype were stimulated for 2 h with LPS and subsequently stimulated with Nigericin or pA and Needle Toxin (LF-YscF) for 2 h. LDH and cytokine secretion are depicted as mean + SEM of three independent experiments.

5.3.3. NF-κB is not necessary for NLRP3 activation in human macrophages

To determine whether the observed IKKβ dependent NLRP3 mediated pyroptosis is also dependent on NF-κB signalling, we generated RelA deficient BLaER1 and THP1 cells. In the BLaER1 cells, we additionally created double knockouts also lacking RelB, to also disrupt non-canonical NF-κB signalling (cf. section 1.5). We stimulated these cells with LPS for four hours and checked the RNA transcription of the NF-κB dependent cytokines *IL1B* and *IL6* via qPCR (Figure 30 A-B). As expected, both in the *RelA*$^{-/-}$ as well as the *RelA*$^{-/-}$ x *RelB*$^{-/-}$ cells transcription levels were completely blunted due to the loss of NF-κB signalling.

We further performed immunoblotting of the phosphorylation of IκBα (pIκBα), a prominent NF-κB activation marker, in a time course stimulation with LPS (Figure 30 D). While phosphorylation levels of IκBα were detectable after one hour of LPS treatment in the wt, in RelA deficient cells no phosphorylation could be detected even after two hours of LPS treatment. Although IκBα phosphorylation takes place upstream of RelA release, our observed loss of IκBα phosphorylation in RelA deficient cells is in line with studies describing a positive feedback control of RelA on the IκBα phosphorylation (*233*). After establishing that the RelA knockout cells were entirely deficient in NF-κB signalling, we analysed the inflammasome activation in these cells. BLaER1 and THP1 cells were primed with LPS for two hours and subsequently stimulated with Nigericin. The NF-κB deficient cells still showed pyroptotic cell death similar to WT cells after NLRP3 activation (Figure 30 C-D). Additional depletion of the non-canonical signalling protein RelB mimicked the RelA single knockout. This indicates that the loss of inflammasome signalling observed cleavage in the IKBKB KO cannot be explained by a loss of NF-κB dependent transcriptional priming.

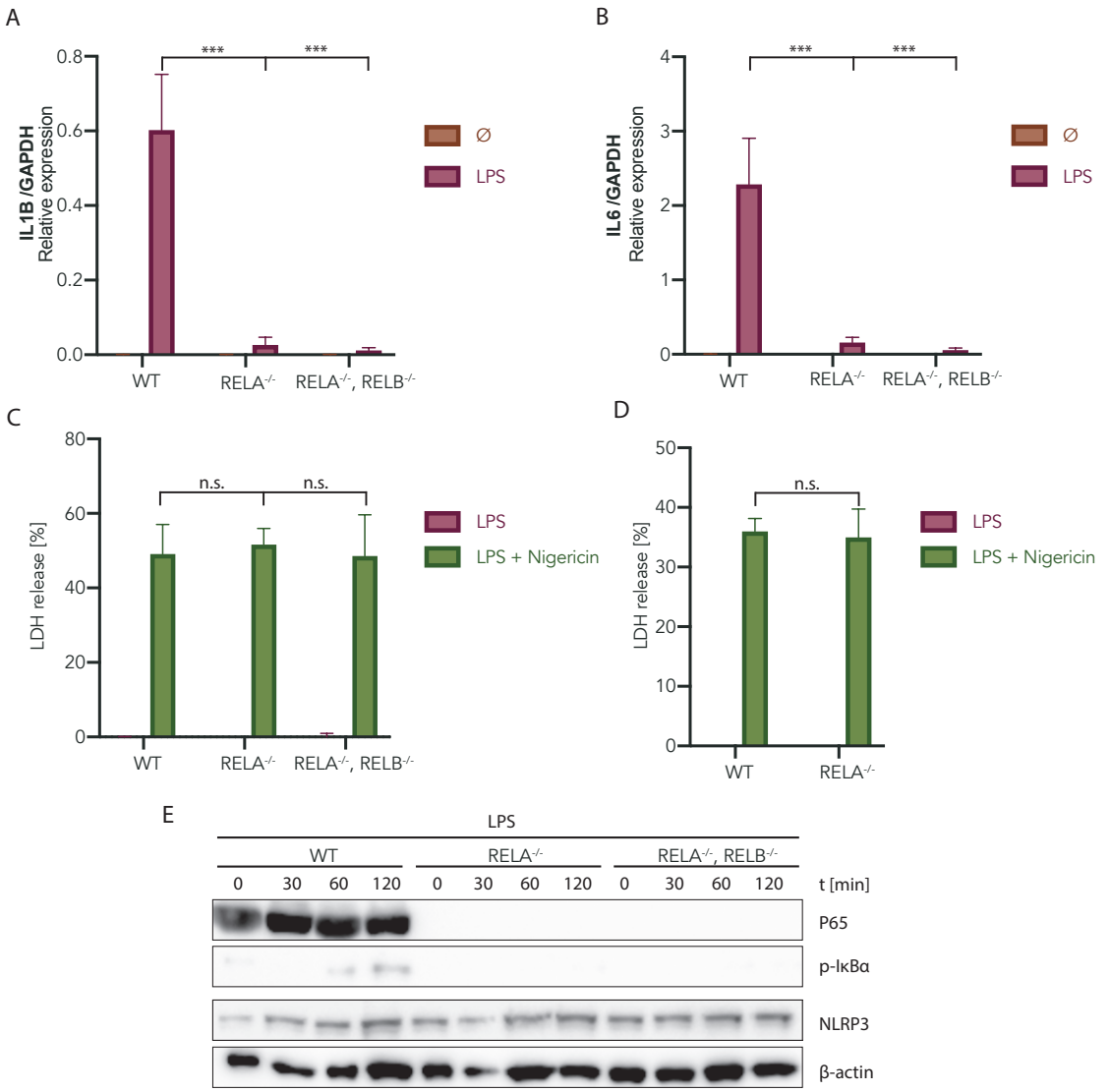

***Figure 30* NF-κB deficiency does not lead to loss of NLRP3 dependent cell death. (A-B)** BLaER1 monocytes of the indicated genotype were stimulated for 4 h with LPS or left untreated. Expression of *IL1B* **(A)** and *IL6* **(B)** was quantified by qRT-PCR. Shown are mean values + SEM of three independent experiments. **(C-D)** THP1 **(D)** and BLaER1 monocytes **(D)** of the indicated genotype were treated with LPS for 2 h and subsequently stimulated with Nigericin. LDH secretion is depicted as mean + SEM of three independent experiments. **(E)** BLaER1 monocytes of the indicated genotype were treated with LPS for the indicated time. Immunoblot of pIκBα and IκBα was performed as markers of NF-κB activation. One representative experiment of two is depicted.

5.3.4. IKKβ plays an NF-κB independent role in NLRP3 activation

As shown in the previous sections, NF-κB disruption is visible both in RelA (Figure 30) and IKBKB deficient cells (Figure 29) when analysing cytokine secretion. LDH release and caspase-1 maturation, on the other hand, can be used as priming independent pyroptosis readouts. Using these readouts, we could observe that in BLaER1 monocytes, while IKKβ is strictly required for NLRP3 signalling, the IKK-complex member IKKα is

dispensable. However, we could observe, that the double knockout of IKKα (CHUCK) and IKKβ, was able to reduce LDH release slightly more than observed in the single IKKβ knockout (Figure 31 A).

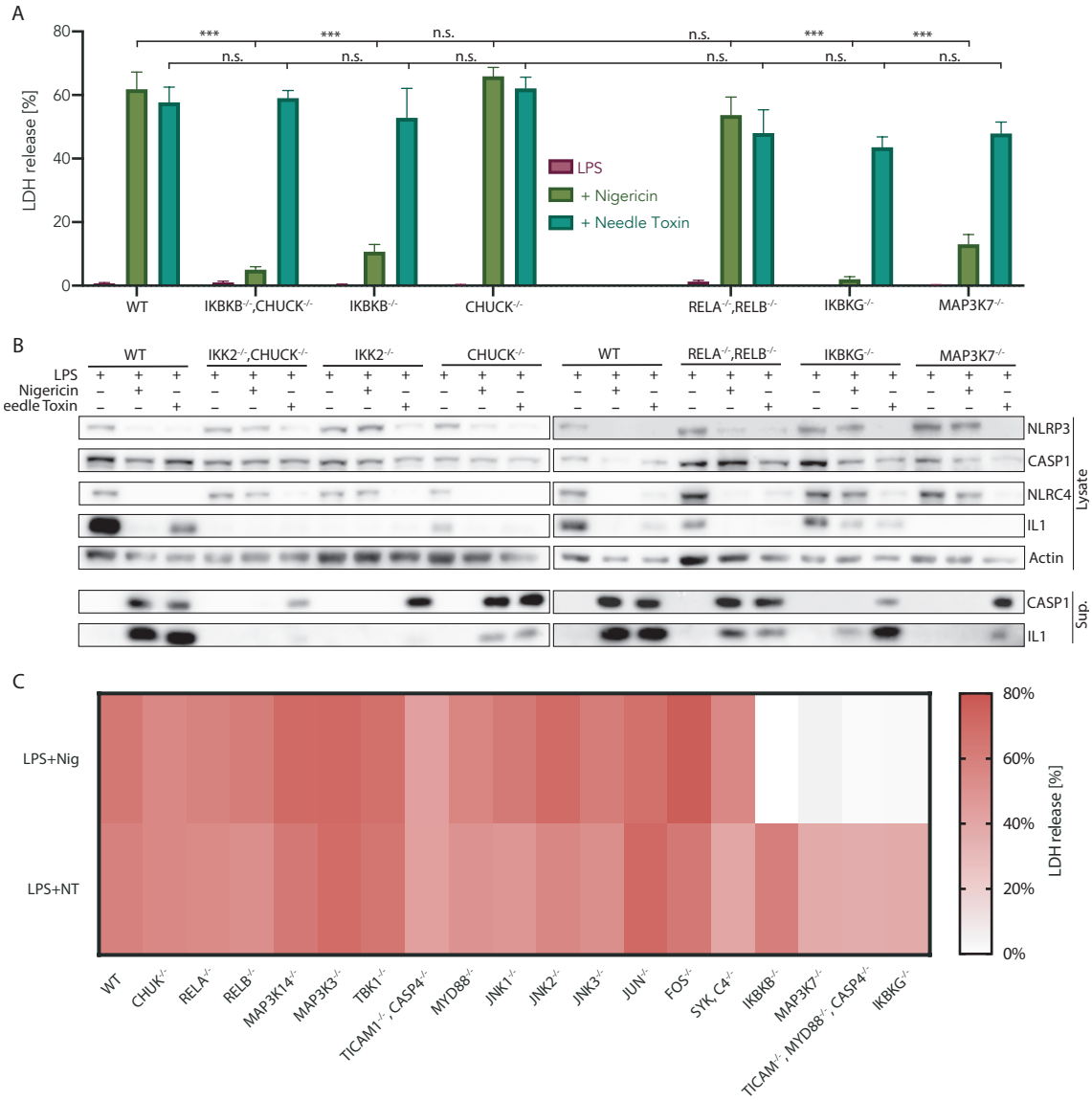

Figure 31 **IKKβ and upstream signalling components are necessary for caspase-1 maturation, while downstream NF-κB signalling is not.** BLaER1 monocytes of the indicated genotype were treated with LPS for 2 h and subsequently stimulated with Nigericin or Needle Toxin for 2 h. **(A)** LDH secretion is depicted as mean + SEM of three independent experiments **(B)** Immunoblot analysis of BLaER1 monocytes lysates and precipitated supernatant of indicated genotype. One representative experiment of two is depicted. **(C)** Heatmap of LDH secretion depicted as mean of at least two independent experiments.

While depleting downstream NF-κB signalling and various upstream signalling components did not show a disruption of NLRP3 activation (Figure 31 C), loss of the upstream molecules TAK1 (MAP3K7) and Nemo (IKBKG) also showed a loss of signalling. By conducting immunoblot analysis of precipitated proteins from the supernatant, we could show that the loss of LDH release corresponded with a loss of mature caspase-1

in all observed conditions (Figure 31 B). IL-1β levels in the supernatant and lysates corresponded to these results.

5.3.5. Primary human macrophages rely on IKKβ for NLRP3 activation

In order to confirm our findings in primary cells, monocytes isolated from PBMCs were differentiated with hM-CSF for seven days to obtain monocyte-derived human macrophages. Cells were primed with 50 pg/ml of LPS (2 h) and stimulated with 6.5 µM Nigericin or 0.25 µg/ml pA and 0.025 µg/ml Needle Toxin (LF-YscF) for two hours. To inhibit IKKβ, 4 µM TPCA1 was added prior to LPS priming. As observed with the knockout cell-lines, the inhibition of IKKβ in primary macrophages also led to a loss of pyroptotic cell death after NLRP3 activation while not affecting NLRC4 signalling (Figure 32 A). The secretion of IL-1β and IL-6 also followed the pattern observed in the cell-line knockouts (Figure 32 B, C). Immunoblotting further validated these results (Figure 32 D).

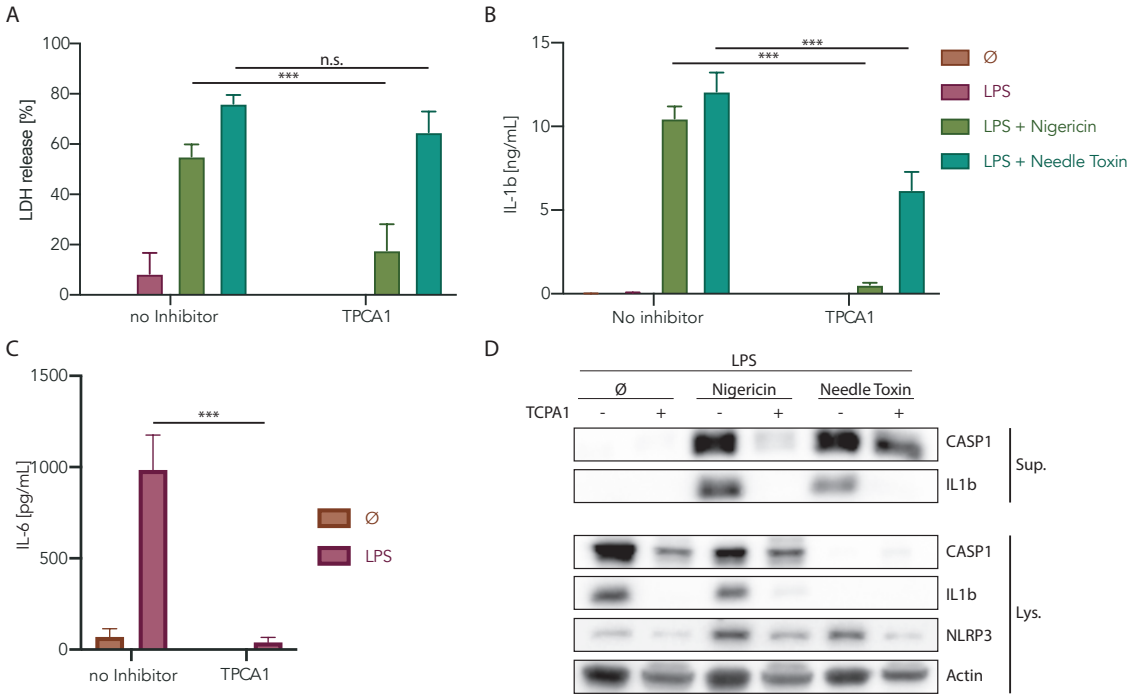

***Figure 32* NLRP3 signalling in Primary human monocytes depends on IKKβ activity.** Human monocytes were isolated from PBMCs were treated with 4 µM TPCA1 or left untreated prior to treatment with LPS for 2 h and subsequently stimulated with Nigericin or Needle Toxin for 2 h. **(A-C)** LDH and cytokine secretion are depicted as mean + SEM of three independent experiments. **(D)** Immunoblot analysis of monocyte lysates and precipitated supernatant. One representative experiment of two is depicted.

Since we also wanted to work with complete genetic ablation instead of inhibitors in primary human cells, we adopted an *in vitro* differentiation protocol in which human iPS cells are differentiated into macrophages (hiPS-Macs) (*195*). The lab of Florent Ginhoux kindly provided iKKβ deficient hiPS-Macs. By analysing the cells via immunoblot, we could validate that no IKKβ was detectable in the knockouts. After differentiating the cells following the procedure published by Takata *et al*., macrophages were primed with LPS for two hours and four hours and subsequently treated with Nigericin or Needle-Toxin. NLRP3 dependent pyroptosis, as measured through LDH, was entirely dependent on IKKβ.

Moreover, IL-1β and IL-18 release were also fully IKKβ dependent (Figure 33 B, E, F). Residual IL-6 and TNF production was observable, albeit notably reduced (Figure 33 C, D). In summary, our data from primary human macrophages and iPS-Macs confirms the role of IKKβ in primary human cells.

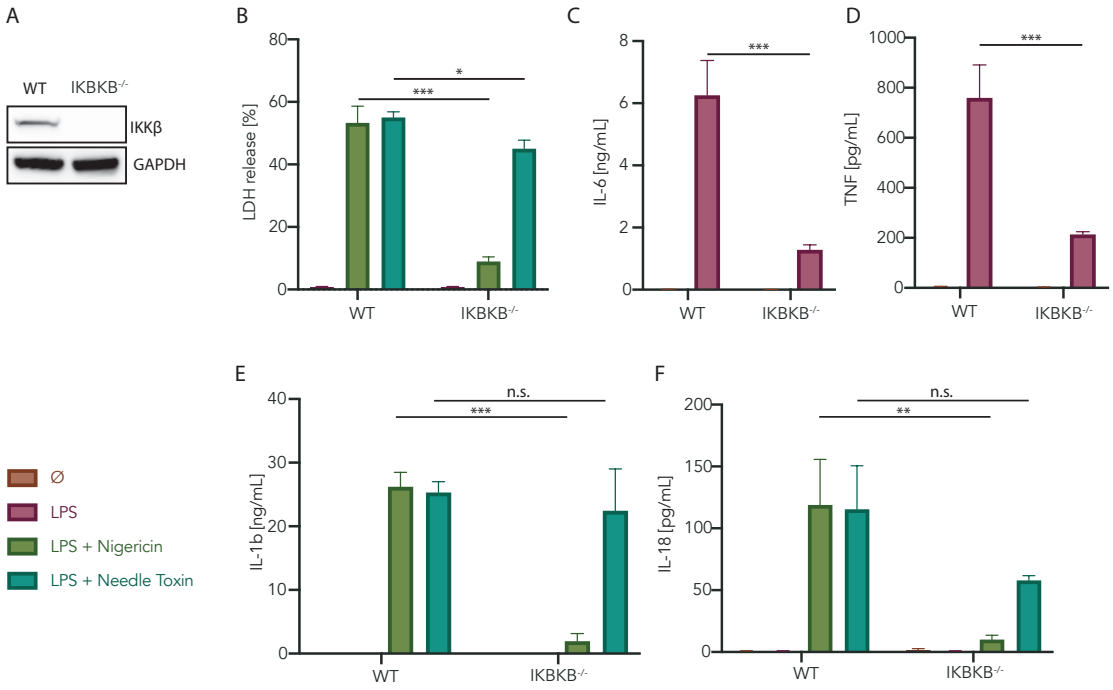

***Figure 33* NLRP3 signalling in human iPS cells depends on IKKβ activity. (A)** hiPS-Macs used for the experiments were analysed by immunoblot for the expression of IKKβ. GAPDH was used as housekeeping gene. **(B-F) WT** and *IKBKB*$^{-/-}$ hiPS-Macs were treated with LPS for 2 h and subsequently stimulated with Nigericin or Needle Toxin for 2 h. LDH release (B), IL-6 (C), TNF (D), IL-1β (E) and IL-18 (F) secretion are depicted as mean + SEM of two independent experiments.

5.3.6. IKKβ is necessary for potassium independent NLRP3 signalling

Previous models have suggested K^+-efflux to lead to rapid interaction between proteins involved in NLRP3 signalling (*153, 154*). Since then, studies have shown a K^+-efflux-independent activation of NLRP3 through the immune modulator imiquimod (ct. section 1.7) (*157*).

We thus set out to study if this K^+-efflux-independent NLRP3 activation also requires IKKβ. We primed BLaER1s for two hours with LPS and treated them with 30 µg/ml imiquimod for two hours. The LDH release after this treatment resembled the results obtained after K^+-dependent NLRP3 stimulation with a loss of LDH release in IKKβ deficient cells and no effect of NF-κB deficiency (Figure 34).

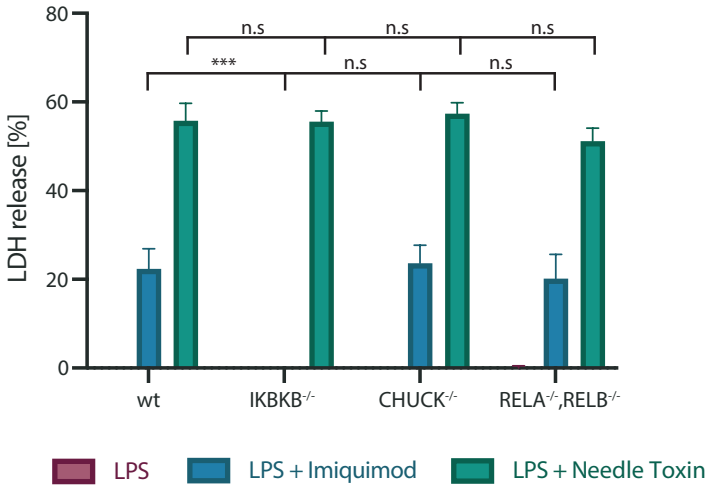

***Figure 34* Potassium independent activation via imiquimod requires IKKβ.** BLaER1 monocytes of the indicated genotype were treated for 2 h with LPS and subsequently stimulated with 30 µg/ml imiquimod for 2 h. LDH secretion is depicted as mean + SEM of three independent experiments.

With the finding that K^+-efflux-independent activation is also dependent on IKKβ we can conclude that IKKβ does not play a role in potassium sensing or signalling, but more likely is involved in a master activator necessary for all forms of NLRP3 activation.

5.3.7. Kinase function of IKKβ is necessary for NLRP3 signalling

After establishing that IKKβ is required both potassium dependent and independent NLRP3 activation, we wanted to further investigate the underlying mechanism of activation. In the IKK complex the scaffolding function of proteins, and not necessarily their enzyme activity, are in some cases essential for signal transduction (ct. section 1.5) (*300-302*). The mitotic spindle kinase NEK7 was also shown to function independently of its kinase role in NLRP3 activation (*153, 154*). Due to these facts, we wanted to investigate whether the kinase function of IKKβ is necessary for its role in NLRP3 activation. For this, we generated BLaER1 *IKBKB*$^{-/-}$ cells expressing the catalytically inactive mutant (K44M) or wildtype IKKβ in a doxycycline dependent manner. Similar levels of both constructs were expressed after doxycycline treatment as verified via immunoblot (Figure 35 A). Cells were primed and stimulated with Nigericin, imiquimod and Needle Toxin. Both in the case of Nigericin and imiquimod stimulation, the WT complementation showed pyroptotic cell death which was absent in the cells complemented with the kinase-dead mutant (Figure 35 B). As expected, as the depletion of IKKβ had no impact on NLRC4 activation, neither did the complementation.

IL-1β secretion of cells transduced with the kinase-dead mutant was blunted for all conditions (Figure 35 C). This is in line with previous studies that showed IKKβ K44M to inhibit RelA nuclear translocation (*93*).

This data show that the scaffold function is not sufficient, but the kinase activity of IKKβ is necessary for NLRP3 signalling.

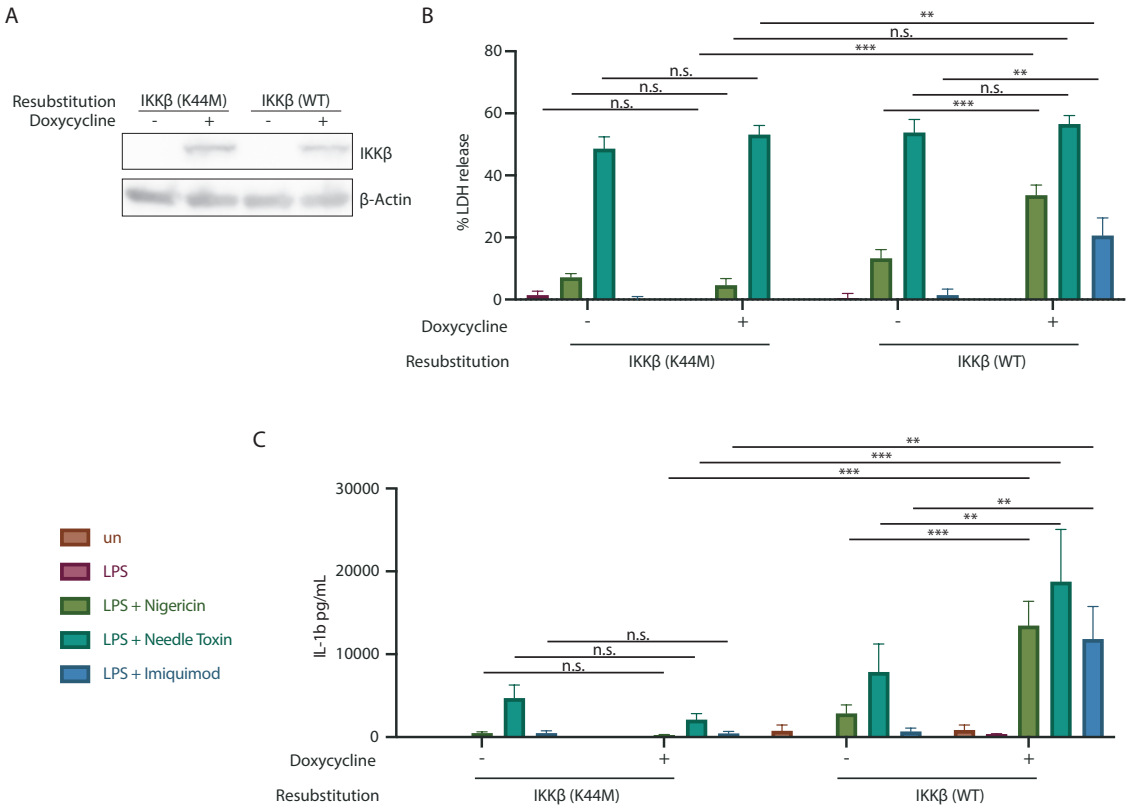

***Figure 35* IKKβ kinase activity is required for NLRP3 signalling. (A-C)** IKKβ knockout BLaER1 cells transduced with an inducible construct for WT or K44M Ikk2 were treated with doxycycline for 8 h or left untreated. **(A)** Cells used for the experiments were analysed by immunoblot for the expression of IKKβ. β-Actin was used as housekeeping gene. **(B, C)** Cells were treated with LPS for 2 h and subsequently stimulated with Nigericin or Needle Toxin for 2 h. LDH release (B) and IL-1β (C) secretion are depicted as mean + SEM of two independent experiments.

5.3.8. IKKβ triggers a rapid short-lived PTM enabling NLRP3 activation

In contrast to transcriptional regulation, post-transcriptional regulation enables a rapid form of regulation. Inhibition of this line of regulation should be effective even when applied at later timepoints. As all of our data discussed in the previous chapters hinted towards such a rapid post-translational modification, we set out to further analyse this by inhibiting IKKβ at different timepoints throughout the stimulation. For this, BLaER1, THP1 and primary human monocytes were treated with TPCA1 at different timepoints of the experiment (with priming; with inflammasome stimulus; after inflammasome stimulus). In all experiments, the addition of TPCA1 together with or even 30 minutes after Nigericin treatment strongly reduced cell death and IL-1β secretion (Figure 36). For NLRC4 inflammasome activation, after Needle Toxin treatment, nearly no reduction in

LDH release was observed and, for late inhibitor treatments, IL-1β secretion was likewise barely affected.

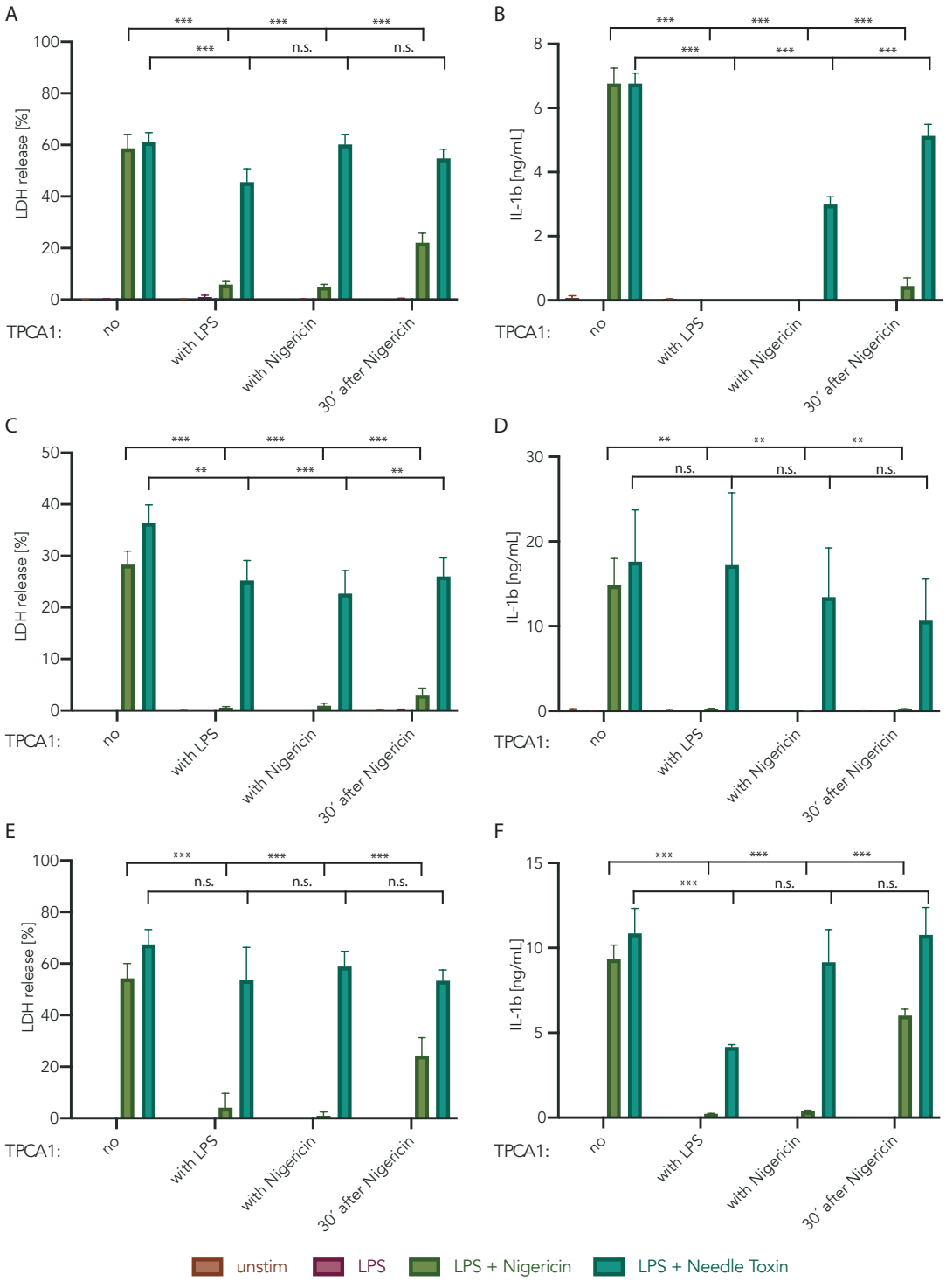

Figure 36 **Rapid effect of IKKβ inhibition on NLRP3 inflammasome. (A, B)** BLaER1 **(C,D)** THP1 cells and **(E, F)** primary human monocytes were treated with LPS for 2 h and subsequently stimulated with Nigericin or Needle Toxin for 2 h. 4 µM TPCA1 was added at different timepoints of the experiment. LDH and cytokine secretion are depicted as mean + SEM of three independent experiments.

In summary, this data - together with our previous findings - suggests a direct and possibly rapid, short-lived phosphorylation event through IKKβ, which is required for further activation of NLRP3.

5.3.9. Analysis of IKKβ dependent phosphoproteome

After determining the importance of the IKKβ kinase function, we set out to search for potential substrates of IKKβ. For this, we studied IKKβ-mediated phosphorylation in label-free cultured BLaER1 cells via phosphoproteomics. We analysed the phospho-proteome of cells left untreated, pre-treated for two hours with LPS alone, or with addition of 30 minutes of Nigericin. As a reference, full proteomes without phosphopeptide enrichment were also measured.

Phosphoproteomic sample preparation and measurement was performed by Dr. M. Tanzer (Mann Department, MPI Munich) following a recently published method (*205*).

In brief, extracted proteins from the SDC lysates (30 x 10^6 cells/condition) were digested with trypsin and phosphopeptides were enriched with titanium dioxide (TiO_2) beads. After further purification by StageTip cleanup, high-resolution mass spectrometry and comprehensive bioinformatics were carried out to identify new proteins that could be potential targets of IKKβ (workflow depicted in Figure 37).

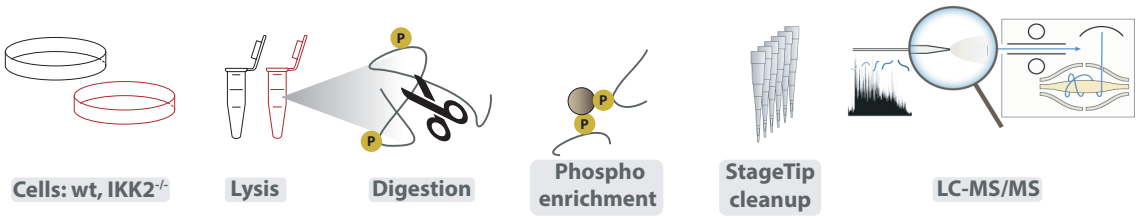

Figure 37 Workflow of Phosphoproteomics. Steps involved in preparing samples using the high-sensitivity workflow described by Humphrey *et al.* (*205*). Samples are lysed, digested and enriched followed by StageTip cleanup and LC-MS/MS measurement.

In total, we identified about 20,000 phosphorylation sites from 4,403 proteins. We first focused on the effect of LPS stimulation of wildtype cells to validate our experimental settings.

Following LPS stimulation, we identified 15727 phosphorylation sites on 3427 proteins, of which 910 phosphorylation sites on 501 proteins were considered significantly regulated compared to the unstimulated samples (Figure 38).

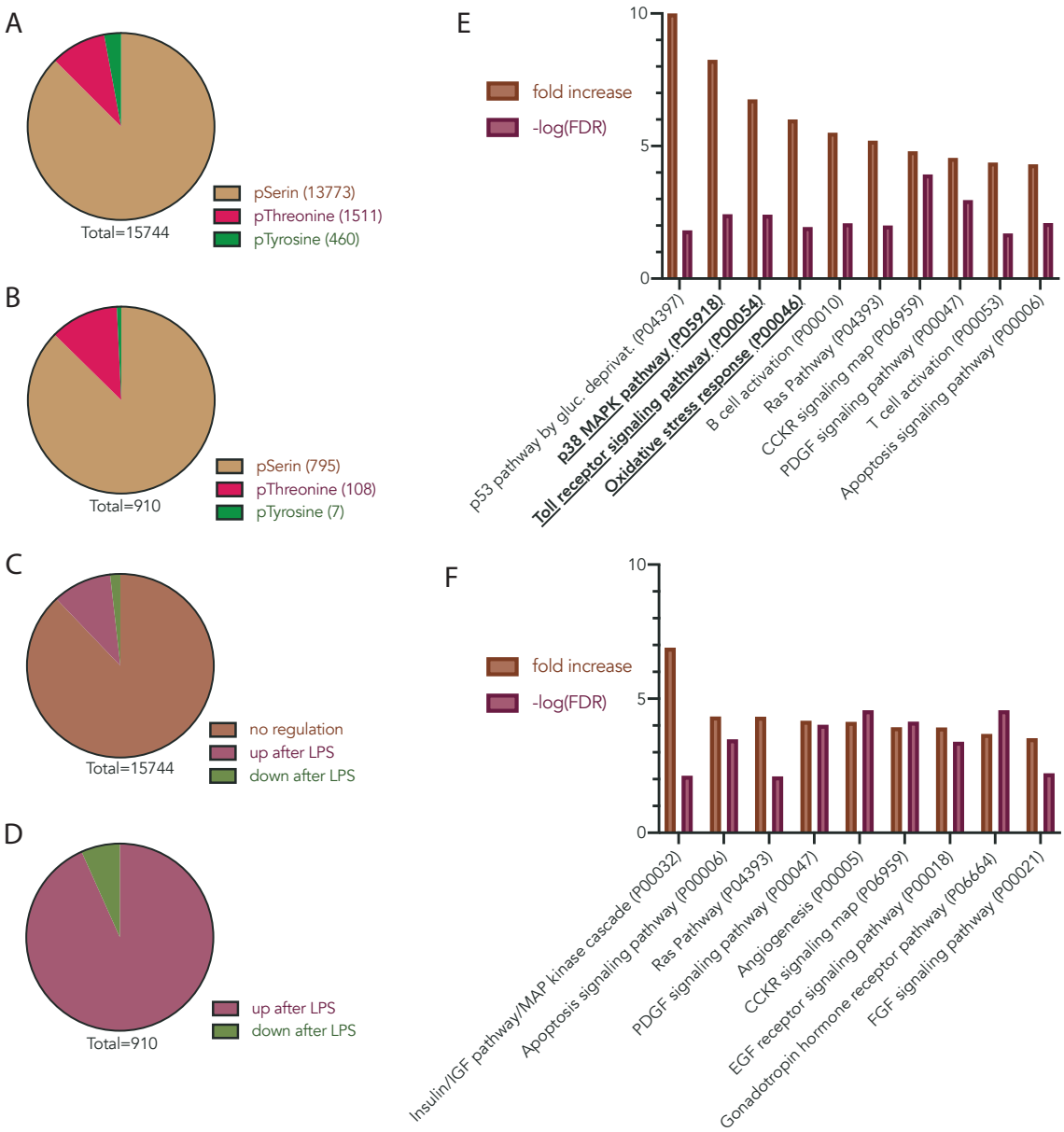

Figure 38 **Analysis of phosphosites in BLaER1 treated with LPS. (A, B)** Distribution of phosphorylated amino acids in WT BLaER1 cells after LPS treatment. Numbers of quantified serine- (pS), threonine- (pT), tyrosine- (pY) phosphorylation sites in total dataset **(A)** and significantly regulated dataset **(B)**. **(C,D)** Extent of regulation by LPS on WT BLaER1 cells. A threshold of at least 1.5-fold-change was used as a threshold to define up-regulated and down-regulated phosphorylation sites in the total dataset **(C)** and significantly regulated dataset **(D)**. **(E, F)** Over-represented signalling pathways after LPS treatment. Proteins with significantly up-regulated phosphosites were assigned to GO Gene Ontology terms for signalling pathways for WT **(E)** and IKKβ Knockout cells **(F)**.

Most phosphorylation sites were on serine (87%) and threonine residues (12%), tyrosine phosphorylation accounting for less than 1% of the sites (Figure 38 A, B). These ratios are consistent with studies analysing phospho-proteomic profiles in human macrophages (*303, 304*). As expected, LPS treatment led mostly to upregulation of phosphosites (Figure 38 C, D). A GO term analysis on proteins with strongly induced

(>1.5 log2 change) phosphosites showed enrichment of proteins relevant in MAPK and TLR signalling (Figure 35 E). An identical GO term analysis conducted with IKKβ knockouts did not show the enrichment of these signature signalling proteins (Figure 38 F).

As we had observed that even late inhibition of IKKβ leads to protection against cell death (chapter 4.2.6), we analysed Nigericin treated samples to find unique phosphosites that are not present after LPS treatment but only occur after Nigericin treatment (Figure 39).

Of note, the GO term analysis on proteins that were only found to be significantly phosphorylated after Nigericin treatment showed high enrichment scoring for the families “inositol phosphate biosynthetic process” and “Golgi to plasma membrane protein transport” (Figure 39 D, E).

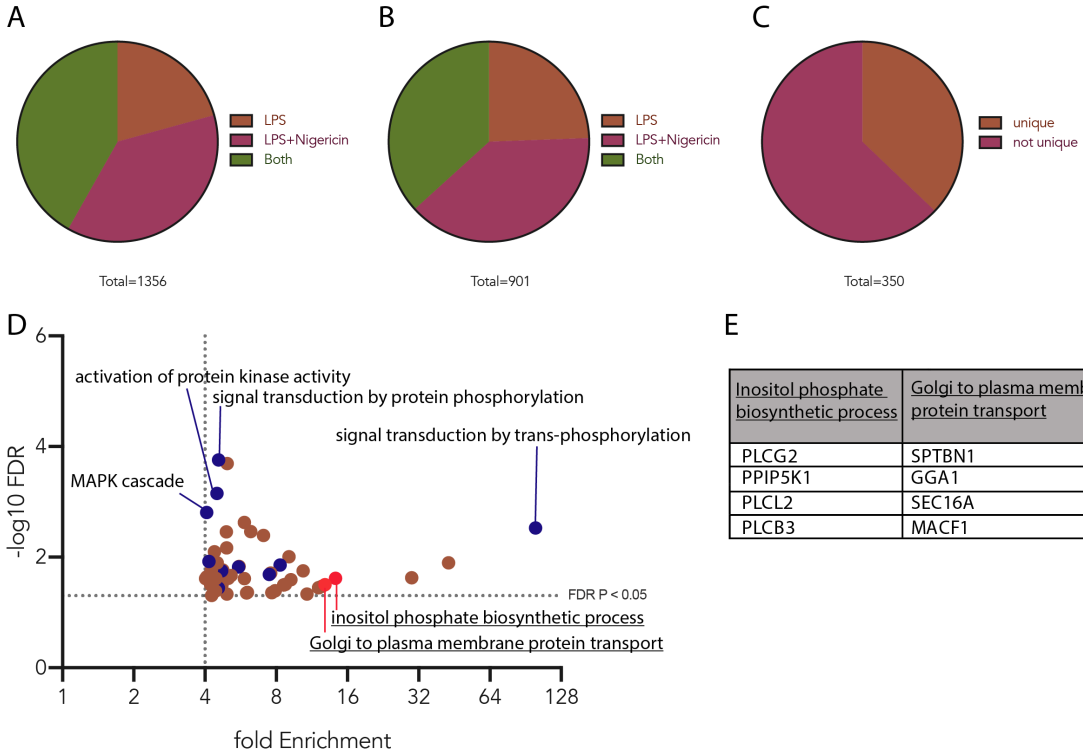

Inositol phosphate biosynthetic process	Golgi to plasma membrane protein transport
PLCG2	SPTBN1
PPIP5K1	GGA1
PLCL2	SEC16A
PLCB3	MACF1

Figure 39 **Analysis of phosphorylation events observed only after Nigericin treatment.** Significantly up-regulated phosphosites (A) and phosphoproteins (B) in BLaER1 WT cells. (C) Significantly up-regulated phosphoproteins (from B) observed after Nigericin treatment were reanalysed for their “unique” appearance exclusively in the Nigericin treated dataset. These unique Nigericin induced phosphoproteins were assigned to GO Gene Ontology terms for GO biological processes. (E) Proteins involved in Inositol phosphate biosynthesis and Golgi to plasma membrane transport.

5.3.10. Investigating NLRP3 as a direct substrate of IKKβ

In the proteomic dataset, we found phosphopeptides mapping to NLRP3. These phosphorylation events could predominantly be found in WT samples and to a much lesser degree in IKKβ KO. The phosphosite identified was on S163, which lies in close proximity to the polybasic region, which was shown to play an important role in NLRP3 activation. To get more detailed data on this region, we conducted a targeted proteomics experiment. Untreated and LPS treated samples were prepared and enriched as described above, while the mass spectrometer was set to focus on ions of a specific mass (m/z) at a specific time, matching the region of interest which were derived from the previous analysis. This detailed and precise analysis also confirmed the reduction of the phosphorylation upon IKKβ depletion and also showed no induction after LPS stimulation. In this, more detailed analysis, also S161 was found to be phosphorylated. S161, in contrast to S163, was also a predicted phosphorylation site of IKKβ by multiple in silico analysis that we conducted (PhosphoNET Kinase Predictor, PHOSIDA, GPS5.0). The recently published phosphosite on S198 is in close proximity, but not on the same peptide as our targeted proteomics was focused on (Figure 40) (*185*). S198 was also not detected in the initial phosphoproteomic experiment. However, this peptide was also not detectable in the total proteome measurement that was conducted in parallel. This is in line with previous proteomics experiments, we and collaborators have conducted, that have shown us that the coverage of NLRP3 is generally very poor in mass spectrometry experiments.

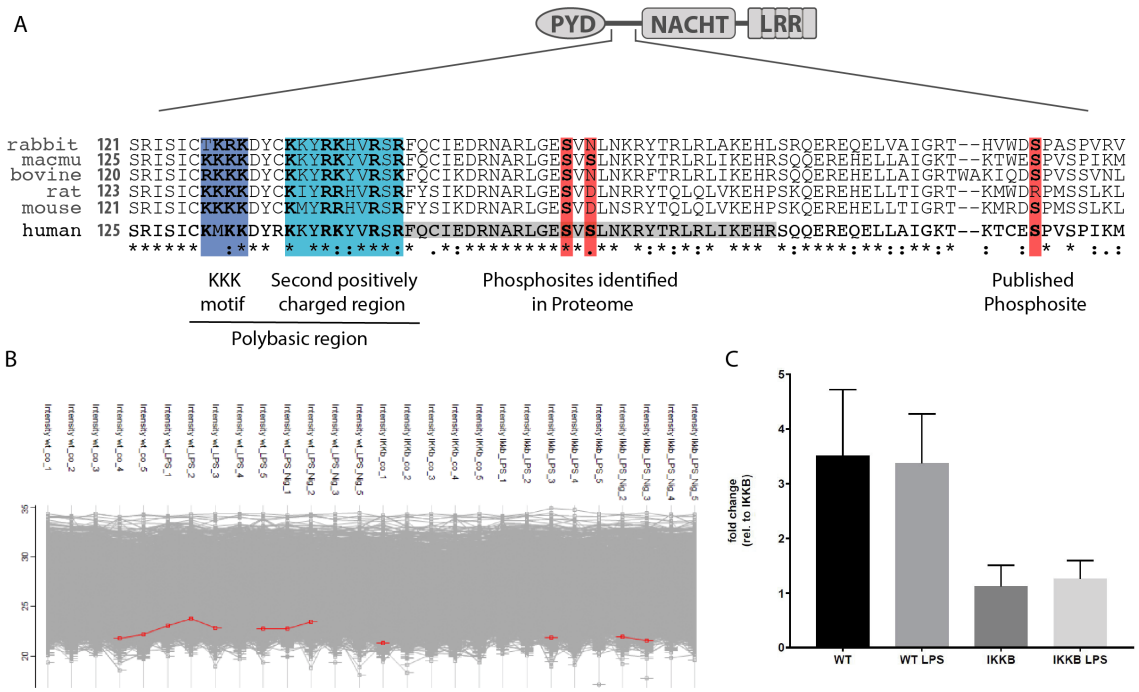

Figure 40 **IKKβ dependent phosphorylation sites detected on NLRP3. (A)** Both the phosphosites found in our proteomic experiments and a previously published phosphosite are located near the polybasic region (highlighted in blue) of NLRP3 which is highly conserved in many NLRP3 orthologues (aligned using Clustal Omega). Detected peptide is highlighted in grey. **(B)** Mass spectrometry traces with indicated detection of phosphorylated S161/S163 in individual samples. **(C)** Fold change of the phosphorylated peptide in the targeted proteomic measurement.

To investigate the role of S161 and S163, NLRP3 knockout BLaER1 cells were transduced with constructs containing phospho-dead (Ala) mutants at the respective sites. Transduction levels were analysed via western blot. Cells were differentiated and stimulated as in previous experiments. Both S161A and S163A, as well as the double mutant, showed no reduction in LDH release after NLRP3 stimulation compared to the WT transfected cells (Figure 38).

Song *et al.* convincingly demonstrated the role of murine S194 (homologue to human S198) in knock-in mice, while the proposed mechanism of JNK1 mediating this phosphorylation was mostly only backed by data using the inhibitor (*185*). However, due to studies that describe JNK independent effects of this inhibitor, its selectivity was disputed (*305*). We thus generated full genetic knockouts of JNK1 and activated the NLRP3 and NLRC4 inflammasome in these cells (Figure 41 C, D). JNK1 depletion did not result in a loss of function upon NLRP3 stimulation. We thus speculated that the phosphorylation observed by Song *et al.* is actually mediated through IKKβ.

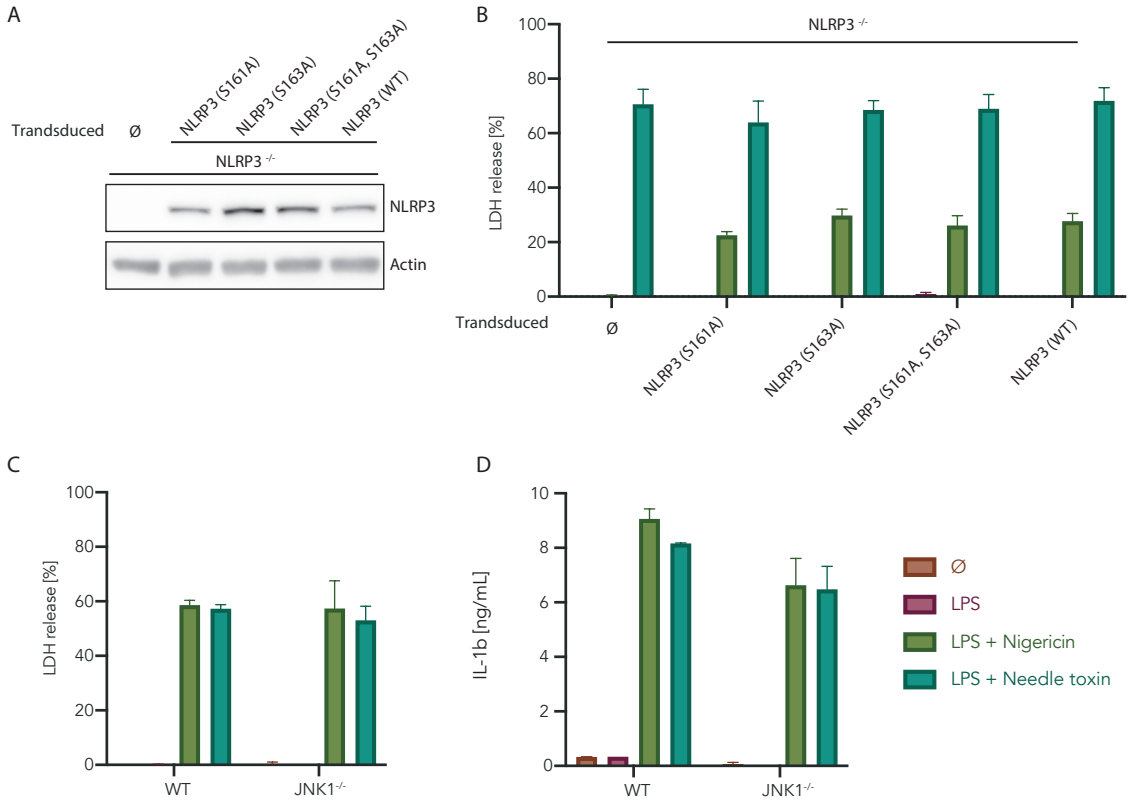

Figure 41 **NLRP3 signalling does not rely on S161, S163 or JNK1. (A-B)** NLRP3 knockout BLaER1 cells stably transduced with constructs containing mutant and WT NLRP3. **(A)** Cells used for the experiments were analysed by immunoblot for the expression of IKKβ. β-Actin was used as housekeeping gene. **(B-D)** Cells were treated with LPS for 2 h and subsequently stimulated with Nigericin or Needle Toxin for 2 h. LDH release and IL-1β secretion are depicted as mean + SEM of two independent experiments.

To further study this theory, a monoclonal antibody against the phosphorylated serine at this position was generated. For the generation of the antibodies (Figure 42), mice were immunised with synthesised peptides containing the phosphorylated serine (KTKTCEpSPVSPIK). After immunisation, antibody-producing B-cells from the spleen were harvested and fused with a myeloma cell line according to standard procedures (this work was performed by the group of Dr. E. Kremmer, Biology LMU Munich). The antibodies from the hybridoma culture supernatants were selected for specificity and high-affinity binding by ELISA. Throughout all immunisation, only one antibody was found to be suitable and was further validated via Western blot. For this purpose, we generated lysates from BLaER1 cells that were either treated with LPS for four hours or were kept untreated. We chose these conditions, as S189 phosphorylation was shown to appear robustly at this timepoint, and we wanted to ensure that any signal from the antibody, was produced due to specific detection of this modification. Unfortunately,

no specific signal was detectable both in whole lysates, as well as after enrichment by IP using a commercial NLRP3 antibody. Further testing will be conducted with other antibodies to further investigate the phosphorylation of this site.

***Figure 42* Schematic of phospho-specific NLRP3 antibody generation.** A synthesised peptide (p-NLRP3) was used for immunisation of mice. The subsequently generated hybridoma cells secrete antibodies towards this peptide into the supernatants which were used for further validation.

5.4. Discussion

5.4.1. IKKβ is essential for NLRP3 inflammasome activation

In the classical model of the NLRP3 inflammasome activation, two signals are required: The first pre-activation signal (priming) is thought to mainly provide sufficient NLRP3 and pro-IL-1β protein levels by transcriptional upregulation via the NF-κB signalling pathway. More recent studies have demonstrated that short, 10 min priming by LPS can facilitate NLRP3 inflammasome activation (so-called rapid priming) (*306*). As the elevated expression of NLRP3 protein occurs at two hours post- LPS stimulation (*137*), it suggests that a more rapid regulation is involved in the priming process. Recent studies have further shown NLRP3 activation occurring independently of transcription and postulated a priming dependent post-translational licensing, as also described in chapter 1.9.

Our data complement these findings by showing that NF-κB signalling, while necessary for IL-1β release, is not required for NLRP3 activation. It seems that the basal expression levels of NLRP3 itself are sufficient for inflammasome formation, which is in line with the studies applying short priming.

Even with NF-κB being dispensable for NLRP3 activation, the priming step itself is required nonetheless. The priming signal acts through TLRs and can activate both NF-κB and MAP kinase signalling. The role of IKKβ has been extensively studied in the context of NF-κB and more recently also in the context of MAPK (*307-309*).

Our data demonstrate that catalytically active IKKβ is essential for NLRP3 inflammasome activation. The mechanism seems to be specific to NLRP3, as no effect could be observed on the activation of the NLRC4 inflammasome. This also shows that IKKβ does not impact on caspase-1 or Gasdermin-D activation.

The adaptor ASC was previously found to be phosphorylated by IKKa. Pyroptosis and LDH release after NLRC4 activation can occur in an ASC independent fashion, whereas IL-1β release always requires ASC. The fact that inhibition of IKKβ after LPS priming, while still fully blocking NLRP3 activation, did not affect IL-1β release after NLRC4 activation strongly suggests no IKKβ dependent effect on ASC. Neither Ikkα nor downstream components of NF-κB signalling seem to be necessary for the process of NLRP3 activation. Overall the findings suggest a role of IKKβ in rapid posttranscriptional licensing of NLRP3.

Recently Chen *et al.* deciphered that the common denominator of all signal two stimuli, including potassium efflux independent inflammasome activation, was the disassembly of the trans-Golgi network (TGN) which then serves as a scaffold for NLRP3 aggregation (cf. section 1.7). The authors found that a polybasic stretch on NLRP3 mediated charge-based interactions with phosphatidylinositol-4-phosphate (PtdIns4P) on the TGN. For most stimuli, this is mediated by potassium efflux, which is thought to promote ionic binding between NLRP3 and PtdIns4P (*158*). Prior to this, other studies have suggested that phosphorylation of NLRP3 at the Golgi controls its activation (*186*).

Our phosphoproteomic investigation showed NLRP3 phosphorylation close to the polybasic motif described to interact with PtdIns4P. Our studies conducted with mutant NLRP3 highlight that phosphorylation on these sites is not required for NLRP3 activation. This is in line with other studies that found these sites to be phosphorylated and investigated these mutants (*185, 188*). The fact that these serine residues are phosphorylated in an IKKβ dependent manner, still suggests IKKβ interaction with NLRP3 close to this residue. S198 is in close proximity and its phosphorylation has been previously shown to be required for NLRP3 phosphorylation. We could demonstrate that

the proposed mechanism of NLRP3 activation was not dependent on JNK1, as full genetic knockouts still signalled normally.

To further investigate this residue and the role IKKβ has in the mechanism, we generated a phospho-specific antibody against S198 and resubstituted NLRP3 knockouts both with phospho-dead (S198A) and phospho-mimetic (S198D) mutants. These recourses will allow future experiments to study the role of IKKβ on the proposed mechanism involving S198.

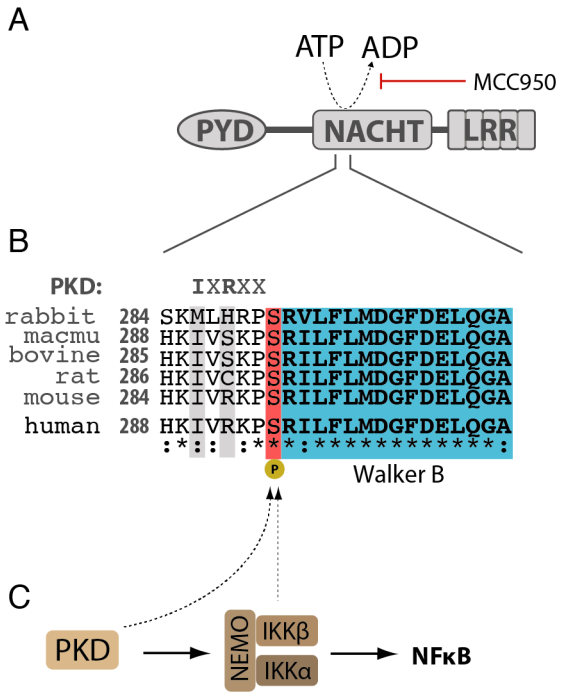

Figure 43 Phosphorylation of S295 as potential mechanism. (A) MCC950 inhibits NLRP3 by directly binding to the Walker B motif within the NACHT domain, preventing ATP hydrolysis and enforcing a inactive conformation. **(B)** Ser295 and the Walker B motif are strongly conserved among NLRP3 orthologous. The PKD consensus sequence (labelled above the alignment) are not as conserved. **(B)** PKD signalling through Ikk-complex in the context of NF-κB and potential involvement in S295 phosphorylation.

Prior to the findings of Chen *et al.* introducing the TGN based mechanism, Zhang *et al.* first implicated the Golgi by suggesting that phosphorylation of NLRP3 at the Golgi controls its activation (283). The phosphorylation was proposed to occur at the conserved Ser295, in the NBD domain of NLRP3, through protein kinase D (PKD). PKD in turn has been shown in multiple studies to regulate the IKK complex. Thus the observed phosphorylation on Ser295 could also be mediated through IKKβ. This site is highly conserved and just adjacent to the Walker B motif. This region is required for NLRP3s ATPase activity (Figure 43) (*310*). The NLRP3 inhibitor MCC950 also binds non-covalently proximal to the Walker B motif (*311, 312*). Future experiments will also focus on this site as a potential target of IKKβ in the context of our observed phenotype.

5.4.2. Species difference (mouse-men)

Previous studies revealed that full genetic knockouts of IKKβ in mice results in embryonic lethality at mid-gestation due to severe liver apoptosis. A similar phenotype was observed in mice deficient in RelA and NEMO. It was suggested that a defect in NF-κB signalling in these animals leads to an absence of survival signalling in response to TNFα stimulation, thus leading to RIPK1 independent apoptotic cell death (*283, 285, 286, 313*). While this pathway is thought to lead to the lethality in the mouse knockouts, it is not present to the same degree in humans. While the homozygous NEMO and RelA loss-of-function mutation appears to be lethal in humans (*314, 315*), this does not hold true for IKBKB. Complete IKKβ deficiency (caused by a homozygous duplication on exon 13 of IKBKB) was discovered in multiple unrelated patients, all from families of Northern Cree ancestry (*287*). A founder effect was later confirmed for the underlying homozygous mutation (c.1292dupG) and the frequency of this allele in the Northern Cree population was assessed (MAF = 0.0076) (*316*). Besides the discussed mutation, other bi-allelic loss-of-function mutations in IKBKB have also been observed in patients with different ancestry (Arabian, Turkish), all showing similar phenotypes (*288, 289, 317*). The existence of these patients with homozygous loss of IKKβ clearly shows that in humans IKBKB is not an essential gene.

While in contrast to mice, the loss of IKKβ is not lethal in humans, individuals indeed show a deficiency in innate and acquired immunity. In the discussed c.1292dupG patients, induction of IL-6 was shown to be absent in response to TLR5 stimulation. This is in line with our findings of a loss of IL-6 signalling after TLR4 stimulation in *IKBKB*$^{-/-}$ cells.

Interestingly, even though the patients produced normal mRNA levels of IKBKG and CHUK they only had low levels of the corresponding proteins indicating that IKKβ stabilises these proteins in the IKK complex in humans (*287, 288*). Although none of these studies analysed IL-1β, it is important to note that in our experiments while transcriptional levels of IL-6 were fully dependent on IKKβ, IL-1β transcription levels were only partially reduced. RNA-seq datasets, further showed that the classical NF-κB

transcripts did not show a complete reduction in *IKBKB*$^{-/-}$ cells. Further experiments are necessary to decipher the exact mechanism leading to this observed redundancy.

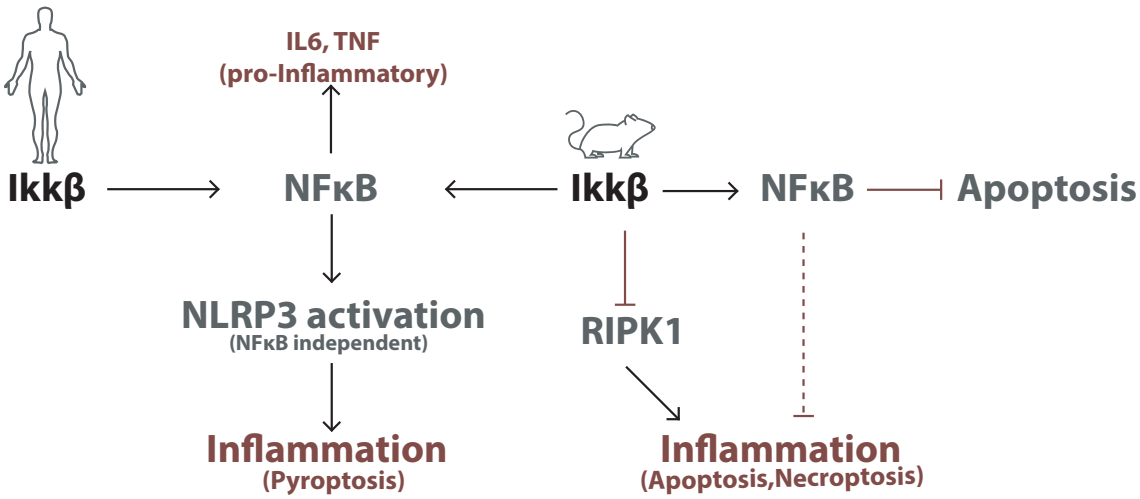

Figure 44 **Proposed schematic model of the roles of IKKβ in mice and men.**

In contrast to the described deficiency in innate immunity described for humans lacking IKKβ, studies in mice using IKKβ inhibitors or conditional knockouts showed spontaneous inflammatory conditions accompanied by increased LPS induced mortality and IL-1β secretion. We could show with both knockout cell lines as well as with using inhibitors on primary BMDMs that mouse cells lacking functional IKKβ trigger pyroptotic cell death mediated through caspase-1 cleavage upon LPS treatment. In our hands, the stimulation did not result in any release of IL-1β. Furthermore, we could show that this response could not be seen in any of our experiments with human cells, thus suggesting a clear difference in the underlying signalling mechanism between mice and humans. An overview of the different proposed cell death mechanisms in mice and men is depicted in Figure 44.

In the context of TNF signalling, it was shown that the IKK complex phosphorylates RIPK1, thus inhibiting it and preventing RIPK1 dependent cell death (*295*). It has been previously shown that activated RIPK1 can both promote apoptosis through the assembly of a RIPK1- FADD-caspase-8 complex (*318*), or necroptosis via activation of the RIPK3-MLKL pathway (*319*).

Preliminary data (not shown) suggests that the observed cell death and LDH release in IKKβ deficient mouse cells treated with LPS is dependent on RIPK1 and independent of NLRP3. Malireddi *et al.* proposed that the absence of TAK1 induces spontaneous RIPK1-dependent NLRP3 inflammasome activation; our preliminary data suggest that the loss of IKKβ (or upstream TAK1) leads to RIPK1 dependent but NLRP3 independent cell death (*320*). Any observed NLRP3 dependent effects are most likely due to necroptosis induced potassium efflux leading to NLRP3 activation. Ongoing experiments will further decipher if the downstream cell death is driven by caspase-8 dependent apoptosis or MLKL dependent necroptosis.

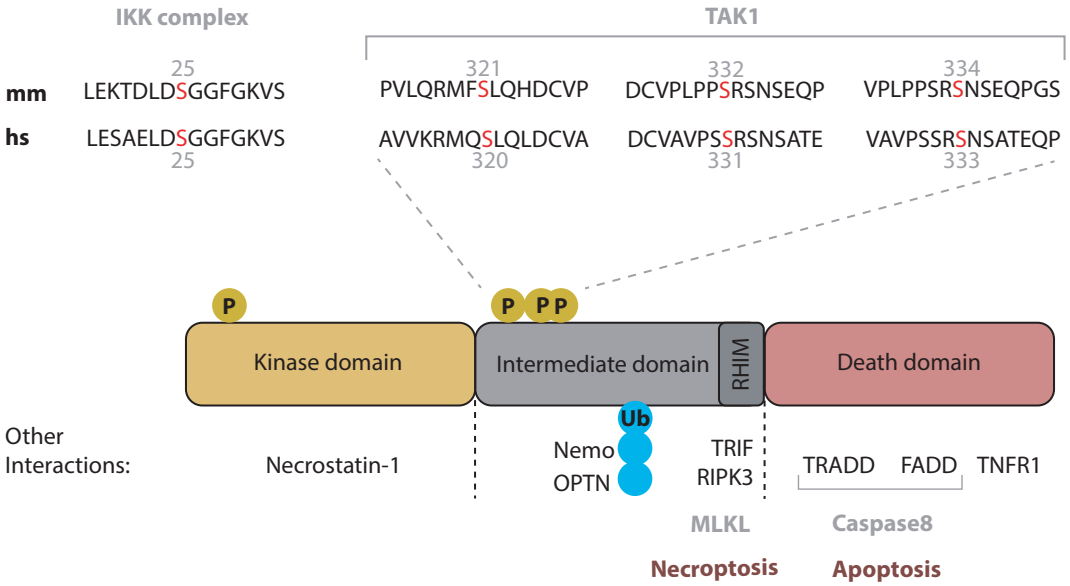

Figure 45 Structural domains of RIPK1 with selected PTMs and Interactions. Sequence of the published phosphorylation sites of the IKK complex and TAK1 are highlighted. (Fig. adapted from (*321*))

RIPK1 has previously been shown to undergo TAK1 dependent phosphorylation at S321, S332 and S334 (*296*). Furthermore, Dondellinger *et al.* recently proposed that during TNF stimulation an inhibitory phosphorylation on S25 through IKKa and IKKβ inhibits RIPK1 kinase-dependent cell death (*322*). The phosphosites are depicted in Figure 45 together with the domain structure of Ripk1. Future experiments using RIPK1 mutants could help explain if these sites are phosphorylated in an IKKβ dependent manner after LPS. As these sites are relatively well conserved between mice and humans, the species-specific signalling difference cannot be explained.

For the classical NLRP3 dependent cell death we could show an IKKβ-dependence both in humans and mice: in mice, we observed that the discussed LPS induced cell death in IKKβ deficient cells masks the effect of NLRP3 inflammasome activation after nigericin treatment. However, by inhibiting IKKβ at late timepoints we could demonstrate that the IKKβ is also required for NLRP3 inflammasome activation in mice.

5.4.3. Physiological relevance of IKKβ mediated NLRP3 activation

Previous studies investigating pharmacological kinase inhibitors in the context of NLRP3 signalling had identified TAK1 inhibitors to block inflammasome activation (*323*). However, the inhibition of TAK1 impacts on several pathways (e.g. NF-κB, cJun, p38 MAPK). With the inhibition of the downstream acting kinase IKKβ, such undesired interference in other signalling is reduced. Furthermore, IKKβ has been frequently targeted in drug development as a primary, druggable mediator of canonical NF-κB signalling. Several clinically approved non-steroidal anti-inflammatory agents (NSAIDs), such as sodium salicylate (aspirin), sulindac sulphide and exisulind, have been proposed to inhibit IKKβ, in addition to their role on cyclooxygenase enzymes (*324-328*). However, aspirin inhibits several other kinases to similar levels as IKKβ, and some studies question if this inhibition observed *in vitro* reflect its inhibitory mechanism *in vivo* (*329, 330*).

Besides these less specific compounds, highly specific IKKβ inhibitors have recently been developed for the treatment of cancer and inflammatory disease. While many candidates show promising efficacy in preclinical models, there are often concerns about the safety of systemic administration of IKKβ inhibitors. Many of these concerns are based on studies conducted in mice, showing embryonic lethality or severe spontaneous inflammatory reaction upon depletion or inhibition of IKKβ. Due to the difference between humans and mice in this regard, these concerns should be re-evaluated (see previous section).

In our experiments using pharmacological inhibitors, we found that the kinetics of NLRP3 inhibition were much faster than the inhibition of NF-κB. Further studies would be necessary, both in animal models and human samples to evaluate if this difference in kinetics can be utilised to specifically target NLRP3 *in vivo*.

In some diseases an inhibition of both NLRP3 and NF-κB might even be of interest: To date, sepsis remains to a major cause of health loss and death worldwide (*331*).

The survival rate after LPS-induced sepsis is significantly increased both by the use of NF-κB inhibitors (*332, 333*) and NLRP3 inhibitors (*334*). TPCA-1, the inhibitor used in this study, has already been successfully tested in various disease models such as arthritis and lung cancer (*298, 335*).

6. Summary

PTMs are covalent modifications of proteins to regulate their size, conformation, location, turnover and interaction with their target. Both NF-κB signalling (Priming) and the assembly and activation of inflammasomes are thought to be also directly controlled by PTMs. However, little is known about the exact mechanism of action. We set out to investigate the role of deubiquitynation through the deubiquitinase USP7 in NLRC4 signalling and the role of phosphorylation through IKKβ in NLRP3 signalling.

The main focus of past research into USP7 is focused on its role in oncology, by regulating p53 and MDM2, which leads to cell growth repression and the activation of apoptosis. Due to embryonically lethality of *USP7*$^{-/-}$ mice, there is a lack of *in vivo* studies characterising the role of USP7. In order to identify the role of USP7 both in NF-κB and inflammasome signalling, we generated BLaER1 knockout cell lines. We could confirm that USP7 deficient cells are not viable, but could be rescued *in vitro* by additionally depleting p53.

Utilising these cells, we could demonstrate a dependence of NF-κB on USP7. We could further show that USP7 deficiency leads to a loss of pyroptotic cell death after NLRC4 activation independent of the observed NF-κB phenotype. Using a special toxin expression system, we could show, USP7 to interfere with intracellular NLRC4 signalling rather than toxin uptake.

We further studied the mechanism of NLRC4 inhibition and found a strong transcriptional regulation dependent on USP7 for both NLRC4 and NAIP. We discovered additional immune regulatory proteins, which were downregulated in the USP7 deficient cells. We demonstrated for two of these immune regulatory proteins revealed by the transcriptomic analysis, NOD2 and TLR2, that the observed transcriptional regulation also shows an effect on the signalling capability.

Finally, we set out to identify the common transcription factor responsible for the regulation of the genes we observed to be affected by USP7. We could show that a depletion of IRF8 lead to a similar phenotype as USP7 deficiency. This is in line with recent findings showing an IRF8 dependent regulation of murine NAIPs.

The main focus of past research into IKKβ has been focused on its role in NF-κB signalling. To further understand the role of IKKβ both in NF-κB dependent and independent inflammasome signalling, we first set out to analyse the effect of IKKβ inhibition in mouse macrophages, as most of the previous studies focus on this model organism.
Our data show that the loss or early inhibition of IKKβ in mouse macrophages leads to pyroptotic cell death mediated through caspase-1 cleavage upon LPS treatment.
At the same time, classical NLRP3 inflammasome signalling seems to be dependent on IKKβ, as could be observed through late-stage IKKβ inhibition.

In human macrophages, no LPS induced proptosis was detectable in IKKβ deficient cells or after IKKβ inhibition, highlighting a critical difference between mice and man. However, we could observe a striking reduction of pyroptosis in the knockouts after NLRP3 activation. We could show that this effect was independent of NF-κB and upstream of caspase-1 activation.
We observed these findings both in immortalised cell lines (BLaER1, THP1) as well as primary cells (primary monocytes, iPS-Macs).
To identify the catalytic IKKβ target responsible for NLRP3 activation, we conducted phosphoproteomics. We could detect an IKKβ dependent phosphosite on NLRP3 close to a motif previously described to be necessary for activation. For the further investigation of the phosphorylation of NLRP3 through IKKβ, cells expressing a variety of different NLRP3-mutant were created and a we initiated the production of a phosphor-specific antibody for NLRP3.

7. Bibliography

1. K. Murphy, Weaver C., Janeway, C. , *Janeway's immunobiology*. (Garland Science, New York, ed. 9, 2017).
2. R. Medzhitov, C. A. Janeway, Jr., Decoding the patterns of self and nonself by the innate immune system. *Science (New York, N.Y.)* **296**, 298-300 (2002).
3. C. A. Janeway, Jr., Approaching the asymptote? Evolution and revolution in immunology. *Cold Spring Harbor symposia on quantitative biology* **54 Pt 1**, 1-13 (1989).
4. A. Aderem, D. M. Underhill, Mechanisms of phagocytosis in macrophages. *Annual review of immunology* **17**, 593-623 (1999).
5. M. Guilliams *et al.*, Dendritic cells, monocytes and macrophages: a unified nomenclature based on ontogeny. *Nature reviews. Immunology* **14**, 571-578 (2014).
6. D. G. Schatz, M. A. Oettinger, M. S. Schlissel, V(D)J recombination: molecular biology and regulation. *Annual review of immunology* **10**, 359-383 (1992).
7. S. L. Nutt, P. D. Hodgkin, D. M. Tarlinton, L. M. Corcoran, The generation of antibody-secreting plasma cells. *Nature reviews. Immunology* **15**, 160-171 (2015).
8. L. L. Lanier, J. C. Sun, Do the terms innate and adaptive immunity create conceptual barriers? *Nature reviews. Immunology* **9**, 302-303 (2009).
9. K. Palucka, J. Banchereau, Dendritic cells: a link between innate and adaptive immunity. *J Clin Immunol* **19**, 12-25 (1999).
10. A. Doria *et al.*, Autoinflammation and autoimmunity: bridging the divide. *Autoimmun Rev* **12**, 22-30 (2012).
11. L. W. Peterson, D. Artis, Intestinal epithelial cells: regulators of barrier function and immune homeostasis. *Nature reviews. Immunology* **14**, 141-153 (2014).
12. K. A. Brogden, Antimicrobial peptides: pore formers or metabolic inhibitors in bacteria? *Nat Rev Microbiol* **3**, 238-250 (2005).
13. B. Bottazzi, A. Doni, C. Garlanda, A. Mantovani, An integrated view of humoral innate immunity: pentraxins as a paradigm. *Annual review of immunology* **28**, 157-183 (2010).
14. A. Morizot, M. Saleh, Non-apoptotic functions of cell death effectors in inflammation and innate immunity. *Microbes Infect* **14**, 1241-1253 (2012).
15. H. Baumann, J. Gauldie, The acute phase response. *Immunol Today* **15**, 74-80 (1994).
16. M. G. Manz, S. Boettcher, Emergency granulopoiesis. *Nature reviews. Immunology* **14**, 302-314 (2014).
17. C. Gabay, I. Kushner, Acute-phase proteins and other systemic responses to inflammation. *N Engl J Med* **340**, 448-454 (1999).
18. G. T. Huang, L. Eckmann, T. C. Savidge, M. F. Kagnoff, Infection of human intestinal epithelial cells with invasive bacteria upregulates apical intercellular adhesion molecule-1 (ICAM)-1) expression and neutrophil adhesion. *J Clin Invest* **98**, 572-583 (1996).
19. R. Rothlein, M. L. Dustin, S. D. Marlin, T. A. Springer, A human intercellular adhesion molecule (ICAM-1) distinct from LFA-1. *Journal of immunology (Baltimore, Md. : 1950)* **137**, 1270-1274 (1986).

20. M. J. Kluger, D. H. Ringler, M. R. Anver, Fever and survival. *Science (New York, N.Y.)* **188**, 166-168 (1975).
21. S. S. Evans, E. A. Repasky, D. T. Fisher, Fever and the thermal regulation of immunity: the immune system feels the heat. *Nature reviews. Immunology* **15**, 335-349 (2015).
22. T. Kawai, S. Akira, The role of pattern-recognition receptors in innate immunity: update on Toll-like receptors. *Nature immunology* **11**, 373-384 (2010).
23. B. Beutler, Tlr4: central component of the sole mammalian LPS sensor. *Curr Opin Immunol* **12**, 20-26 (2000).
24. F. Martinon, V. Petrilli, A. Mayor, A. Tardivel, J. Tschopp, Gout-associated uric acid crystals activate the NALP3 inflammasome. *Nature* **440**, 237-241 (2006).
25. A. G. Kutikhin, A. E. Yuzhalin, C-type lectin receptors and RIG-I-like receptors: new points on the oncogenomics map. *Cancer Manag Res* **4**, 39-53 (2012).
26. T. H. Mogensen, Pathogen recognition and inflammatory signaling in innate immune defenses. *Clin Microbiol Rev* **22**, 240-273, Table of Contents (2009).
27. S. Akira, S. Uematsu, O. Takeuchi, Pathogen recognition and innate immunity. *Cell* **124**, 783-801 (2006).
28. L. Alexopoulou, A. C. Holt, R. Medzhitov, R. A. Flavell, Recognition of double-stranded RNA and activation of NF-kappaB by Toll-like receptor 3. *Nature* **413**, 732-738 (2001).
29. F. Heil, Species-Specific Recognition of Single-Stranded RNA via Toll-like Receptor 7 and 8. *Science (New York, N.Y.)* **303**, 1526-1529 (2004).
30. S. S. Diebold, T. Kaisho, H. Hemmi, S. Akira, C. Reis e Sousa, Innate antiviral responses by means of TLR7-mediated recognition of single-stranded RNA. *Science (New York, N.Y.)* **303**, 1529-1531 (2004).
31. V. Hornung *et al.*, Sequence-specific potent induction of IFN-alpha by short interfering RNA in plasmacytoid dendritic cells through TLR7. *Nature medicine* **11**, 263-270 (2005).
32. H. Hemmi *et al.*, A Toll-like receptor recognizes bacterial DNA. *Nature* **408**, 740-745 (2000).
33. A. O. Aliprantis *et al.*, Cell activation and apoptosis by bacterial lipoproteins through toll-like receptor-2. *Science (New York, N.Y.)* **285**, 736-739 (1999).
34. E. Lien *et al.*, Toll-like receptor 2 functions as a pattern recognition receptor for diverse bacterial products. *The Journal of biological chemistry* **274**, 33419-33425 (1999).
35. D. M. Underhill *et al.*, The Toll-like receptor 2 is recruited to macrophage phagosomes and discriminates between pathogens. *Nature* **401**, 811-815 (1999).
36. O. Takeuchi *et al.*, Cutting edge: role of Toll-like receptor 1 in mediating immune response to microbial lipoproteins. *Journal of immunology (Baltimore, Md. : 1950)* **169**, 10-14 (2002).
37. O. Takeuchi *et al.*, Discrimination of bacterial lipoproteins by Toll-like receptor 6. *Int Immunol* **13**, 933-940 (2001).
38. M. S. Jin *et al.*, Crystal structure of the TLR1-TLR2 heterodimer induced by binding of a tri-acylated lipopeptide. *Cell* **130**, 1071-1082 (2007).
39. R. B. Yang *et al.*, Toll-like receptor-2 mediates lipopolysaccharide-induced cellular signalling. *Nature* **395**, 284-288 (1998).

40. J. C. Chow, D. W. Young, D. T. Golenbock, W. J. Christ, F. Gusovsky, Toll-like receptor-4 mediates lipopolysaccharide-induced signal transduction. *The Journal of biological chemistry* **274**, 10689-10692 (1999).
41. K. Hoshino *et al.*, Cutting edge: Toll-like receptor 4 (TLR4)-deficient mice are hyporesponsive to lipopolysaccharide: evidence for TLR4 as the Lps gene product. *Journal of immunology (Baltimore, Md. : 1950)* **162**, 3749-3752 (1999).
42. A. Poltorak *et al.*, Defective LPS signaling in C3H/HeJ and C57BL/10ScCr mice: mutations in Tlr4 gene. *Science (New York, N.Y.)* **282**, 2085-2088 (1998).
43. H. Heine *et al.*, Cutting edge: cells that carry A null allele for toll-like receptor 2 are capable of responding to endotoxin. *Journal of immunology (Baltimore, Md. : 1950)* **162**, 6971-6975 (1999).
44. H. M. Kim *et al.*, Crystal structure of the TLR4-MD-2 complex with bound endotoxin antagonist Eritoran. *Cell* **130**, 906-917 (2007).
45. N. Lamping *et al.*, LPS-binding protein protects mice from septic shock caused by LPS or gram-negative bacteria. *J Clin Invest* **101**, 2065-2071 (1998).
46. J. Pugin *et al.*, Lipopolysaccharide activation of human endothelial and epithelial cells is mediated by lipopolysaccharide-binding protein and soluble CD14. *Proceedings of the National Academy of Sciences of the United States of America* **90**, 2744-2748 (1993).
47. Y. Kamio, H. Nikaido, Outer membrane of Salmonella typhimurium: accessibility of phospholipid head groups to phospholipase c and cyanogen bromide activated dextran in the external medium. *Biochemistry* **15**, 2561-2570 (1976).
48. C. R. Raetz, C. Whitfield, Lipopolysaccharide endotoxins. *Annu Rev Biochem* **71**, 635-700 (2002).
49. J. S. Gunn *et al.*, PmrA-PmrB-regulated genes necessary for 4-aminoarabinose lipid A modification and polymyxin resistance. *Mol Microbiol* **27**, 1171-1182 (1998).
50. L. Guo *et al.*, Lipid A acylation and bacterial resistance against vertebrate antimicrobial peptides. *Cell* **95**, 189-198 (1998).
51. A. M. Hajjar, R. K. Ernst, J. H. Tsai, C. B. Wilson, S. I. Miller, Human Toll-like receptor 4 recognizes host-specific LPS modifications. *Nature immunology* **3**, 354-359 (2002).
52. F. Hayashi *et al.*, The innate immune response to bacterial flagellin is mediated by Toll-like receptor 5. *Nature* **410**, 1099-1103 (2001).
53. H. C. Ramos, M. Rumbo, J. C. Sirard, Bacterial flagellins: mediators of pathogenicity and host immune responses in mucosa. *Trends in microbiology* **12**, 509-517 (2004).
54. M. Leone, R. Moreau, Leukocyte Toll-like Receptor 2-mitochondria Axis in Sepsis. **121**, 1147-1149 (2014).
55. O. Adachi *et al.*, Targeted disruption of the MyD88 gene results in loss of IL-1- and IL-18-mediated function. *Immunity* **9**, 143-150 (1998).
56. H. Ohnishi *et al.*, Structural basis for the multiple interactions of the MyD88 TIR domain in TLR4 signaling. *Proceedings of the National Academy of Sciences of the United States of America* **106**, 10260-10265 (2009).
57. S. C. Lin, Y. C. Lo, H. Wu, Helical assembly in the MyD88-IRAK4-IRAK2 complex in TLR/IL-1R signalling. *Nature* **465**, 885-890 (2010).

58. M. Yamamoto *et al.*, TRAM is specifically involved in the Toll-like receptor 4-mediated MyD88-independent signaling pathway. *Nature immunology* **4**, 1144-1150 (2003).
59. K. A. Fitzgerald *et al.*, Mal (MyD88-adapter-like) is required for Toll-like receptor-4 signal transduction. *Nature* **413**, 78-83 (2001).
60. Y. Lin *et al.*, Characterization of the immune defense related tissues, cells, and genes in amphioxus. *Science China. Life sciences* **54**, 999-1004 (2011).
61. S. Li, A. Strelow, E. J. Fontana, H. Wesche, IRAK-4: a novel member of the IRAK family with the properties of an IRAK-kinase. *Proceedings of the National Academy of Sciences of the United States of America* **99**, 5567-5572 (2002).
62. L. Deng *et al.*, Activation of the IkappaB kinase complex by TRAF6 requires a dimeric ubiquitin-conjugating enzyme complex and a unique polyubiquitin chain. *Cell* **103**, 351-361 (2000).
63. G. Takaesu *et al.*, TAB2, a Novel Adaptor Protein, Mediates Activation of TAK1 MAPKKK by Linking TAK1 to TRAF6 in the IL-1 Signal Transduction Pathway. *Molecular cell* **5**, 649-658 (2000).
64. H. Sakurai, H. Miyoshi, J. Mizukami, T. Sugita, Phosphorylation-dependent activation of TAK1 mitogen-activated protein kinase kinase kinase by TAB1. *FEBS Lett* **474**, 141-145 (2000).
65. N. Cusson-Hermance, S. Khurana, T. H. Lee, K. A. Fitzgerald, M. A. Kelliher, Rip1 mediates the Trif-dependent toll-like receptor 3- and 4-induced NF-{kappa}B activation but does not contribute to interferon regulatory factor 3 activation. *The Journal of biological chemistry* **280**, 36560-36566 (2005).
66. A. Kanayama *et al.*, TAB2 and TAB3 activate the NF-kappaB pathway through binding to polyubiquitin chains. *Molecular cell* **15**, 535-548 (2004).
67. C. Wang *et al.*, TAK1 is a ubiquitin-dependent kinase of MKK and IKK. *Nature* **412**, 346-351 (2001).
68. Z. J. Chen, L. Parent, T. Maniatis, Site-specific phosphorylation of IkappaBalpha by a novel ubiquitination-dependent protein kinase activity. *Cell* **84**, 853-862 (1996).
69. J. A. DiDonato, M. Hayakawa, D. M. Rothwarf, E. Zandi, M. Karin, A cytokine-responsive IkappaB kinase that activates the transcription factor NF-kappaB. *Nature* **388**, 548-554 (1997).
70. S. Yamaoka *et al.*, Complementation cloning of NEMO, a component of the IkappaB kinase complex essential for NF-kappaB activation. *Cell* **93**, 1231-1240 (1998).
71. N. Dey, T. Liu, R. P. Garofalo, A. Casola, TAK1 regulates NF-KB and AP-1 activation in airway epithelial cells following RSV infection. *Virology* **418**, 93-101 (2011).
72. J. Hess, P. Angel, M. Schorpp-Kistner, AP-1 subunits: quarrel and harmony among siblings. *J Cell Sci* **117**, 5965-5973 (2004).
73. T. D. Gilmore, Introduction to NF-kappaB: players, pathways, perspectives. *Oncogene* **25**, 6680-6684 (2006).
74. A. S. Baldwin, THE NF-κB AND IκB PROTEINS: New Discoveries and Insights. *Annual review of immunology* **14**, 649-681 (1996).
75. T. Huxford, S. Malek, G. Ghosh, Structure and mechanism in NF-kappa B/I kappa B signaling. *Cold Spring Harbor symposia on quantitative biology* **64**, 533-540 (1999).

76. Y. Hou, F. Moreau, K. Chadee, PPARgamma is an E3 ligase that induces the degradation of NFkappaB/p65. *Nat Commun* **3**, 1300 (2012).
77. H. Li *et al.*, Regulation of NF-kappaB activity by competition between RelA acetylation and ubiquitination. *Oncogene* **31**, 611-623 (2012).
78. G. Wu *et al.*, Structure of a beta-TrCP1-Skp1-beta-catenin complex: destruction motif binding and lysine specificity of the SCF(beta-TrCP1) ubiquitin ligase. *Molecular cell* **11**, 1445-1456 (2003).
79. Y. Kravtsova-Ivantsiv *et al.*, KPC1-mediated ubiquitination and proteasomal processing of NF-kappaB1 p105 to p50 restricts tumor growth. *Cell* **161**, 333-347 (2015).
80. M. S. Hayden, S. Ghosh, Signaling to NF-kappaB. *Genes & development* **18**, 2195-2224 (2004).
81. C. Scheidereit, IκB kinase complexes: gateways to NF-κB activation and transcription. *Oncogene* **25**, 6685-6705 (2006).
82. J. Napetschnig, H. Wu, Molecular basis of NF-kappaB signaling. *Annu Rev Biophys* **42**, 443-468 (2013).
83. E. Derudder *et al.*, RelB/p50 dimers are differentially regulated by tumor necrosis factor-alpha and lymphotoxin-beta receptor activation: critical roles for p100. *The Journal of biological chemistry* **278**, 23278-23284 (2003).
84. S. Vallabhapurapu, M. Karin, Regulation and function of NF-kappaB transcription factors in the immune system. *Annual review of immunology* **27**, 693-733 (2009).
85. H. Hacker, M. Karin, Regulation and function of IKK and IKK-related kinases. *Sci STKE* **2006**, re13 (2006).
86. S.-C. Sun, Non-canonical NF-κB signaling pathway. *Cell research* **21**, 71-85 (2011).
87. F. Liu, Y. Xia, A. S. Parker, I. M. Verma, IKK biology. *Immunological reviews* **246**, 239-253 (2012).
88. S. Polley *et al.*, Structural Basis for the Activation of IKK1/α. *Cell reports* **17**, 1907-1914 (2016).
89. S. Polley *et al.*, A Structural Basis for IκB Kinase 2 Activation Via Oligomerization-Dependent Trans Auto-Phosphorylation. **11**, e1001581 (2013).
90. F. Mercurio *et al.*, IKK-1 and IKK-2: cytokine-activated IkappaB kinases essential for NF-kappaB activation. *Science (New York, N.Y.)* **278**, 860-866 (1997).
91. M. Delhase, Positive and Negative Regulation of IB Kinase Activity Through IKK Subunit Phosphorylation. *Science (New York, N.Y.)* **284**, 309-313 (1999).
92. J. Scholefield *et al.*, Super-resolution microscopy reveals a preformed NEMO lattice structure that is collapsed in incontinentia pigmenti. **7**, 12629 (2016).
93. F. Mercurio, IKK-1 and IKK-2: Cytokine-Activated IB Kinases Essential for NF-B Activation. *Science (New York, N.Y.)* **278**, 860-866 (1997).
94. T. Henkel *et al.*, Rapid proteolysis of IκB-α is necessary for activation of transcription factor NF-κB. *Nature* **365**, 182-185 (1993).
95. K. Brown, S. Gerstberger, L. Carlson, G. Franzoso, U. Siebenlist, Control of I kappa B-alpha proteolysis by site-specific, signal-induced phosphorylation. *Science (New York, N.Y.)* **267**, 1485-1488 (1995).
96. J. Zhang, K. Clark, T. Lawrence, M. W. Peggie, P. Cohen, An unexpected twist to the activation of IKKbeta: TAK1 primes IKKbeta for activation by autophosphorylation. *The Biochemical journal* **461**, 531-537 (2014).

97. A. Chariot, The NF-kappaB-independent functions of IKK subunits in immunity and cancer. *Trends Cell Biol* **19**, 404-413 (2009).
98. M. C. Hu *et al.*, IkappaB kinase promotes tumorigenesis through inhibition of forkhead FOXO3a. *Cell* **117**, 225-237 (2004).
99. D. F. Lee *et al.*, IKK beta suppression of TSC1 links inflammation and tumor angiogenesis via the mTOR pathway. *Cell* **130**, 440-455 (2007).
100. A. Fontalba, O. Gutierrez, J. L. Fernandez-Luna, NLRP2, an inhibitor of the NF-kappaB pathway, is transcriptionally activated by NF-kappaB and exhibits a nonfunctional allelic variant. *Journal of immunology (Baltimore, Md. : 1950)* **179**, 8519-8524 (2007).
101. P. Rosenstiel *et al.*, TNF-alpha and IFN-gamma regulate the expression of the NOD2 (CARD15) gene in human intestinal epithelial cells. *Gastroenterology* **124**, 1001-1009 (2003).
102. Y. M. Loo, M. Gale, Jr., Immune signaling by RIG-I-like receptors. *Immunity* **34**, 680-692 (2011).
103. V. Hornung *et al.*, AIM2 recognizes cytosolic dsDNA and forms a caspase-1-activating inflammasome with ASC. *Nature* **458**, 514-518 (2009).
104. N. Inohara, G. Nunez, The NOD: a signaling module that regulates apoptosis and host defense against pathogens. *Oncogene* **20**, 6473-6481 (2001).
105. A. Ablasser *et al.*, Cell intrinsic immunity spreads to bystander cells via the intercellular transfer of cGAMP. *Nature* **503**, 530-534 (2013).
106. V. Hornung, R. Hartmann, A. Ablasser, K. P. Hopfner, OAS proteins and cGAS: unifying concepts in sensing and responding to cytosolic nucleic acids. *Nature reviews. Immunology* **14**, 521-528 (2014).
107. M. Proell, S. J. Riedl, J. H. Fritz, A. M. Rojas, R. Schwarzenbacher, The Nod-like receptor (NLR) family: a tale of similarities and differences. *PLoS One* **3**, e2119 (2008).
108. F. Martinon, K. Burns, J. Tschopp, The inflammasome: a molecular platform triggering activation of inflammatory caspases and processing of proIL-beta. *Molecular cell* **10**, 417-426 (2002).
109. N. Inohara *et al.*, An induced proximity model for NF-kappa B activation in the Nod1/RICK and RIP signaling pathways. *The Journal of biological chemistry* **275**, 27823-27831 (2000).
110. E. Marquenet, E. Richet, How integration of positive and negative regulatory signals by a STAND signaling protein depends on ATP hydrolysis. *Molecular cell* **28**, 187-199 (2007).
111. E. Latz, T. S. Xiao, A. Stutz, Activation and regulation of the inflammasomes. *Nature reviews. Immunology* **13**, 397-411 (2013).
112. Y. K. Kim, J. S. Shin, M. H. Nahm, NOD-Like Receptors in Infection, Immunity, and Diseases. *Yonsei Med J* **57**, 5-14 (2016).
113. Y. Yang *et al.*, NOD2 pathway activation by MDP or Mycobacterium tuberculosis infection involves the stable polyubiquitination of Rip2. *The Journal of biological chemistry* **282**, 36223-36229 (2007).
114. M. Hasegawa *et al.*, A critical role of RICK/RIP2 polyubiquitination in Nod-induced NF-kappaB activation. *The EMBO journal* **27**, 373-383 (2008).
115. P. R. Vajjhala, R. E. Mirams, J. M. Hill, Multiple binding sites on the pyrin domain of ASC protein allow self-association and interaction with NLRP3 protein. *The Journal of biological chemistry* **287**, 41732-41743 (2012).

116. T. Fernandes-Alnemri *et al.*, The pyroptosome: a supramolecular assembly of ASC dimers mediating inflammatory cell death via caspase-1 activation. *Cell Death Differ* **14**, 1590-1604 (2007).
117. M. Proell, M. Gerlic, P. D. Mace, J. C. Reed, S. J. Riedl, The CARD plays a critical role in ASC foci formation and inflammasome signalling. *The Biochemical journal* **449**, 613-621 (2013).
118. Y. Gu *et al.*, Activation of interferon-gamma inducing factor mediated by interleukin-1beta converting enzyme. *Science (New York, N.Y.)* **275**, 206-209 (1997).
119. B. T. Cookson, M. A. Brennan, Pro-inflammatory programmed cell death. *Trends in microbiology* **9**, 113-114 (2001).
120. X. Liu *et al.*, Inflammasome-activated gasdermin D causes pyroptosis by forming membrane pores. *Nature* **535**, 153-158 (2016).
121. J. Shi *et al.*, Cleavage of GSDMD by inflammatory caspases determines pyroptotic cell death. *Nature* **526**, 660-665 (2015).
122. W. T. He *et al.*, Gasdermin D is an executor of pyroptosis and required for interleukin-1beta secretion. *Cell research* **25**, 1285-1298 (2015).
123. J. Ding *et al.*, Pore-forming activity and structural autoinhibition of the gasdermin family. *Nature* **535**, 111-116 (2016).
124. B. S. Franklin *et al.*, The adaptor ASC has extracellular and 'prionoid' activities that propagate inflammation. *Nature immunology* **15**, 727-737 (2014).
125. E. A. Miao *et al.*, Caspase-1-induced pyroptosis is an innate immune effector mechanism against intracellular bacteria. *Nature immunology* **11**, 1136-1142 (2010).
126. L. Broderick, D. De Nardo, B. S. Franklin, H. M. Hoffman, E. Latz, The inflammasomes and autoinflammatory syndromes. *Annu Rev Pathol* **10**, 395-424 (2015).
127. H. M. Hoffman, J. L. Mueller, D. H. Broide, A. A. Wanderer, R. D. Kolodner, Mutation of a new gene encoding a putative pyrin-like protein causes familial cold autoinflammatory syndrome and Muckle-Wells syndrome. *Nat Genet* **29**, 301-305 (2001).
128. H. M. Hoffman *et al.*, Efficacy and safety of rilonacept (interleukin-1 Trap) in patients with cryopyrin-associated periodic syndromes: results from two sequential placebo-controlled studies. *Arthritis Rheum* **58**, 2443-2452 (2008).
129. J. W. Yu *et al.*, Cryopyrin and pyrin activate caspase-1, but not NF-kappaB, via ASC oligomerization. *Cell Death Differ* **13**, 236-249 (2006).
130. S. L. Masters *et al.*, Activation of the NLRP3 inflammasome by islet amyloid polypeptide provides a mechanism for enhanced IL-1beta in type 2 diabetes. *Nature immunology* **11**, 897-904 (2010).
131. H. M. Lee *et al.*, Upregulated NLRP3 inflammasome activation in patients with type 2 diabetes. *Diabetes* **62**, 194-204 (2013).
132. P. Duewell *et al.*, NLRP3 inflammasomes are required for atherogenesis and activated by cholesterol crystals. *Nature* **464**, 1357-1361 (2010).
133. A. Halle *et al.*, The NALP3 inflammasome is involved in the innate immune response to amyloid-beta. *Nature immunology* **9**, 857-865 (2008).
134. M. T. Heneka *et al.*, NLRP3 is activated in Alzheimer's disease and contributes to pathology in APP/PS1 mice. *Nature* **493**, 674-678 (2013).

135. G. Codolo *et al.*, Triggering of inflammasome by aggregated alpha-synuclein, an inflammatory response in synucleinopathies. *PLoS One* **8**, e55375 (2013).
136. Y. Yan *et al.*, Dopamine controls systemic inflammation through inhibition of NLRP3 inflammasome. *Cell* **160**, 62-73 (2015).
137. F. G. Bauernfeind *et al.*, Cutting edge: NF-kappaB activating pattern recognition and cytokine receptors license NLRP3 inflammasome activation by regulating NLRP3 expression. *Journal of immunology (Baltimore, Md. : 1950)* **183**, 787-791 (2009).
138. D. M. Thiboutot, Inflammasome activation by Propionibacterium acnes: the story of IL-1 in acne continues to unfold. *J Invest Dermatol* **134**, 595-597 (2014).
139. K. Schroder *et al.*, Acute lipopolysaccharide priming boosts inflammasome activation independently of inflammasome sensor induction. *Immunobiology* **217**, 1325-1329 (2012).
140. S. Mariathasan *et al.*, Cryopyrin activates the inflammasome in response to toxins and ATP. *Nature* **440**, 228-232 (2006).
141. V. Hornung *et al.*, Silica crystals and aluminum salts activate the NALP3 inflammasome through phagosomal destabilization. *Nature immunology* **9**, 847-856 (2008).
142. S. Mariathasan *et al.*, Differential activation of the inflammasome by caspase-1 adaptors ASC and Ipaf. *Nature* **430**, 213-218 (2004).
143. G. L. Horvath, J. E. Schrum, C. M. De Nardo, E. Latz, Intracellular sensing of microbes and danger signals by the inflammasomes. *Immunological reviews* **243**, 119-135 (2011).
144. J. Shi *et al.*, Inflammatory caspases are innate immune receptors for intracellular LPS. *Nature* **514**, 187-192 (2014).
145. J. L. Schmid-Burgk *et al.*, Caspase-4 mediates non-canonical activation of the NLRP3 inflammasome in human myeloid cells. *European journal of immunology* **45**, 2911-2917 (2015).
146. N. Kayagaki *et al.*, Non-canonical inflammasome activation targets caspase-11. *Nature* **479**, 117-121 (2011).
147. N. Kayagaki *et al.*, Caspase-11 cleaves gasdermin D for non-canonical inflammasome signalling. *Nature* **526**, 666-671 (2015).
148. R. Zhou, A. S. Yazdi, P. Menu, J. Tschopp, A role for mitochondria in NLRP3 inflammasome activation. *Nature* **469**, 221-225 (2011).
149. G. S. Lee *et al.*, The calcium-sensing receptor regulates the NLRP3 inflammasome through Ca2+ and cAMP. *Nature* **492**, 123-127 (2012).
150. R. Munoz-Planillo *et al.*, K(+) efflux is the common trigger of NLRP3 inflammasome activation by bacterial toxins and particulate matter. *Immunity* **38**, 1142-1153 (2013).
151. S. Ruhl, P. Broz, Caspase-11 activates a canonical NLRP3 inflammasome by promoting K(+) efflux. *European journal of immunology* **45**, 2927-2936 (2015).
152. P. J. Baker *et al.*, NLRP3 inflammasome activation downstream of cytoplasmic LPS recognition by both caspase-4 and caspase-5. *European journal of immunology* **45**, 2918-2926 (2015).
153. Y. He, M. Y. Zeng, D. Yang, B. Motro, G. Nunez, NEK7 is an essential mediator of NLRP3 activation downstream of potassium efflux. *Nature* **530**, 354-357 (2016).

154. H. Shi *et al.*, NLRP3 activation and mitosis are mutually exclusive events coordinated by NEK7, a new inflammasome component. *Nature immunology* **17**, 250-258 (2016).
155. J. L. Schmid-Burgk *et al.*, A Genome-wide CRISPR (Clustered Regularly Interspaced Short Palindromic Repeats) Screen Identifies NEK7 as an Essential Component of NLRP3 Inflammasome Activation. *The Journal of biological chemistry* **291**, 103-109 (2016).
156. M. M. Gaidt *et al.*, Human Monocytes Engage an Alternative Inflammasome Pathway. *Immunity* **44**, 833-846 (2016).
157. C. J. Gross *et al.*, K(+) Efflux-Independent NLRP3 Inflammasome Activation by Small Molecules Targeting Mitochondria. *Immunity* **45**, 761-773 (2016).
158. J. Chen, Z. J. Chen, PtdIns4P on dispersed trans-Golgi network mediates NLRP3 inflammasome activation. *Nature* **564**, 71-76 (2018).
159. P. Broz, V. M. Dixit, Inflammasomes: mechanism of assembly, regulation and signalling. *Nature reviews. Immunology* **16**, 407-420 (2016).
160. E. M. Kofoed, R. E. Vance, Innate immune recognition of bacterial ligands by NAIPs determines inflammasome specificity. *Nature* **477**, 592-595 (2011).
161. Y. Zhao *et al.*, The NLRC4 inflammasome receptors for bacterial flagellin and type III secretion apparatus. *Nature* **477**, 596-600 (2011).
162. J. Kortmann, S. W. Brubaker, D. M. Monack, Cutting Edge: Inflammasome Activation in Primary Human Macrophages Is Dependent on Flagellin. *Journal of immunology (Baltimore, Md. : 1950)* **195**, 815-819 (2015).
163. J. Yang, Y. Zhao, J. Shi, F. Shao, Human NAIP and mouse NAIP1 recognize bacterial type III secretion needle protein for inflammasome activation. *Proceedings of the National Academy of Sciences of the United States of America* **110**, 14408-14413 (2013).
164. J. L. Tenthorey, E. M. Kofoed, M. D. Daugherty, H. S. Malik, R. E. Vance, Molecular basis for specific recognition of bacterial ligands by NAIP/NLRC4 inflammasomes. *Molecular cell* **54**, 17-29 (2014).
165. Z. Hu *et al.*, Structural and biochemical basis for induced self-propagation of NLRC4. *Science (New York, N.Y.)* **350**, 399-404 (2015).
166. L. Zhang *et al.*, Cryo-EM structure of the activated NAIP2-NLRC4 inflammasome reveals nucleated polymerization. *Science (New York, N.Y.)* **350**, 404-409 (2015).
167. H. Guo, J. B. Callaway, J. Ting, Inflammasomes: mechanism of action, role in disease, and therapeutics. *Nature medicine* **21**, 677-687 (2015).
168. P. Broz, J. von Moltke, J. W. Jones, R. E. Vance, D. M. Monack, Differential requirement for Caspase-1 autoproteolysis in pathogen-induced cell death and cytokine processing. *Cell Host Microbe* **8**, 471-483 (2010).
169. O. Gutierrez, C. Pipaon, J. L. Fernandez-Luna, Ipaf is upregulated by tumor necrosis factor-alpha in human leukemia cells. *FEBS Lett* **568**, 79-82 (2004).
170. R. Karki *et al.*, IRF8 Regulates Transcription of Naips for NLRC4 Inflammasome Activation. *Cell* **173**, 920-933 e913 (2018).
171. S. Sadasivam *et al.*, Caspase-1 activator Ipaf is a p53-inducible gene involved in apoptosis. *Oncogene* **24**, 627-636 (2005).
172. J. A. Duncan, S. W. Canna, The NLRC4 Inflammasome. *Immunological reviews* **281**, 115-123 (2018).

173. L. Abrami, B. Kunz, F. G. van der Goot, Anthrax toxin triggers the activation of src-like kinases to mediate its own uptake. *Proceedings of the National Academy of Sciences of the United States of America* **107**, 1420-1424 (2010).
174. C. A. Moore, S. K. Milano, J. L. Benovic, Regulation of receptor trafficking by GRKs and arrestins. *Annu Rev Physiol* **69**, 451-482 (2007).
175. L. Abrami, M. Bischofberger, B. Kunz, R. Groux, F. G. van der Goot, Endocytosis of the anthrax toxin is mediated by clathrin, actin and unconventional adaptors. *PLoS Pathog* **6**, e1000792 (2010).
176. J. Chavarria-Smith, R. E. Vance, The NLRP1 inflammasomes. *Immunological reviews* **265**, 22-34 (2015).
177. B. C. Frew, V. R. Joag, J. Mogridge, Proteolytic processing of Nlrp1b is required for inflammasome activity. *PLoS Pathog* **8**, e1002659 (2012).
178. S. K. Goru, A. Pandey, A. B. Gaikwad, E3 ubiquitin ligases as novel targets for inflammatory diseases. *Pharmacol Res* **106**, 1-9 (2016).
179. V. K. Chaugule, H. Walden, Specificity and disease in the ubiquitin system. *Biochemical Society transactions* **44**, 212-227 (2016).
180. S. Fulda, K. Rajalingam, I. Dikic, Ubiquitylation in immune disorders and cancer: from molecular mechanisms to therapeutic implications. *EMBO Mol Med* **4**, 545-556 (2012).
181. I. E. Wertz *et al.*, De-ubiquitination and ubiquitin ligase domains of A20 downregulate NF-kappaB signalling. *Nature* **430**, 694-699 (2004).
182. L. Catrysse, L. Vereecke, R. Beyaert, G. van Loo, A20 in inflammation and autoimmunity. *Trends in immunology* **35**, 22-31 (2014).
183. Y. Yang, H. Wang, M. Kouadir, H. Song, F. Shi, Recent advances in the mechanisms of NLRP3 inflammasome activation and its inhibitors. *Cell death & disease* **10**, (2019).
184. J. Yang, Z. Liu, T. S. Xiao, Post-translational regulation of inflammasomes. *Cellular & Molecular Immunology* **14**, 65-79 (2017).
185. N. Song *et al.*, NLRP3 Phosphorylation Is an Essential Priming Event for Inflammasome Activation. *Molecular cell* **68**, 185-197 e186 (2017).
186. Z. Zhang *et al.*, Protein kinase D at the Golgi controls NLRP3 inflammasome activation. *J Exp Med* **214**, 2671-2693 (2017).
187. L. Mortimer, F. Moreau, J. A. MacDonald, K. Chadee, NLRP3 inflammasome inhibition is disrupted in a group of auto-inflammatory disease CAPS mutations. *Nature immunology* **17**, 1176-1186 (2016).
188. A. Stutz *et al.*, NLRP3 inflammasome assembly is regulated by phosphorylation of the pyrin domain. *The Journal of Experimental Medicine* **214**, 1725-1736 (2017).
189. M. R. Spalinger *et al.*, NLRP3 tyrosine phosphorylation is controlled by protein tyrosine phosphatase PTPN22. *J Clin Invest* **126**, 4388 (2016).
190. C. F. Sandall, J. A. MacDonald, Effects of phosphorylation on the NLRP3 inflammasome. *Arch Biochem Biophys* **670**, 43-57 (2019).
191. T. Schmidt, J. L. Schmid-Burgk, V. Hornung, Synthesis of an arrayed sgRNA library targeting the human genome. *Sci Rep* **5**, 14987 (2015).
192. T. G. Montague, J. M. Cruz, J. A. Gagnon, G. M. Church, E. Valen, CHOPCHOP: a CRISPR/Cas9 and TALEN web tool for genome editing. *Nucleic Acids Res* **42**, W401-407 (2014).

193. K. Labun *et al.*, CHOPCHOP v3: expanding the CRISPR web toolbox beyond genome editing. *Nucleic Acids Res* **47**, W171-W174 (2019).
194. F. Rapino *et al.*, C/EBPalpha induces highly efficient macrophage transdifferentiation of B lymphoma and leukemia cell lines and impairs their tumorigenicity. *Cell reports* **3**, 1153-1163 (2013).
195. K. Takata *et al.*, Induced-Pluripotent-Stem-Cell-Derived Primitive Macrophages Provide a Platform for Modeling Tissue-Resident Macrophage Differentiation and Function. *Immunity* **47**, 183-198 e186 (2017).
196. R. H. Kutner, X.-Y. Zhang, J. Reiser, Production, concentration and titration of pseudotyped HIV-1-based lentiviral vectors. *Nature Protocols* **4**, 495-505 (2009).
197. J. L. Schmid-Burgk *et al.*, OutKnocker: a web tool for rapid and simple genotyping of designer nuclease edited cell lines. *Genome research* **24**, 1719-1723 (2014).
198. C. Girardot, J. Scholtalbers, S. Sauer, S. Y. Su, E. E. Furlong, Je, a versatile suite to handle multiplexed NGS libraries with unique molecular identifiers. *BMC Bioinformatics* **17**, 419 (2016).
199. L. Wang, S. Wang, W. Li, RSeQC: quality control of RNA-seq experiments. *Bioinformatics* **28**, 2184-2185 (2012).
200. A. Roberts, L. Pachter, Streaming fragment assignment for real-time analysis of sequencing experiments. *Nat Methods* **10**, 71-73 (2013).
201. C. Soneson, M. I. Love, M. D. Robinson, Differential analyses for RNA-seq: transcript-level estimates improve gene-level inferences. *F1000Res* **4**, 1521 (2015).
202. M. I. Love, W. Huber, S. Anders, Moderated estimation of fold change and dispersion for RNA-seq data with DESeq2. *Genome Biol* **15**, 550 (2014).
203. P. Shannon *et al.*, Cytoscape: a software environment for integrated models of biomolecular interaction networks. *Genome research* **13**, 2498-2504 (2003).
204. J. Cox, M. Mann, MaxQuant enables high peptide identification rates, individualized p.p.b.-range mass accuracies and proteome-wide protein quantification. *Nat Biotechnol* **26**, 1367-1372 (2008).
205. S. J. Humphrey, O. Karayel, D. E. James, M. Mann, High-throughput and high-sensitivity phosphoproteomics with the EasyPhos platform. *Nature Protocols* **13**, 1897-1916 (2018).
206. A. K. Raghawan *et al.*, A Disease-associated Mutant of NLRC4 Shows Enhanced Interaction with SUG1 Leading to Constitutive FADD-dependent Caspase-8 Activation and Cell Death. *Journal of Biological Chemistry* **292**, 1218-1230 (2017).
207. B. Giardine *et al.*, Galaxy: a platform for interactive large-scale genome analysis. *Genome research* **15**, 1451-1455 (2005).
208. C. Wang *et al.*, GPS 5.0: An Update on the Prediction of Kinase-specific Phosphorylation Sites in Proteins. *Genomics Proteomics Bioinformatics*, (2020).
209. R. S. Janky *et al.*, iRegulon: From a Gene List to a Gene Regulatory Network Using Large Motif and Track Collections. *PLoS Computational Biology* **10**, e1003731 (2014).
210. H. Mi, A. Muruganujan, D. Ebert, X. Huang, P. D. Thomas, PANTHER version 14: more genomes, a new PANTHER GO-slim and improvements in enrichment analysis tools. *Nucleic Acids Res* **47**, D419-D426 (2019).

211. F. Gnad, J. Gunawardena, M. Mann, PHOSIDA 2011: the posttranslational modification database. *Nucleic Acids Res* **39**, D253-260 (2011).
212. H. Han *et al.*, TRRUST v2: an expanded reference database of human and mouse transcriptional regulatory interactions. *Nucleic Acids Res* **46**, D380-D386 (2018).
213. J. Zhou *et al.*, USP7: Target Validation and Drug Discovery for Cancer Therapy. *Med Chem* **14**, 3-18 (2018).
214. W. Jager *et al.*, The ubiquitin-specific protease USP7 modulates the replication of Kaposi's sarcoma-associated herpesvirus latent episomal DNA. *J Virol* **86**, 6745-6757 (2012).
215. S. Chavoshi *et al.*, Identification of Kaposi Sarcoma Herpesvirus (KSHV) vIRF1 Protein as a Novel Interaction Partner of Human Deubiquitinase USP7. *The Journal of biological chemistry* **291**, 6281-6291 (2016).
216. S. Bhattacharya, D. Chakraborty, M. Basu, M. K. Ghosh, Emerging insights into HAUSP (USP7) in physiology, cancer and other diseases. *Signal Transduction and Targeted Therapy* **3**, (2018).
217. A. Kovalenko *et al.*, The tumour suppressor CYLD negatively regulates NF-kappaB signalling by deubiquitination. *Nature* **424**, 801-805 (2003).
218. E. Trompouki *et al.*, CYLD is a deubiquitinating enzyme that negatively regulates NF-kappaB activation by TNFR family members. *Nature* **424**, 793-796 (2003).
219. R. B. Damgaard *et al.*, The Deubiquitinase OTULIN Is an Essential Negative Regulator of Inflammation and Autoimmunity. *Cell* **166**, 1215-1230 e1220 (2016).
220. V. Schaeffer *et al.*, Binding of OTULIN to the PUB domain of HOIP controls NF-kappaB signaling. *Molecular cell* **54**, 349-361 (2014).
221. E. G. Lee *et al.*, Failure to regulate TNF-induced NF-kappaB and cell death responses in A20-deficient mice. *Science (New York, N.Y.)* **289**, 2350-2354 (2000).
222. T. Li, J. Guan, S. Li, X. Zhang, X. Zheng, HSCARG downregulates NF-κB signaling by interacting with USP7 and inhibiting NEMO ubiquitination. **5**, e1229 (2014).
223. S. Daubeuf *et al.*, HSV ICP0 recruits USP7 to modulate TLR-mediated innate response. *Blood* **113**, 3264-3275 (2009).
224. A. Colleran *et al.*, Deubiquitination of NF- B by Ubiquitin-Specific Protease-7 promotes transcription. *Proceedings of the National Academy of Sciences* **110**, 618-623 (2013).
225. N. Kon *et al.*, Inactivation of HAUSP in vivo modulates p53 function. *Oncogene* **29**, 1270-1279 (2010).
226. Z. Wang *et al.*, USP7: Novel Drug Target in Cancer Therapy. *Front Pharmacol* **10**, 427 (2019).
227. N. Kon *et al.*, Roles of HAUSP-mediated p53 regulation in central nervous system development. **18**, 1366-1375 (2011).
228. C. L. Brooks, W. Gu, p53 ubiquitination: Mdm2 and beyond. *Molecular cell* **21**, 307-315 (2006).
229. F. Colland, The therapeutic potential of deubiquitinating enzyme inhibitors. *Biochemical Society transactions* **38**, 137-143 (2010).
230. L. Kategaya *et al.*, USP7 small-molecule inhibitors interfere with ubiquitin binding. *Nature* **550**, 534-538 (2017).

231. I. Lamberto *et al.*, Structure-Guided Development of a Potent and Selective Non-covalent Active-Site Inhibitor of USP7. *Cell Chem Biol* **24**, 1490-1500 e1411 (2017).
232. G. Gavory *et al.*, Discovery and characterization of highly potent and selective allosteric USP7 inhibitors. *Nat Chem Biol* **14**, 118-125 (2018).
233. L. Yang, K. Ross, E. E. Qwarnstrom, RelA Control of IκBα Phosphorylation: A POSITIVE FEEDBACK LOOP FOR HIGH AFFINITY NF-κB COMPLEXES. *Journal of Biological Chemistry* **278**, 30881-30888 (2003).
234. L. Novellasdemunt *et al.*, USP7 Is a Tumor-Specific WNT Activator for APC-Mutated Colorectal Cancer by Mediating beta-Catenin Deubiquitination. *Cell reports* **21**, 612-627 (2017).
235. P. Palazón-Riquelme *et al.*, USP7 and USP47 deubiquitinases regulate NLRP3 inflammasome activation. *EMBO reports* **19**, e44766 (2018).
236. L. Abrami, S. H. Leppla, F. G. Van Der Goot, Receptor palmitoylation and ubiquitination regulate anthrax toxin endocytosis. *Journal of Cell Biology* **172**, 309-320 (2006).
237. X. Sun *et al.*, Usp7 regulates Hippo pathway through deubiquitinating the transcriptional coactivator Yorkie. *Nature Communications* **10**, (2019).
238. B. K. Fiil *et al.*, OTULIN restricts Met1-linked ubiquitination to control innate immune signaling. *Molecular cell* **50**, 818-830 (2013).
239. K. Ellwanger *et al.*, XIAP controls RIPK2 signaling by preventing its deposition in speck-like structures. *Life Science Alliance* **2**, e201900346 (2019).
240. C. Hu *et al.*, Functional characterization of the NF-κB binding site in the human NOD2 promoter. **7**, 288-295 (2010).
241. M. Yamamoto *et al.*, Shared and Distinct Functions of the Transcription Factors IRF4 and IRF8 in Myeloid Cell Development. **6**, e25812 (2011).
242. V. Shukla, R. Lu, IRF4 and IRF8: governing the virtues of B lymphocytes. **9**, 269-282 (2014).
243. O. Fornes *et al.*, JASPAR 2020: update of the open-access database of transcription factor binding profiles. *Nucleic Acids Research*, (2019).
244. J. S. Bednash, R. K. Mallampalli, Regulation of inflammasomes by ubiquitination. *Cellular & Molecular Immunology* **13**, 722-728 (2016).
245. D. L. Boone *et al.*, The ubiquitin-modifying enzyme A20 is required for termination of Toll-like receptor responses. *Nature immunology* **5**, 1052-1060 (2004).
246. M. S. Ritorto *et al.*, Screening of DUB activity and specificity by MALDI-TOF mass spectrometry. *Nature Communications* **5**, 4763 (2014).
247. R. D. Everett *et al.*, A novel ubiquitin-specific protease is dynamically associated with the PML nuclear domain and binds to a herpesvirus regulatory protein. *The EMBO journal* **16**, 1519-1530 (1997).
248. M. M. McDaniel, L. C. Kottyan, H. Singh, C. Pasare, Suppression of Inflammasome Activation by IRF8 and IRF4 in cDCs Is Critical for T Cell Priming. *Cell reports* **31**, 107604 (2020).
249. C. Bovolenta *et al.*, Molecular interactions between interferon consensus sequence binding protein and members of the interferon regulatory factor family. *Proceedings of the National Academy of Sciences of the United States of America* **91**, 5046-5050 (1994).

250. E. A. Eklund, A. Jalava, R. Kakar, PU.1, interferon regulatory factor 1, and interferon consensus sequence-binding protein cooperate to increase gp91(phox) expression. *The Journal of biological chemistry* **273**, 13957-13965 (1998).
251. M. S. Lee, Y. J. Kim, Signaling pathways downstream of pattern-recognition receptors and their cross talk. *Annu Rev Biochem* **76**, 447-480 (2007).
252. K. A. Fitzgerald *et al.*, IKKepsilon and TBK1 are essential components of the IRF3 signaling pathway. *Nature immunology* **4**, 491-496 (2003).
253. S. Sharma *et al.*, Triggering the interferon antiviral response through an IKK-related pathway. *Science (New York, N.Y.)* **300**, 1148-1151 (2003).
254. M. Iwanaszko, M. Kimmel, NF-kappaB and IRF pathways: cross-regulation on target genes promoter level. *BMC Genomics* **16**, 307 (2015).
255. V. Quesada *et al.*, Cloning and enzymatic analysis of 22 novel human ubiquitin-specific proteases. *Biochemical and biophysical research communications* **314**, 54-62 (2004).
256. R. Lin *et al.*, USP4 interacts and positively regulates IRF8 function via K48-linked deubiquitination in regulatory T cells. *FEBS Lett* **591**, 1677-1686 (2017).
257. Z. Li *et al.*, USP4 inhibits p53 and NF-kappaB through deubiquitinating and stabilizing HDAC2. *Oncogene* **35**, 2902-2912 (2016).
258. X. Zhang, F. G. Berger, J. Yang, X. Lu, USP4 inhibits p53 through deubiquitinating and stabilizing ARF-BP1. *The EMBO journal* **30**, 2177-2189 (2011).
259. S. J. Ward *et al.*, The structure of the deubiquitinase USP15 reveals a misaligned catalytic triad and an open ubiquitin-binding channel. *The Journal of biological chemistry* **293**, 17362-17374 (2018).
260. X. Zhu, R. Menard, T. Sulea, High incidence of ubiquitin-like domains in human ubiquitin-specific proteases. *Proteins* **69**, 1-7 (2007).
261. R. Q. Kim, T. K. Sixma, Regulation of USP7: A High Incidence of E3 Complexes. *J Mol Biol* **429**, 3395-3408 (2017).
262. J. Liang *et al.*, Novel NLRC4 Mutation Causes a Syndrome of Perinatal Autoinflammation With Hemophagocytic Lymphohistiocytosis, Hepatosplenomegaly, Fetal Thrombotic Vasculopathy, and Congenital Anemia and Ascites. *Pediatr Dev Pathol* **20**, 498-505 (2017).
263. Y. Kawasaki *et al.*, Identification of a High-Frequency Somatic NLRC4 Mutation as a Cause of Autoinflammation by Pluripotent Cell-Based Phenotype Dissection. *Arthritis Rheumatol* **69**, 447-459 (2017).
264. S. W. Canna *et al.*, An activating NLRC4 inflammasome mutation causes autoinflammation with recurrent macrophage activation syndrome. *Nat Genet* **46**, 1140-1146 (2014).
265. C. Bracaglia *et al.*, Anti interferon-gamma (IFNγ) monoclonal antibody treatment in a patient carrying an NLRC4 mutation and severe hemophagocytic lymphohistiocytosis. *Pediatric Rheumatology* **13**, O68 (2015).
266. S. W. Canna *et al.*, Life-threatening NLRC4-associated hyperinflammation successfully treated with IL-18 inhibition. *J Allergy Clin Immunol* **139**, 1698-1701 (2017).
267. N. Romberg *et al.*, Mutation of NLRC4 causes a syndrome of enterocolitis and autoinflammation. *Nat Genet* **46**, 1135-1139 (2014).

268. A. Kitamura, Y. Sasaki, T. Abe, H. Kano, K. Yasutomo, An inherited mutation in NLRC4 causes autoinflammation in human and mice. *J Exp Med* **211**, 2385-2396 (2014).
269. C. M. Volker-Touw *et al.*, Erythematous nodes, urticarial rash and arthralgias in a large pedigree with NLRC4-related autoinflammatory disease, expansion of the phenotype. *Br J Dermatol* **176**, 244-248 (2017).
270. C. T. Chear *et al.*, A novel de novo NLRC4 mutation reinforces the likely pathogenicity of specific LRR domain mutation. *Clin Immunol* **211**, 108328 (2020).
271. I. Jeru *et al.*, Mutations in NALP12 cause hereditary periodic fever syndromes. *Proceedings of the National Academy of Sciences of the United States of America* **105**, 1614-1619 (2008).
272. E. E. Zoller *et al.*, Hemophagocytosis causes a consumptive anemia of inflammation. *Journal of Experimental Medicine* **208**, 1203-1214 (2011).
273. S. W. Canna, E. M. Behrens, Not all hemophagocytes are created equally: appreciating the heterogeneity of the hemophagocytic syndromes. *Current opinion in rheumatology* **24**, 113 (2012).
274. J. Cui *et al.*, NLRP4 negatively regulates type I interferon signaling by targeting the kinase TBK1 for degradation via the ubiquitin ligase DTX4. *Nature immunology* **13**, 387-395 (2012).
275. X. Wang *et al.*, The proteasome deubiquitinase inhibitor VLX1570 shows selectivity for ubiquitin-specific protease-14 and induces apoptosis of multiple myeloma cells. *Sci Rep* **6**, 26979 (2016).
276. D. Chauhan *et al.*, A small molecule inhibitor of ubiquitin-specific protease-7 induces apoptosis in multiple myeloma cells and overcomes bortezomib resistance. *Cancer cell* **22**, 345-358 (2012).
277. Q. Wang *et al.*, Stabilization of histone demethylase PHF8 by USP7 promotes breast carcinogenesis. *J Clin Invest* **126**, 2205-2220 (2016).
278. O. Tavana *et al.*, HAUSP deubiquitinates and stabilizes N-Myc in neuroblastoma. *Nature medicine* **22**, 1180-1186 (2016).
279. C. Cheng, C. Niu, Y. Yang, Y. Wang, M. Lu, Expression of HAUSP in gliomas correlates with disease progression and survival of patients. *Oncol Rep* **29**, 1730-1736 (2013).
280. L. Zhang, H. Wang, L. Tian, H. Li, Expression of USP7 and MARCH7 Is Correlated with Poor Prognosis in Epithelial Ovarian Cancer. *The Tohoku journal of experimental medicine* **239**, 165-175 (2016).
281. Y. Peng *et al.*, USP7 is a novel Deubiquitinase sustaining PLK1 protein stability and regulating chromosome alignment in mitosis. *Journal of Experimental & Clinical Cancer Research* **38**, 468 (2019).
282. J. Chen *et al.*, Selective and cell-active inhibitors of the USP1/ UAF1 deubiquitinase complex reverse cisplatin resistance in non-small cell lung cancer cells. *Chem Biol* **18**, 1390-1400 (2011).
283. Q. Li, Severe Liver Degeneration in Mice Lacking the IB Kinase 2 Gene. **284**, 321-325 (1999).
284. Y. Hu, Abnormal Morphogenesis But Intact IKK Activation in Mice Lacking the IKK Subunit of IB Kinase. *Science (New York, N.Y.)* **284**, 316-320 (1999).

285. A. A. Beg, W. C. Sha, R. T. Bronson, S. Ghosh, D. Baltimore, Embryonic lethality and liver degeneration in mice lacking the RelA component of NF-κB. *Nature* **376**, 167-170 (1995).
286. M. Tanaka *et al.*, Embryonic Lethality, Liver Degeneration, and Impaired NF-κB Activation in IKK-β-Deficient Mice. *Immunity* **10**, 421-429 (1999).
287. U. Pannicke *et al.*, Deficiency of Innate and Acquired Immunity Caused by an IKBKB Mutation. *New England Journal of Medicine* **369**, 2504-2514 (2013).
288. T. Mousallem *et al.*, A nonsense mutation in IKBKB causes combined immunodeficiency. *Blood* **124**, 2046-2050 (2014).
289. C. Nielsen *et al.*, Immunodeficiency Associated with a Nonsense Mutation of IKBKB. *Journal of Clinical Immunology* **34**, 916-921 (2014).
290. F. R. Greten *et al.*, IKKβ Links Inflammation and Tumorigenesis in a Mouse Model of Colitis-Associated Cancer. *Cell* **118**, 285-296 (2004).
291. J. Yang *et al.*, Conditional ablation of Ikkb inhibits melanoma tumor development in mice. *Journal of Clinical Investigation* **120**, 2563-2574 (2010).
292. J. Ling *et al.*, KrasG12D-Induced IKK2/β/NF-κB Activation by IL-1α and p62 Feedforward Loops Is Required for Development of Pancreatic Ductal Adenocarcinoma. **21**, 105-120 (2012).
293. Y.-N. Gong *et al.*, Chemical probing reveals insights into the signaling mechanism of inflammasome activation. *Cell research* **20**, 1289-1305 (2010).
294. C. Juliana *et al.*, Anti-inflammatory Compounds Parthenolide and Bay 11-7082 Are Direct Inhibitors of the Inflammasome. **285**, 9792-9802 (2010).
295. Y. Dondelinger *et al.*, NF-κB-Independent Role of IKKα/IKKβ in Preventing RIPK1 Kinase-Dependent Apoptotic and Necroptotic Cell Death during TNF Signaling. **60**, 63-76 (2015).
296. J. Geng *et al.*, Regulation of RIPK1 activation by TAK1-mediated phosphorylation dictates apoptosis and necroptosis. *Nat Commun* **8**, 359 (2017).
297. R. K. S. Malireddi *et al.*, TAK1 restricts spontaneous NLRP3 activation and cell death to control myeloid proliferation. *Journal of Experimental Medicine* **215**, 1023-1034 (2018).
298. P. L. Podolin *et al.*, Attenuation of murine collagen-induced arthritis by a novel, potent, selective small molecule inhibitor of IkappaB Kinase 2, TPCA-1 (2-[(aminocarbonyl)amino]-5-(4-fluorophenyl)-3-thiophenecarboxamide), occurs via reduction of proinflammatory cytokines and antigen-induced T cell Proliferation. *J Pharmacol Exp Ther* **312**, 373-381 (2005).
299. F. R. Greten *et al.*, NF-κB Is a Negative Regulator of IL-1β Secretion as Revealed by Genetic and Pharmacological Inhibition of IKKβ. *Cell* **130**, 918-931 (2007).
300. D. M. Rothwarf, E. Zandi, G. Natoli, M. Karin, IKK-γ is an essential regulatory subunit of the IκB kinase complex. *Nature* **395**, 297-300 (1998).
301. L. A. Solt, L. A. Madge, M. J. May, NEMO-binding Domains of Both IKK and IKK Regulate I B Kinase Complex Assembly and Classical NF- B Activation. **284**, 27596-27608 (2009).
302. C.-K. Ea, L. Deng, Z.-P. Xia, G. Pineda, Z. J. Chen, Activation of IKK by TNFα Requires Site-Specific Ubiquitination of RIP1 and Polyubiquitin Binding by NEMO. **22**, 245-257 (2006).

303. V. Sjoelund, M. Smelkinson, A. Nita-Lazar, Phosphoproteome Profiling of the Macrophage Response to Different Toll-Like Receptor Ligands Identifies Differences in Global Phosphorylation Dynamics. **13**, 5185-5197 (2014).
304. G. Weintz *et al.*, The phosphoproteome of toll-like receptor-activated macrophages. **6**, (2010).
305. J. A. Kim, J. Lee, R. L. Margolis, R. Fotedar, SP600125 suppresses Cdk1 and induces endoreplication directly from G2 phase, independent of JNK inhibition. **29**, 1702-1716 (2010).
306. C. Juliana *et al.*, Non-transcriptional priming and deubiquitination regulate NLRP3 inflammasome activation. *The Journal of biological chemistry* **287**, 36617-36622 (2012).
307. M. Waterfield, W. Jin, W. Reiley, M. Zhang, S. C. Sun, IkappaB kinase is an essential component of the Tpl2 signaling pathway. *Molecular and cellular biology* **24**, 6040-6048 (2004).
308. G. Tang *et al.*, Inhibition of JNK activation through NF-kappaB target genes. *Nature* **414**, 313-317 (2001).
309. E. De Smaele *et al.*, Induction of gadd45beta by NF-kappaB downregulates pro-apoptotic JNK signalling. *Nature* **414**, 308-313 (2001).
310. J. A. Duncan *et al.*, Cryopyrin/NALP3 binds ATP/dATP, is an ATPase, and requires ATP binding to mediate inflammatory signaling. *Proceedings of the National Academy of Sciences of the United States of America* **104**, 8041-8046 (2007).
311. R. C. Coll *et al.*, MCC950 directly targets the NLRP3 ATP-hydrolysis motif for inflammasome inhibition. *Nat Chem Biol* **15**, 556-559 (2019).
312. A. Tapia-Abellan *et al.*, MCC950 closes the active conformation of NLRP3 to an inactive state. *Nat Chem Biol* **15**, 560-564 (2019).
313. D. J. Van Antwerp, S. J. Martin, T. Kafri, D. R. Green, I. M. Verma, Suppression of TNF-alpha-induced apoptosis by NF-kappaB. *Science (New York, N.Y.)* **274**, 787-789 (1996).
314. F. Fusco *et al.*, Alterations of the IKBKG locus and diseases: an update and a report of 13 novel mutations. *Hum Mutat* **29**, 595-604 (2008).
315. Y. R. Badran *et al.*, Human RELA haploinsufficiency results in autosomal-dominant chronic mucocutaneous ulceration. *J Exp Med* **214**, 1937-1947 (2017).
316. T. S. Rubin *et al.*, Newborn Screening for IKBKB Deficiency in Manitoba, Using Genetic Mutation Analysis. *J Clin Immunol* **38**, 742-744 (2018).
317. S. O. Burns *et al.*, Immunodeficiency and disseminated mycobacterial infection associated with homozygous nonsense mutation of IKKbeta. *J Allergy Clin Immunol* **134**, 215-218 (2014).
318. N. S. Wilson, V. Dixit, A. Ashkenazi, Death receptor signal transducers: nodes of coordination in immune signaling networks. *Nature immunology* **10**, 348-355 (2009).
319. M. Pasparakis, P. Vandenabeele, Necroptosis and its role in inflammation. *Nature* **517**, 311-320 (2015).
320. R. K. S. Malireddi *et al.*, TAK1 restricts spontaneous NLRP3 activation and cell death to control myeloid proliferation. *The Journal of Experimental Medicine* **215**, 1023-1034 (2018).

321. D. Ofengeim, J. Yuan, Regulation of RIP1 kinase signalling at the crossroads of inflammation and cell death. *Nature reviews. Molecular cell biology* **14**, 727-736 (2013).
322. Y. Dondelinger *et al.*, Serine 25 phosphorylation inhibits RIPK1 kinase-dependent cell death in models of infection and inflammation. *Nat Commun* **10**, 1729 (2019).
323. Y.-N. Gong *et al.*, Chemical probing reveals insights into the signaling mechanism of inflammasome activation. *Cell research* **20**, 1289-1305 (2010).
324. E. Kopp, S. Ghosh, Inhibition of NF-kappa B by sodium salicylate and aspirin. **265**, 956-959 (1994).
325. M.-J. Yin, Y. Yamamoto, R. B. Gaynor, The anti-inflammatory agents aspirin and salicylate inhibit the activity of IκB kinase-β. *Nature* **396**, 77-80 (1998).
326. T. P. McDade, R. A. Perugini, F. J. Vittimberga, R. C. Carrigan, M. P. Callery, Salicylates Inhibit NF-κB Activation and Enhance TNF-α-Induced Apoptosis in Human Pancreatic Cancer Cells. *Journal of Surgical Research* **83**, 56-61 (1999).
327. Y. Yamamoto, M.-J. Yin, K.-M. Lin, R. B. Gaynor, Sulindac Inhibits Activation of the NF-κB Pathway. *Journal of Biological Chemistry* **274**, 27307-27314 (1999).
328. L. Alfonso, G. Ai, R. C. Spitale, G. J. Bhat, Molecular targets of aspirin and cancer prevention. *British Journal of Cancer* **111**, 61-67 (2014).
329. P. Schwenger, D. Alpert, E. Y. Skolnik, J. Vilček, Activation of p38 Mitogen-Activated Protein Kinase by Sodium Salicylate Leads to Inhibition of Tumor Necrosis Factor-Induced IκBα Phosphorylation and Degradation. **18**, 78-84 (1998).
330. D. Alpert, Inhibition of Ikappa B Kinase Activity by Sodium Salicylate in Vitro Does Not Reflect Its Inhibitory Mechanism in Intact Cells. **275**, 10925-10929 (2000).
331. K. E. Rudd *et al.*, Global, regional, and national sepsis incidence and mortality, 1990–2017: analysis for the Global Burden of Disease Study. *The Lancet* **395**, 200-211 (2020).
332. D. Altavilla *et al.*, Inhibition of nuclear factor-kappaB activation by IRFI 042, protects against endotoxin-induced shock. *Cardiovasc Res* **54**, 684-693 (2002).
333. M. Sheehan *et al.*, Parthenolide, an inhibitor of the nuclear factor-kappaB pathway, ameliorates cardiovascular derangement and outcome in endotoxic shock in rodents. *Mol Pharmacol* **61**, 953-963 (2002).
334. L. G. Danielski, A. D. Giustina, S. Bonfante, T. Barichello, F. Petronilho, The NLRP3 Inflammasome and Its Role in Sepsis Development. *Inflammation* **43**, 24-31 (2020).
335. J. Nan *et al.*, TPCA-1 is a direct dual inhibitor of STAT3 and NF-kappaB and regresses mutant EGFR-associated human non-small cell lung cancers. *Mol Cancer Ther* **13**, 617-629 (2014).

8. Abbreviations

AD	Acid transactivation domain
AIM2	Absent in melanoma 2
ALR	Aim2-like receptor
AP	Alkaline phosphatase
AP-1	Activating protein-1
APC	Antigen-presenting cell
APP	Amyloid precursor protein
ARD	Ankyrin repeats
ASC	An apoptosis-associated speck-like protein containing CARD
ATP	Adenosine triphosphate
BCA	Bicinchoninic acid
BIR	Baculovirus inhibitor repeat
BMDM	Bone marrow derived macrophage
BSA	Bovine serum albumin
CARD	Caspase recruitment domain
CAPS	Cryopyrin-associated periodic syndromes
CD	Cluster of differentiation
cGAMP	Cyclic GMP-AMP
cGAS	Cyclic GMP AMP synthase
CIITA	Class II transactivator
CLRs	Type lectin receptors
CMV	Cytomegalovirus
CTB	Cell titer-blue
DAMP	Damage-associated molecular pattern
DCs	Dendritic cells
DMSO	Dimethyl sulfoxide
DNA	Deoxyribonucleic acid
dNTP	Deoxynucleoside triphosphate
ds	Double-stranded
DTT	Dithiothreitol
DUB	Deubiquitinase
ECL	Electrochemiluminescence
EDTA	Ethylenediaminetetraacetic acid
ELISA	Enzyme-linked Immunosorbent Assay
ER	Endoplasmic reticulum
FACS	Fluorescence-activated cell sorting
FCAS	Familial cold autoinflammatory syndrome
FADD	Fas associated death domain
FCS	Fetal cow serum
GSDMD	Gasdermin D
HEPES	Hydroxyethyl-piperazineethanesulfonic acid
ICAM	Intracellular adhesion molecule
IFN	Interferon

IkB	Inhibitor of nuclear factor B
IKK	Ikb kinase complex
IL	Interleukin
iNOS	Inducible nitric oxide synthase
IRAK	IL-1 receptor-activated protein kinase
IRF	Interferon regulatory factor
JAK	Janus kinase
JNK	C-Jun N-terminal kinase
LB	Luria broth
LBP	LPS binding protein
LDH	Lactate dehydrogenase lps
LPS	Lipopolysaccharide
LRR	Leucin reach repeat
LT	Lymphotoxin
LUBAC	Linear ubiquitin chain assembly complex
M-CSF	Macrophage colony-stimulating factor
MACS	Magnetic-activated cell sorting
MAL	Myd88 adaptor like protein
MAM	Mitochondria-associated ER membrane
MAPK	Mitogen-activated protein kinase
MAVS	Mitochondrial antiviral signaling protein
MDP	Muramyl dipeptide
MDA5	Melanoma differentiation-associated protein 5
MHC	Major histocompatibility complex
MLKL	Mixed lineage kinase domain-like protein
MPD	Membrane proximal domain
MSU	Monosodium urate
MWS	Muckle-Wells syndrome
Myd88	Myeloid differentiation primary response gene 88
NACHT	Nucleotide-binding domain
NADPH	Nicotinamide adenine dinucleotide phosphate
NAIP	Nlr family apoptosis inhibitory protein
NEK7	Never in mitosis gene a – related expressed kinase 7
NF-kB	Nuclear factor kappa-light-chain-enhancer of activated B cells
NIK	NF-κb inducing kinase
NLCR	NLR family CARD domain-containing protein
NLRP	NOD-, LRR- and pyrin domain-containing protein
NLR	NOD like receptor
NOMID	Neonatal-onset multisystem inflammatory disorder
OLR	Oas-like receptor
PAMP	Pathogen associated molecular pattern
PBMC	Peripheral blood mononuclear cell
PBS	Phosphate-buffered saline
PCR	Polymerase chain reaction
PK	Protein kinase
PMA	Phorbol 12-myristate 13-acetate
PRR	Pathogen recognition receptors

PtdIns4P	Phosphatidylinositol-4-phosphate
PTM	Post-translational modification
PYD	Pyrin domain
RHD	Rel homology domain
RHIM	RIP homotypic interaction motif
RIG-I	Retinoic-acid inducible gene I
RIPK	Receptor-interacting serine/threonine-protein kinase
RLH	Rig-i-like receptor
RLR	RIG-I like receptor
RNA	Ribonucleic acid
RNaseL	Ribonuclease L
ROS	Reactive oxygen species
SDD	Scaffold/dimerisation domain
SDC	Sodium deoxycholate
SDS	Sodium dodecyl sulfate
STAT	Signal transducers and activators of transcription
STING	Stimulator of interferon genes
TAE	Tris base, acetic acid and EDTA
TBS	Tris-buffered saline

9. Acknowledgments

I would like to thank all the people who supported me during the time of my doctorate.

First and foremost, I want to thank my family.

Micheál and Barbara, for believing in and supporting me in every possible way throughout my life and education.

Miriam for her inexhaustible commitment of scientific and life advice, guidance and motivation (and the countless proofreading).

Teresa for rejuvenating me and holding up the cultural, musical and philological parts of live that I also hold so dear.

I would like to express my gratitude to Prof. Veit Hornung for giving me the opportunity to do my PhD in his group, as well as for all the support and guidance he has offered me over the years.

I am further grateful to Prof. Julian Stingele for agreeing to be second reviewer of my thesis, as well as to Prof. Förstemann, Prof. Jae, Prof. Pichlmaier and PD Martin for their interest shown in this manuscript by accepting to be members of my defence committee.

I am thankful for the ERC for providing me with financial support to undertake my research; at the same time, I want to highlight the importance now more than ever to continue to fund basic science. A time of pandemics and misinformation is not a time to cut funding.

A very warm thanks also go to all the people I have worked together with and everyone in the Hornung lab, for the time in and outside of the lab.

A special thanks to

Gunnar, for bioinformatic skills and for being my office partner from the very beginning

Che, for both your scientific input and your positivity and sense of humour

Maria, for her great work in the mass spectrometry experiments

Andi, for the excellent technical support

And, everyone else that I can´t thank individually: you know who you are!

A special thanks goes to my former study colleagues and friends in Munich ("*WYB*" & "*Parofal*"). Thank you for the awesome time together, and reminding me that *all work and no play makes Fion a dull boy*. You made the last nearly 10 years unforgettable.

Finally, I want to thank Caroline.

You shared the ups and downs of my PhD journey more than anyone else and enriched the process more than you know.